

Volume 11 | Number 1 | January-December 2022

JCB

Journal of
Circulating Biomarkers



ABOUTSCIENCE

Aims and Scope

Journal of Circulating Biomarkers is an international, peer-reviewed, open access, scientific, online only journal, published once a year. It focuses on all aspects of the rapidly growing field of circulating blood-based biomarkers and diagnostics using circulating protein and lipid markers, circulating tumor cells (CTC), circulating cell-free DNA (cfDNA) and extracellular vesicles. The journal publishes high-impact articles that deal with all fields related to circulating biomarkers and diagnostics, ranging from basic science to translational and clinical applications. Included within the scope are a broad array of specialties including (but not limited to) cancer, immunology, neurology, metabolic diseases, cardiovascular medicine, regenerative medicine, nosology, physiology, pathology, technological applications in diagnostics, therapeutics, vaccine, drug delivery, regenerative medicine, drug development and clinical trials. The journal also hosts reviews, perspectives and news on specific topics. Interdisciplinary studies are especially suitable for this journal.

Abstracting and Indexing

CNKI Scholar
CrossRef
DOAJ
Ebsco Discovery Service
Embase
Google Scholar
J-Gate
OCLC WorldCat
Opac-ACNP (Catalogo Italiano dei Periodici)
Opac-SBN (Catalogo del servizio bibliotecario nazionale)
PubMed Central
Researcher
ROAD (Directory of Open Access Scholarly Resources)
Scilit
Scimago
Scopus
Sherpa Romeo
Transpose

Publication process

Peer review
Papers submitted to JCB are subject to a rigorous peer review process, to ensure that the research published is valuable for its readership. JCB applies a single-blind review process and does not disclose the identity of its reviewers.

Lead times

Submission to final decision: 6-8 weeks
Acceptance to publication: 2 weeks

Publication fees

All manuscripts are submitted under Open Access terms. Article processing fees cover any other costs, that is no fee will be applied for supplementary material or for colour illustrations. Where applicable, article processing fees are subject to VAT.

Open access and copyright

All articles are published and licensed under Creative Commons Attribution-NonCommercial 4.0 International license (CC BY-NC 4.0).

Author information and manuscript submission

For full author guidelines and online submission visit www.aboutscience.eu

EDITORIAL BOARD**Editor in Chief**

Winston Kuo
Prophet Genomics, San José - USA

Co-Editor

Luis Zerbini
International Centre for Genetic Engineering and Biotechnology (ICGEB), Cape Town - South Africa

Associate Editors

Roger Chammas - *Universidade de Sao Paulo, Sao Paulo, Brazil*
Alain Charest - *Harvard University, Boston, USA*
Clark Chen - *UC San Diego Medical Center, San Diego, USA*
Stefano Fais - *Istituto Superiore di Sanità (National Institute of Health), Rome, Italy*
Ionita Ghiran - *Beth Israel Deaconess Medical Center, Boston, USA*
Nancy Raab-Traub - *University of North Carolina, Chapel Hill, USA*
Lawrence Rajendran - *University of Zurich, Zurich, Switzerland*
John Sinden - *ReNeuron, Bridgend, UK*
Johan Skog - *Exosome Diagnostics, Cambridge, USA*
Alexander Vlassov - *Thermo Fisher Scientific, Austin, USA*
David T. Wong - *University of California Los Angeles, Los Angeles, USA*
Hang Yin - *University of Colorado Boulder, Boulder, USA*

Editorial Board

Angel Ayuso-Sacido - *Madrid, Spain*
Leonora Balaj - *Charlestown, USA*
Pauline Carnell-Morris - *Amesbury, UK*
Cesar Castro - *Boston, USA*
Chih Chen - *Hsinchu, China*
William Cho - *Hong Kong*
Pui-Wah Choi - *Hong Kong*
Emanuele Cocucci - *Columbus, USA*
Utkan Demirci - *Stanford, USA*
Dolores Di Vizio - *Los Angeles, USA*
Jiang He - *Charlottesville, USA*
Stefano Holdenrieder - *Munich, Germany*
Bo Huang - *Huazhong, China*
Takanori Ichiki - *Tokyo, Japan*
Alexander Ivanov - *Boston, USA*
Won Jong Rhee - *Incheon, South Korea*
Mehmet Kesimer - *Chapel Hill, USA*
Miroslaw Kornek - *Homburg, Germany*
Masahiko Kuroda - *Tokyo, Japan*
Heedoo Lee - *Changwon, South Korea*
Marcis Leja - *Riga, Latvia*
Sai-Kiang Lim - *Singapore, Singapore*
Aija Line - *Riga, Latvia*
Jan Lotvall - *Gothenburg, Sweden*
Todd Lowe - *Santa Cruz, USA*
Pierre-Yves Mantel - *Fribourg, Switzerland*
David G. Meckes - *Tallahassee, USA*
Andreas Moller - *Brisbane, Australia*
Fatemeh Momen-Heravi - *New York, USA*
Shannon Pendergrast - *Cambridge, USA*
Eva Rohde - *Salzburg, Austria*
Shivani Sharma - *Los Angeles, USA*
Kiyotaka Shiba - *Tokyo, Japan*
Yoshinobu Takakura - *Kyoto, Japan*
Yaoliang Tang - *Georgia, USA*
John Tigges - *Boston, USA*
Matt Trau - *Queensland, Australia*
Jody Vykoukal - *Houston, USA*
ShuQi Wang - *Hangzhou, China*
Gareth Willis - *Boston, USA*
Matthew J. Wood - *Oxford, UK*
Cynthia Yamamoto - *Irvine, USA*
Milis Yuana - *Utrecht, USA*
Huang-ge Zhang - *Louisville, USA*
Davide Zocco - *Siena, Italy*

ABOUTSCIENCE

Aboutscience Srl
Piazza Duca d'Aosta, 12 - 20124 Milano (Italy)

Disclaimer

The statements, opinions and data contained in this publication are solely those of the individual authors and contributors and do not reflect the opinion of the Editors or the Publisher. The Editors and the Publisher disclaim responsibility for any injury to persons or property resulting from any ideas or products referred to in the articles or advertisements. The use of registered names and trademarks in this publication does not imply, even in the absence of a specific statement, that such names are exempt from the relevant protective laws and regulations and therefore free for general use.

Editorial and production enquiries
jcb@aboutscience.eu

Supplements, reprints and commercial enquiries
Lucia Steele - email: lucia.steele@aboutscience.eu

Publication data
eISSN: 1849-4544
Continuous publication
Vol. 11 is published in 2022

- 1** Diagnostic utility of FGF-23 in mineral bone disorder during chronic kidney disease
Luisa Albanese, Gemma Caliendo, Giovanna D'Elia, Luana Passariello, Anna Maria Molinari, Claudio Napoli, Maria Teresa Vietri
- 5** MicroRNAs from urinary exosomes as alternative biomarkers in the differentiation of benign and malignant prostate diseases
Jonas Holdmann, Lukas Markert, Claudia Klinger, Michael Kaufmann, Karin Schork, Michael Turewicz, Martin Eisenacher, Stephan Degener, Nici M. Dreger, Stephan Roth, Andreas Savelsbergh
- 14** The role of microRNAs in COVID-19 with a focus on miR-200c
Hadi Sodagar, Shahriar Alipour, Sepideh Hasani, Shiva Gholizadeh-Ghaleh Aziz, Mohammad Hasan Khadem Ansari, Rahim Asghari
- 24** Assessment of background levels of autoantibodies as a prognostic marker for severe SARS-CoV-2 infection
Frank M. Sullivan, Agnes Tello, Petra Rauchhaus, Virginia Hernandez Santiago, Fergus Daly
- 28** Soluble IL-33 receptor predicts survival in acute kidney injury
Stefan Erfurt, Meike Hoffmeister, Stefanie Oess, Katharina Asmus, Susann Patschan, Oliver Ritter, Daniel Patschan
- 36** Characterization of extracellular vesicles isolated from different liquid biopsies of uveal melanoma patients
Carmen Luz Pessuti, Deise Fialho Costa, Kleber S. Ribeiro, Mohamed Abdouh, Thupten Tsering, Heloisa Nascimento, Alessandra G. Commodaro, Allexya Affonso Antunes Marcos, Ana Claudia Torrecilhas, Rubens N. Belfort, Rubens Belfort Jr, Julia Valdemarin Burnier
- 48** Effectiveness of periodontal intervention on the levels of N-terminal pro-brain natriuretic peptide in chronic periodontitis patients
Ibrahim Fazal, Bhavya Shetty, Umesh Yadalam, Safiya Fatima Khan, Manjusha Nambiar
- 57** Diagnostic impact of CEA and CA 15-3 on monitoring chemotherapy of breast cancer patients
Chemotherapy monitoring by serum markers
Diya Hasan

Diagnostic utility of FGF-23 in mineral bone disorder during chronic kidney disease

Luisa Albanese¹, Gemma Caliendo¹, Giovanna D'Elia¹, Luana Passariello¹, Anna Maria Molinari^{1,2}, Claudio Napoli^{3,4}, Maria Teresa Vietri^{1,2}

¹Unity of Clinical and Molecular Pathology, AOU, University of Campania "Luigi Vanvitelli", Naples - Italy

²Department of Precision Medicine, University of Campania "Luigi Vanvitelli", Naples - Italy

³Department of Advanced Medical and Surgical Sciences (DAMSS), University of Campania "Luigi Vanvitelli", Naples - Italy

⁴Clinical Department of Internal Medicine and Specialistic Units, AOU, University of Campania "Luigi Vanvitelli", Naples - Italy

ABSTRACT

Our data confirm that intact fibroblast growth factor 23 (iFGF-23) concentration is increased in patients with chronic kidney disease (CKD) and that it increases with disease progression (stages I-V). Therefore, iFGF-23 could be considered an early biomarker in the course of chronic kidney disease-mineral bone disorder (CKD-MBD), which has several aspects that make it potentially useful in clinical practice. The availability of an automated method for iFGF-23 assay may represent an added value in the management of the patient with CKD-MBD already from the early stages of the disease, before the increase of the routinely used laboratory parameters, 1-84 parathyroid hormone (PTH) and 25-OH-vitamin D (25-OH-vitD), which occur in more advanced stages of the disease.

Keywords: Bone density, CKD, FGF-23

Introduction

The term "chronic kidney disease-mineral bone disorder" (CKD-MBD) is defined as a systemic disorder of bone and mineral metabolism due to CKD, which occurs in the presence of one or a combination of the following conditions: alterations in laboratory parameters (calcemia, phosphoremia, parathormone, vitamin D); abnormalities in turnover, mineralization, volume, linear growth, or bone strength; vascular or soft tissue calcifications secondary to CKD (1). The three alterations present in CKD-MBD have different prevalence in patients; that is, metabolic alterations are the first to appear followed by bone alterations and vascular calcifications.

Recently, molecules that are produced by the bone and kidney have been identified. These paths play a pivotal role in the mechanisms of bone and cardiovascular alterations during CKD-MBD. Fibroblast growth factor 23 (FGF-23)/Klotho axis, in addition to the parathyroid hormone (PTH)/vitamin D

axis, has a key role in the pathophysiology of CKD-MBD, as it is involved in calcium, phosphorus, and calcitriol homeostasis, as well as in mechanisms of cellular aging (2).

FGF-23 is a glycoprotein of 252 amino acids (32 kDa), encoded by the homonymous gene located on chromosome 12. FGF-23 exerts its biological activity through interaction with one of four specific receptors (FGFR 1-4) by a paracrine mechanism (3). FGF-23 is metabolized to its inactive C-terminal and N-terminal fragments and intact FGF-23 (iFGF-23) represents its biologically active form (4). At the cellular level, FGF-23 acts by binding to an FGF-23-FGFR complex with Klotho. Although the receptors are ubiquitously expressed, Klotho expression is restricted primarily at the level of renal tubules, parathyroid glands, and choroid plexus, determining the tissue specificity of FGF-23 (2,5).

FGF-23 acts at the level of renal tubules by reducing phosphorus reabsorption and inhibiting the expression of the sodium/phosphate cotransporter (Npt2a and Npt2c) on the cell membrane in the proximal tubule. It also reduces the conversion of 25-OH-vitamin D (25-OH-vitD) to its active form 1,25(OH) by inhibiting the expression of 1 α -hydroxylase and increases its degradation by increasing the activity of 24-hydroxylase.

In CKD there is a progressive increase in FGF-23 levels associated with reduced renal function. Several factors may contribute to this phenomenon, such as hyperphosphatemia, hypercalcemia, secondary hyperparathyroidism, and Klotho deficiency (6). Serum levels of FGF-23 increase in the early stages of CKD as a compensatory mechanism to prevent the onset of hyperphosphatemia and secondary

Received: August 4, 2021

Accepted: December 4, 2021

Published online: January 8, 2022

Corresponding author:

Maria Teresa Vietri
Department of Precision Medicine
University of Campania "Luigi Vanvitelli"
Via L. De Crecchio, 7
80138 Naples - Italy
mariateresa.vietri@unicampania.it



hyperparathyroidism (7). Even transient increase in phosphoremia, in the early stages of CKD, stimulates FGF-23 production, which then tends to normalize phosphoremia but at the same time causes a reduction in 1,25(OH)vitD resulting both in increased parathormone synthesis and secretion (8,9).

Extrarenal manifestations of FGF-23 in CKD can be Klotho-dependent and/or Klotho-independent, receptor action of FGF-23 that does not require the presence of the membrane coreceptor. Klotho-independent effects of FGF-23 in CKD are expressed at the cardiac level, with hypertrophy of left ventricular myocytes, and at the hepatic level, with increased synthesis of proinflammatory cytokines (10).

During renal failure, effects of both Klotho-dependent and -independent FGF-23 are instead expressed at the level of the central nervous system, the immune system, and the vascular system.

Enzyme immunoassays, used until now to assay FGF-23, recognized both the C-terminal portion and the intact form of FGF-23. The current availability of a new automated chemiluminescence immunoassay (CLIA) for the determination of the intact molecule only allows overcoming these methodological limitations, favoring a routine use of the FGF-23 assay in clinical practice, in association with parameters already used routinely such as parathormone and vitamin D (11,12).

The aim of the present descriptive study was to assess the circulating levels of iFGF-23 in patients with CKD at various stages in specialist follow-up with the Liaison iFGF-23 assay.

Methods

Sixty-three patients (35 males and 28 females, aged 20-80 years) diagnosed with CKD-MBD were selected; all underwent renal transplantation. The patients were hospitalized at the Teaching Hospital of the University of Campania "Luigi Vanvitelli" of Naples (Italy) and signed an informed consent at the admission time.

Patients aged <18 years, with inflammatory bowel disease, acute infectious or inflammatory disease, or advanced neoplasia were excluded from the study.

Circulating levels of iFGF-23, 1-84 PTH, 25-OH-vitD, creatinine, and albumin were assayed for each patient.

Blood samples were collected at 8 am from fasting patients, centrifuged, and stored at -20°C until assayed.

1-84 PTH, 25-OH-vitD, and iFGF-23 were assayed using chemoluminescence (CLIA) methods on the LIAISON XL platform (DiaSorin spa, Italy).

Albumin and creatinine were assayed by the colorimetric method (Architect Abbott Diagnostics).

Reference values for 1-84 PTH ranged from 4.6 to 58.1 pg/mL, whereas for 25-OH-vitD it was <10 ng/mL (deficiency), 10-30 ng/mL (insufficiency), 30-100 ng/mL (sufficiency).

The reference range for iFGF-23 was 25.1-95.5 pg/mL; for creatinine it was 0.72-1.25 mg/dL for males and 0.57-1.11 mg/dL for females; and for albumin it was 3.5-5.2 g/dL.

Glomerular filtrate was estimated using clearance of creatinine according to the eGFR-EPI equation for the classification of patients at a given stage of CKD. Thus, of the 63 patients with eGFR between 16 and 104 mL/min/1.73 m²,

10 had stage I, 19 stage II, 22 stage III, 7 stage IV, and 5 stage V CKD.

Statistical analysis

Data are reported as means ± standard deviation (SD), unless otherwise stated. Comparison between the groups was performed using χ^2 test. Significance was assumed for p-values less than 0.05.

Results

About 39.7% (25/63) of patients with CKD had iFGF-23 levels above normal (>95.5 pg/mL), 14.3% (9/63) of patients had 1-84 PTH values increased beyond the normal range (>58.1 pg/mL), and 7.9% (5/63) had insufficient 25-OH-vitD values (<10 ng/mL).

Table I shows the number of patients distributed in the different stages of CKD with iFGF-23 and 1-84 PTH values above the cutoff and with 25-OH-vitD deficiency.

TABLE I - Percentage of patients with increased values of iFGF-23 and 1-84 PTH and 25-OH-vitD deficiency divided into the five stages of CKD

Patients with CKD (total 63)	iFGF-23 (>95.5 pg/mL)	1-84 PTH (>58.1 pg/mL)	25-OH-vitD (<10 ng/mL)
Stage I (n = 10)	2/10 (20%)	–	–
Stage II (n = 19)	5/19 (26.3%)	2/19 (10.5%)	–
Stage III (n = 22)	9/22 (40.9%)	4/22 (18.2%)	2/22 (9%)
Stage IV (n = 7)	6/7 (85.7%)	1/7 (14.3%)	2/7 (28.6%)
Stage V (n = 5)	3/5 (60%)	2/5 (40%)	1/5 (20%)

CKD = chronic kidney disease; iFGF-23 = intact fibroblast growth factor 23; PTH = parathyroid hormone; 25-OH-vitD = 25-OH-vitamin D.

Specifically, 20% of stage I, 26.3% of stage II, 40.9% of stage III, 85.7% of stage IV, and 60% of stage V CKD patients had iFGF-23 levels above the cutoff. No statistically significant differences are found among the CKD stages ($p < 0.05$).

Values of 1-84 PTH above the normal range were observed in 10.5% of stage II, 18.2% of stage III, and 14.3% and 40% of stage IV and stage V CKD patients, respectively. For stage I CKD patients, increased values of 1-84 PTH were not found.

In addition, insufficient 25-OH-vitD values were found in 9%, 28.6%, and 20% of patients at CKD stages III, IV, and V, respectively.

Table II shows the percentages of patients with increased serum values of iFGF-23, 1-84 PTH, and 25-OH-vitD deficiency divided according to the number of years since transplantation (<10 years, 11-20 years, and >20 years).

Thirty-two of the 63 patients had received transplantation for <10 years, 20 for 11-20 years, and 11 for >21 years.

Values of iFGF-23 beyond the normal range were found in 43.7% of organ transplant patients received less than 10 years, 35% received between 11 and 20 years, and 36% received >20 years.



TABLE II - Percentage of patients with elevated iFGF-23 and 1-84 PTH levels and 25-OH-vitD deficiency according to years since transplantation

Renal Transplantation	iFGF-23 (>95.5 pg/mL)	1-84 PTH (>58.1 pg/mL)	25-OH-vitD (<10 ng/mL)
<10 years (n = 32)	14/32 (43.7%)	6/32 (18.7%)	3/32 (9.4%)
11-20 years (n = 20)	7/20 (35%)	2/20 (10%)	2/20 (10%)
>20 years (n = 11)	4/11 (36%)	1/11 (9.1%)	–

iFGF-23 = intact fibroblast growth factor 23; PTH = parathyroid hormone; 25-OH-vitD = 25-OH-vitamin D.

Increased values of 1-84 PTH have been detected in 18.7% of transplant patients received less than 10 years, 10% of transplant patients received 11-20 years, and 9.1% of transplant patients received more than 20 years.

A 25-OH-vitD deficiency existed in 9.4% of patients who had received transplantation for less than 10 years and 10% of patients who had received transplantation for more than 11 years. No deficient 25-OH-vitD values were found for patients who had been transplanted for more than 20 years.

Discussion

Increased serum FGF-23 levels from the earliest stages of CKD represent the first indicator of alterations in mineral metabolism. Increased levels of FGF-23, 1-84 PTH, and phosphorus with a concomitant reduction in serum levels of active vitamin D are closely related to reduced glomerular filtration rate (GFR).

The increase in FGF-23 concentration may be caused by the abnormal stimulation of its secretion exerted by substances released from the damaged renal parenchyma or by the effects exerted by the uremic state on bone mineralization processes. Other shreds of evidence, instead, suggest the crucial role that phosphorus plays in the uncontrolled stimulation of FGF-23 secretion (3). Limitation of our study is the distribution of samples by disease stage. Out of 63 enrolled patients, 41 had CKD stages II-III.

Despite this limitation, our results show increased FGF-23 levels in a high percentage of patients with CKD, which is in line with what has been recently reported (12). Moreover, our data show that the percentage of patients with iFGF-23 values above reference limits increases with disease progression (stages I-V).

In the early stages of CKD, increasing iFGF-23 could represent a compensatory mechanism to prevent the establishment of hyperphosphatemia and secondary hyperparathyroidism. Starting from stage IV, with a further reduction of residual renal function, Klotho levels are also reduced, resulting in peripheral resistance due to the FGF-23 action and further increase in the iFGF-23 levels.

Renal transplantation represents the therapy of choice in CKD, allowing, compared to dialysis, a better quality of life and increased survival (13-15).

Indeed, it is reported that after renal transplantation the concentration of FGF-23 decreases rapidly. Here, we noticed a correlation between plasma iFGF-23 concentration and years

since transplantation. Indeed, iFGF-23 values above the normal limit were found in 43.7% of patients transplanted less than 10 years, in 35% of patients transplanted 10-20 years, and in 36% of patients who had received transplantation for more than 20 years.

In addition, increased levels of 1-84 PTH have been observed in 18.7% of patients after renal transplantation less than 10 years while 10% of patients with transplantation for 10-20 years, and 9% of patients with transplantation for more than 20 years. These data indicate, as has been pointed out, that after renal transplantation, persistent hyperparathyroidism is associated with elevated iFGF-23 levels, which may occur with inhibition of the synthesis of the active form of vitamin D, resulting in the persistence of elevated levels of 1-84 PTH.

The persistence of high levels of iFGF-23 after renal transplantation can be interpreted as a mechanism of compensation and adaptation to the new metabolic balance created in the early posttransplant phases. Factors that may favor the persistence of high levels of FGF-23 after transplantation may include immunosuppressive therapy: corticosteroids, calcineurin inhibitors, and mammalian target of rapamycin (mTOR) inhibitors, which stimulate the production of iFGF-23 (16).

Conclusions

The availability of an automated method for iFGF-23 assay may represent an added value in the management of the patient with CKD-MBD already from the early stages of the disease, before the increase of the routinely used laboratory parameters, 1-84 PTH and 25-OH-vitD, which occur in more advanced stages of the disease.

Disclosures

Conflict of interest: The authors declare no conflict of interest. Financial support: This research received no specific grant from any funding agency in the public, commercial, or not-for-profit sectors. Authors contribution: all authors contributed equally to this manuscript.

References

1. Moe S, Drüeke T, Cunningham J, et al; Kidney Disease: Improving Global Outcomes (KDIGO). Definition, evaluation, and classification of renal osteodystrophy: a position statement from Kidney Disease: Improving Global Outcomes (KDIGO). *Kidney Int.* 2006;69(11):1945-1953. [CrossRef PubMed](#)
2. Hu MC, Shiizaki K, Kuro-o M, Moe OW. Fibroblast growth factor 23 and Klotho: physiology and pathophysiology of an endocrine network of mineral metabolism. *Annu Rev Physiol.* 2013;75(1):503-533. [CrossRef PubMed](#)
3. Ho BB, Bergwitz C. FGF23 signalling and physiology. *J Mol Endocrinol.* 2021;66(2):R23-R32. [CrossRef PubMed](#)
4. Shimada T, Urakawa I, Isakova T, et al. Circulating fibroblast growth factor 23 in patients with end-stage renal disease treated by peritoneal dialysis is intact and biologically active. *J Clin Endocrinol Metab.* 2010;95(2):578-585. [CrossRef PubMed](#)
5. Angelin B, Larsson TE, Rudling M. Circulating fibroblast growth factors as metabolic regulators—a critical appraisal. *Cell Metab.* 2012;16(6):693-705. [CrossRef PubMed](#)



6. Wolf M. Update on fibroblast growth factor 23 in chronic kidney disease. *Kidney Int.* 2012;82(7):737-747. [CrossRef PubMed](#)
7. Bergwitz C, Jüppner H. Regulation of phosphate homeostasis by PTH, vitamin D, and FGF23. *Annu Rev Med.* 2010;61(1):91-104. [CrossRef PubMed](#)
8. Isakova T, Wahl P, Vargas GS, et al. Fibroblast growth factor 23 is elevated before parathyroid hormone and phosphate in chronic kidney disease. *Kidney Int.* 2011;79(12):1370-1378. [CrossRef PubMed](#)
9. Isakova T, Xie H, Yang W, et al; Chronic Renal Insufficiency Cohort (CRIC) Study Group. Fibroblast growth factor 23 and risks of mortality and end-stage renal disease in patients with chronic kidney disease. *JAMA.* 2011;305(23):2432-2439. [CrossRef PubMed](#)
10. Takashi Y, Fukumoto S. FGF23 beyond phosphotropic hormone. *Trends Endocrinol Metab.* 2018;29(11):755-767. [CrossRef PubMed](#)
11. Shimizu Y, Fukumoto S, Fujita T. Evaluation of a new automated chemiluminescence immunoassay for FGF23. *J Bone Miner Metab.* 2012;30(2):217-221. [CrossRef PubMed](#)
12. Souberbielle JC, Prié D, Piketty ML, et al. Evaluation of a new fully automated assay for plasma intact FGF23. *Calcif Tissue Int.* 2017;101(5):510-518. [CrossRef PubMed](#)
13. Napoli C, Casamassimi A, Crudele V, Infante T, Abbondanza C. Kidney and heart interactions during cardiorenal syndrome: a molecular and clinical pathogenic framework. *Future Cardiol.* 2011;7(4):485-497. [CrossRef PubMed](#)
14. Vasco M, Benincasa G, Fiorito C, et al. Clinical epigenetics and acute/chronic rejection in solid organ transplantation: an update. *Transplant Rev (Orlando).* 2021;35(2):100609. [CrossRef PubMed](#)
15. Bellastella G, Maiorino MI, De Bellis A et al. Serum but not salivary cortisol levels are influenced by daily glycemic oscillations in type 2 diabetes. *Endocrine.* 2016;53(1):220-6. [CrossRef PubMed](#)
16. Economidou D, Dovas S, Papagianni A, Pateinakis P, Memmos D. FGF-23 levels before and after renal transplantation. *J Transplant.* 2009;2009:379082. [CrossRef PubMed](#)



MicroRNAs from urinary exosomes as alternative biomarkers in the differentiation of benign and malignant prostate diseases

Jonas Holdmann^{1*}, Lukas Markert^{1*}, Claudia Klinger^{1,2}, Michael Kaufmann^{1,2}, Karin Schork^{3,4}, Michael Turewicz^{3,4}, Martin Eisenacher^{3,4}, Stephan Degener⁵, Nici M. Dreger⁵, Stephan Roth⁵, Andreas Savelsbergh^{1,2}

¹Chair for Biochemistry and Molecular Medicine, Division of Functional Genomics, Witten/Herdecke University, Witten - Germany

²Center for Biomedical Education and Research (ZBAF), Witten/Herdecke University, Witten - Germany

³Medizinisches Proteom-Center, Ruhr-University Bochum, Bochum - Germany

⁴Center for Protein Diagnostics (PRODI), Medical Proteome Analysis, Ruhr-University, Bochum - Germany

⁵Department of Urology, Helios University Hospital Wuppertal, Center for Clinical and Translational Research, Witten/Herdecke University, Wuppertal - Germany

*Contributed equally

ABSTRACT

Introduction: Prostate cancer (PCa) is the second most frequently diagnosed cancer and the fifth most cancer-related cause of death worldwide. Various tools are used in the diagnosis of PCa, such as the Prostate-Specific Antigen (PSA) value or digital rectal examination. A final differentiation from benign prostate diseases such as benign prostatic hyperplasia (BPH) can often only be made by a transrectal prostate biopsy. This procedure carries post-procedural complications for the patients and may lead to hospitalization.

Urinary exosomes contain unique components, such as microRNAs (miRNAs) with information about their original tissue. As miRNAs appear to play a role in the development of PCa, they might be useful to develop procedures that could potentially make transrectal biopsies avoidable in certain situations.

Methods: The current study aimed to investigate whether miRNAs from urinary exosomes can be used to differentiate PCa from BPH. For this purpose, urine samples from 28 patients with PCa and 25 patients with BPH were collected and analysed using next-generation sequencing to obtain expression profiles.

Results and conclusion: The two miRNAs hsa-miR-532-3p and hsa-miR-6749-5p showed a significant differential expression within the group of patients with PCa in a training subset of the data containing 32 patients. They were further validated on the independent test data subset containing 20 patients. Additionally, a machine learning algorithm was used to generate a miRNA pattern to distinguish the two disease entities. Both approaches seem to be suitable for the search of alternative diagnostic tools for the differentiation of benign and malignant prostate diseases.

Keywords: Biomarker, Extracellular vesicles, Liquid biopsy, microRNA, Prostate cancer, Urine

Introduction

The prostate is an accessory gland, located below the bladder. It consists of three different zones that are clinically and histologically relevant: the peripheral zone makes up the

largest part, the central zone surrounds the ejaculatory ducts and the transition zone encircles the urethra (1).

With increasing age, the prostate grows, causing an enlargement of the transition zone, which can lead to a benign prostatic hyperplasia (BPH) and obstruction (BPO). About 50% to 75% of men among the age of 50, and more than 80% of men over 70 years of age are affected by BPO (2,3). The symptoms caused by this vary and may also resemble those of prostate cancer (PCa), such as incomplete bladder emptying, a decreased urinary stream, nocturia or infections of the urinary tract. However, prognosis and outcome differ substantially.

PCa is the second-most diagnosed cancer in the world. Among cancer-related death in men, it is the fifth leading cause with a mortality of 7.6 per 100,000 worldwide (4,5).

The distinction between the two entities is made using different diagnostic parameters. A digital rectal examination

Received: July 31, 2021

Accepted: January 12, 2022

Published online: February 10, 2022

Corresponding author:

Jonas Holdmann

Chair for Biochemistry and Molecular Medicine,

Division of Functional Genomics,

Witten/Herdecke University, Germany

Stockumer Straße 10, 58453 Witten - Germany

Jonas.holdmann@uni-wh.de



and the determination of the PSA value are carried out as screening tools. In case of suspicion, further procedures such as multiparametric magnetic resonance imaging (MRI) and targeted and systematic biopsy are indicated (6). So far, the diagnostic gold standard is transrectal or transperineal biopsy that carries a certain risk of post-procedural complications (7), leading to an ongoing need for other non-invasively available and effective diagnostic tools (8).

MicroRNAs (miRNAs) from urinary exosomes might have the potential to serve as early biomarkers. Accordingly, this study investigates its use to differentiate patients with BPH and those with PCa.

Exosomes are extracellular vesicles (EVs) secreted by almost all cell types. They can be isolated from urine, an easily and non-invasively available body fluid. EVs are produced in the endosomal system and actively secreted. As they contain different molecular components, such as proteins, mRNAs and miRNAs of their respective origin cell (9,10), several studies propose their potential as biomarkers in early stages of disease (11).

MiRNAs are single-stranded, non-coding RNA molecules consisting of ~22 nucleotides. More than 60% of human protein-coding genes are targeted by miRNAs (12). Thus, miRNAs are implicated in a variety of biological processes including cell differentiation, development, proliferation, stress response and apoptosis (13). Various studies investigated the connection between miRNA expression profiles and certain types of cancer. An association between chronic lymphatic leukaemia and miRNA deregulation was shown for the first time in 2007 (14). The stability of miRNAs from solid tumour tissues was proven in serum and plasma samples (15), as well as miRNAs in urine and urinary exosomes (16), supporting their potential to serve as ideal biomarker. Recently, the high potential of small RNAs from urine to distinguish benign and malignant prostate diseases was shown (17).

It should be emphasized that this study compares the miRNA expression patterns of two cohorts of diseased patients who may suffer from similar symptoms (BPH or PCa). Since the differentiation of BPH from PCa represents a certain difficulty in clinical practice, it can often only be definitively determined with a transrectal biopsy. The vision is to establish a biomarker from a potentially easily available source, such as urine, as an alternative diagnostic to avoid the invasive transrectal biopsy.

Materials and methods

Ethical approval

The study was approved by the ethics committee of the University of Witten/Herdecke in 3/2014 (application number: 07/2014). It was planned as a monocentric, comparative study. A following ethics application to investigate the same patient data and samples with an alternative method was approved in 2018.

Sample collection

The recruitment of 85 patients was realized from 03/2014 until 02/2015 at the Helios University Hospital Wuppertal,

Department of Urology. Included were patients who underwent prostate biopsy due to elevated PSA levels or who were admitted for surgical BPO treatment (holmium laser enucleation of the prostate).

For this study, a subset of PCa samples (n = 28) and BPH samples (n = 25) was analysed. The number of samples was limited by the amount of urine available, at least 8 mL, as 4 mL was used for each assay run. A previous sample size determination was not performed due to lack of comparative data with respect to the method used here.

Exclusion criteria were infectious diseases (HIV, hepatitis, tuberculosis), received antiandrogen therapy (due to potential effects on the PCa), radiotherapy of the little pelvis and the inability to agree to give informed consent to participate in this study.

Isolation of RNA from urinary exosomes

Urinary exosomes were isolated using the Norgen Urine Exosome RNA Isolation Kit (#47200, Norgen Biotek Corporation). While the kit allows the isolation of exosomal RNA from 1 to 10 mL urine samples, 4 mL starting volume was used in this study. The isolation was performed as specified in the related protocol (Norgen Biotek Corporation, 2018). The exosomal miRNA input for the library preparation was measured using the Qubit Fluorimeter 3.0 (Invitrogen Life Technologies Corp.) and the microRNA Assay Kit (#Q32881, Thermo Fisher Scientific).

Library preparation and next-generation sequencing

Library preparation was performed using the QIAseq miRNA Library Kit (cat no: 331505, Qiagen) following the QIAseq miRNA Library Kit Handbook (Qiagen, 2018). Implemented was a prolonged three-ligation step to 18 hours, due to previous experiments.

The kit operates with unique molecular identifiers (UMIs), unique sequences that are integrated into the reverse transcription. Consequently, each miRNA is assigned to a unique sequence, enabling the exact quantification of input miRNA by next-generation sequencing (NGS). This approach reduces the usual amplification bias during polymerase chain reaction.

Quality and quantity control of the libraries was conducted using an automated electrophoresis (Agilent 2100 Bioanalyzer, DNA 1000 Kit), following the corresponding protocol (Agilent Technologies, 2016). NGS was carried out using an illumina sequencing platform (NextSeq 500) with a single read length of 75 bp and around 400 million reads per run.

Statistical and bioinformatic analysis

For raw data analysis the sequencing files were uploaded to the GeneGlobe Data Analysis Center and processed using the QIAseq miRNA Primary Quantification software (Qiagen, 2018).

A downstream analysis was performed using R 3.5.3 (18) and RStudio 1.2.1335 and R-scripts created by the de.NBI service centre BioInfra.Prot (19). The data table was read and



imported with R package openxlsx 4.1.0.1 (20). Two steps of filtering were conducted for cleaning of the relevant data. From the R package caret 6.0-84 (21) the nearZeroVar function was used, removing 100 miRNAs due to their low variance and therefore no ability to separate the groups. Additionally, miRNAs with more than three zero counts in each group were removed, 115 miRNAs remained. Normalization and statistical testing was performed using the R package DESeq2 1.22.2 (22). Considering multiple testing and a potentially increased type I error rate, an adjusted p-value was calculated using the Benjamini-Hochberg procedure.

One sample was removed due to an insufficient variance resulting from a large proportion of zero counts. The 52 remaining samples were randomly divided into a training set (PCa = 17 samples, BPH = 15 samples) and a test set (PCa and BPH = 10 samples each) to validate the results.

Graphics such as the volcano plot and Principal Component Analysis (PCA) were created with R package ggplot2 3.1.1 (23) and aligned with cowplot 0.9.4 (24); the volcano plots were labelled with ggrepel 0.8.1 (25). The performance of potential biomarker candidates to discriminate the two groups was additionally visualized with the help of receiver operating characteristic (ROC) curve, conducted with R package pROC 1.15.0 (26).

Data analysis to find a miRNA panel was carried out using a previously published machine learning algorithm (17). Briefly, on the training dataset a random forest (27) model with 100,000 trees was trained using the R-package randomForest (28) to acquire a random forest-specific variable importance measure (mean decrease of the Gini index). For panel sizes m between 1 and 50, the m variables with the highest variable importance in the model were chosen as a panel. For each of these 50 sets of variables, the random forest was retrained on the training dataset. To evaluate all 50 specific models (one for each panel size m) the samples of test dataset were classified. ROC curves were drawn and the panel with the best area under the curve (AUC) was chosen from the 50 sets of variables. For comparison, an additional ROC curve was drawn to show the performance of the chosen panel on the training dataset (by splitting it 1,000 times randomly into a training and test subset with the ratio 2:1). In a heat map (z-scored values) the miRNAs from the chosen panel were visualized with dendrograms from hierarchical clustering.

Results

Demographic and clinicopathological characteristics

A detailed list of demographic and clinicopathological characteristics of the participants is displayed (Tab. I). The two cohorts of patients with PCa and BPH demonstrate a nearly even distribution, regarding patient age, PSA level, fPSA level and PSA ratio. Within the patient cohort with BPH, the increased prostate volume measured via transrectal ultrasound (TRUS) and the bacterial positive urinary status could be attributed to the urethral obstruction, the leading symptom of the underlying disease. In summary, two highly matching and therefore comparable patient cohorts were evaluated in this study.

Normalization

The dataset was normalized as described above, resulting in an apparently higher comparable dataset for further analysis (Fig. 1).

Comparison of expression profiles

The statistical analysis resulted in two miRNAs with a significant overexpression within the group of PCa samples. Both have a high log₂-fold-change (>1.65), displaying their differential expression compared to other biomarker candidates (Tab. II).

Compared to the group of BPH, five miRNAs are upregulated with a log₂-fold-change >1 among the PCa group, while

Table I - Demographic and clinicopathological characteristics of study participants

Characteristics	Patients with BPH	Patients with PCa
Number (n)	25	27
Age in years (median)	68	70
PSA in ng/mL (median)	6.89	8.34
fPSA in ng/mL (median)	1.43	1.095
PSA ratio (median)	0.18	0.165
Prostate volume in mL (median)	50	38.5
Urinary status: bacterial positive	48% (n = 12)	14.8% (n = 4)

Table II - Differentially expressed exosomal miRNAs

miRNA	Log ₂ -Fold-Change	p-value	adjusted p-value	AUC (Test Dataset)
hsa-miR-6749-5p	2.05598389	0.00053395	0.03070213	0.678
hsa-miR-532-3p	1.6532989	6.0461E-05	0.00695299	0.644
hsa-miR-6756-3p	1.40729735	0.00169959	0.06515094	0.544
hsa-miR-3960	-1.4405426	0.00877074	0.16810583	0.589
hsa-miR-363-3p	-1.0276721	0.00680747	0.16167405	0.7

Adjusted p-values <0.05 are marked in bold, corresponding to a significance niveau of 5%. Area under the curve (AUC) values were calculated on the test dataset, shown in the last column. Subsequent over- and under-expressed miRNAs are also displayed (complete data are available at the following data repository: [Online](#))

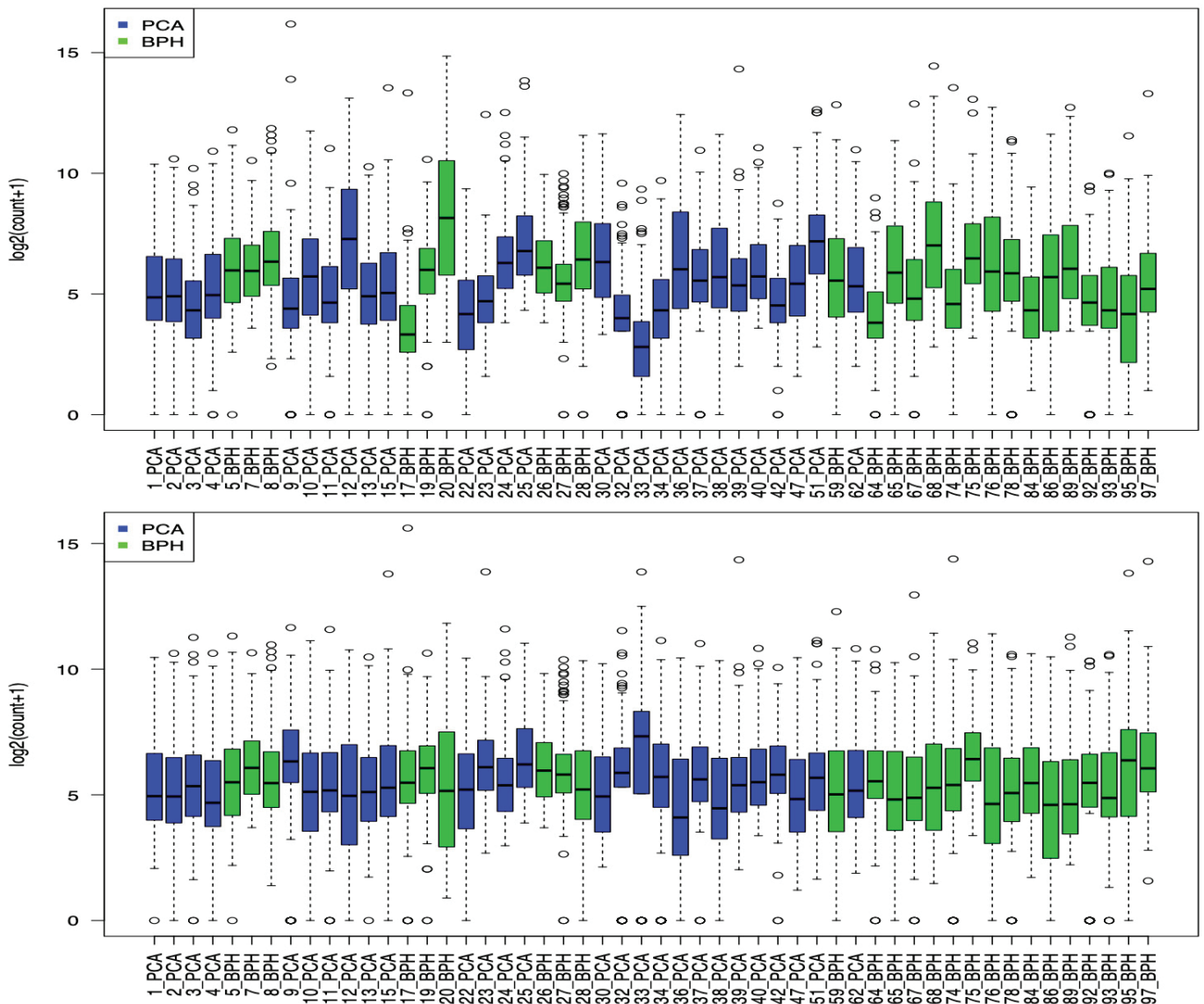


Fig. 1 - Distribution of exosomal miRNAs. Before (top) and after (bottom) normalization

two of them meet the criterion for the adjusted p-value (<0.05). The results of the analysis are visualized in a volcano plot (Fig. 2).

Due to its upregulation with a \log_2 -fold-change of ~ 1.65 in urinary exosomes in patients with PCa, hsa-miR-532-3p is considered as a novel biomarker in the differentiation of PCa and BPH.

According to miRNA database (miRBase), hsa-mir-532-3p was found in 139 experiments (29). The exact understanding of its biological function in cancer genesis is an ongoing research process, in which hsa-mir-532-3p is mainly described as a putative tumour suppressing miRNA. For example, it directly regulates the expression of the water channel protein aquaporin 9 (AQP9), which is significantly associated with poor prognosis in renal cell carcinoma (30). A decreased level of intracellular hsa-miR-523-3p is

associated with metastatic progression in hepatocellular cancer, due to its direct regulation of the oncogenic kinase family member C1 (KIFC1) (31). Moreover, a decreased level of intracellular hsa-miR-532-3p in colorectal cancer promotes cell growth and metastasis. It directly regulates E26 oncogene homolog 1 (ETS1) and transglutaminase 2 (TGM2), which are associated with cell proliferation via the Wnt/ β -catenin pathway. Interestingly, it also shows potential as an in vitro chemotherapy sensitizer in colorectal cancer (32). In non-small cell lung cancer, hsa-miR-532-3p regulates the forkhead box P3 (FOXP3) and thereby inhibits proliferation and metastasis (33). It must be noted that in terms of cancer research, the understanding of one dysregulated miRNA affecting a specific target mRNA is limited until further understanding of other miRNAs affecting the same mRNA is available (34).

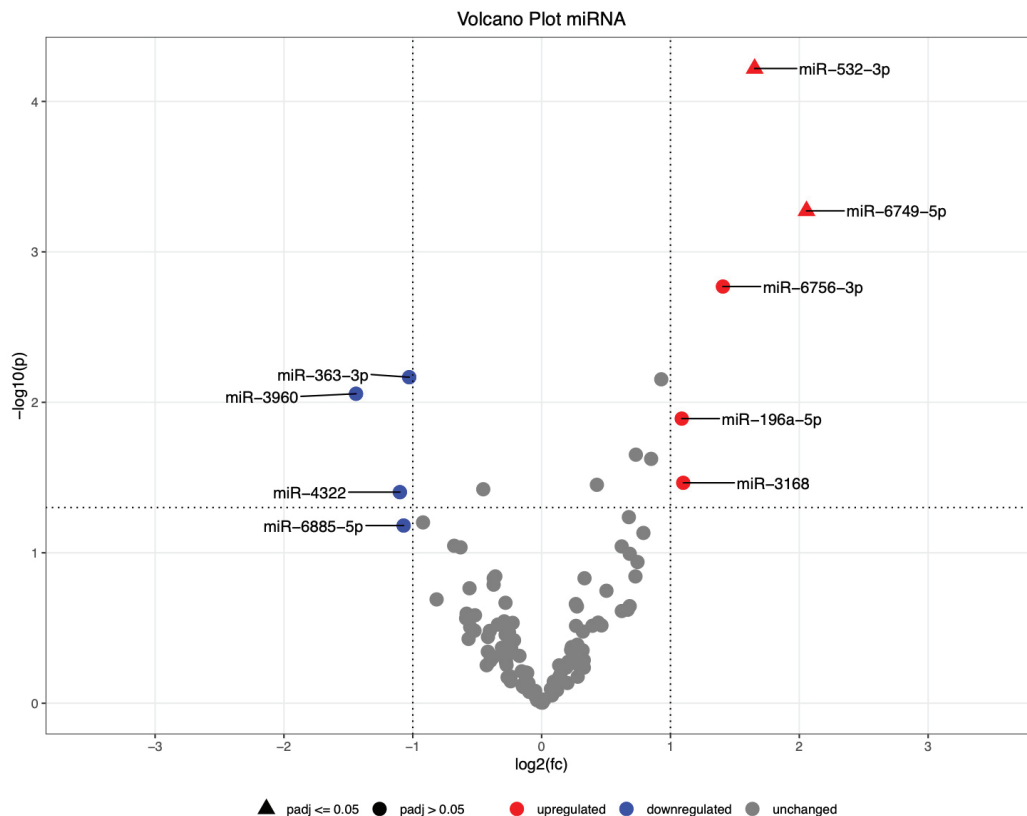


Fig. 2 - Volcano plot of the comparison of PCa vs. BPH. Fold changes ($\log_2(fc)$) are displayed on the x-axis, the y-axis shows the t-statistic calculated as the negative decimal logarithm of the p-value ($-\log_{10}(p)$). Thresholds are highlighted with dotted lines presenting the promising miRNAs in the upper left and upper right corners.

A rather new potential biomarker is hsa-miR-6749-5p. It was found in 16 experiments (29), for instance, it was differently expressed in serum of patients with breast cancer (35). Moreover, it was significantly upregulated in serum of patients with nasopharyngeal cancer (36). In the current study, hsa-miR-6749-5p was significantly upregulated with a \log_2 -fold-change of ~ 2.0 within the group of patients with PCa. The validation on the test set shows a diagnostic test accuracy of 80% specificity and 66.7% sensitivity. Among the compared data, hsa-miR-6749-5p has the highest fold change and therefore might be an interesting new biomarker in the differentiation of PCa and BPH.

Both miRNAs, especially hsa-miR-532-3p, seem to play a role in the genesis of different types of cancer. It should be considered that the present study only found a correlation of two upregulated miRNAs in urinary exosomes in patients with PCa. Conclusions about the causality of this upregulation cannot be drawn as the dysregulated miRNAs can either be the cause or the effect of cancer development. As shown in two further studies, hsa-miR-532 is presented once upregulated and once downregulated as a potential biomarker. In serum of patients with breast cancer, it was significantly upregulated as a part of the miR-532-502 cluster (37), whereas it was found significantly downregulated in urine supernatant of patients with bladder cancer (38).

Considering the found candidates, it is not known if those are prostate-specific miRNAs, as the prostate gland

can be grouped with salivary glands, seminal vesicles and the lactating breast, regarding their miRNA expression profiles (39) and no prostate-specific miRNAs are described so far. However, further experiments need to proof their reliability and enhance the understanding of its biological function, such as target genes and signalling pathways in the human body.

Validation

The two significant differentially expressed miRNAs (hsa-miR-6749-5p, hsa-miR-532-3p) were validated, using the remaining 10 samples of each group (BPH/PCa), which were not used for the selection (i.e. the test set). Specificity and sensitivity were determined and visualized in ROC curves (Fig. 3). The calculated AUCs show that the miRNAs do not reach the set limit of 0.7, thereby the two groups cannot be finally distinguished.

Panel calculation

The panel calculation resulted in a panel of eight miRNAs:

hsa-miR-4322	hsa-miR-4532	hsa-miR-532-3p	hsa-miR-1307-3p
hsa-miR-3656	hsa-miR-196a-5p	hsa-miR-6749-5p	hsa-miR-92a-3p



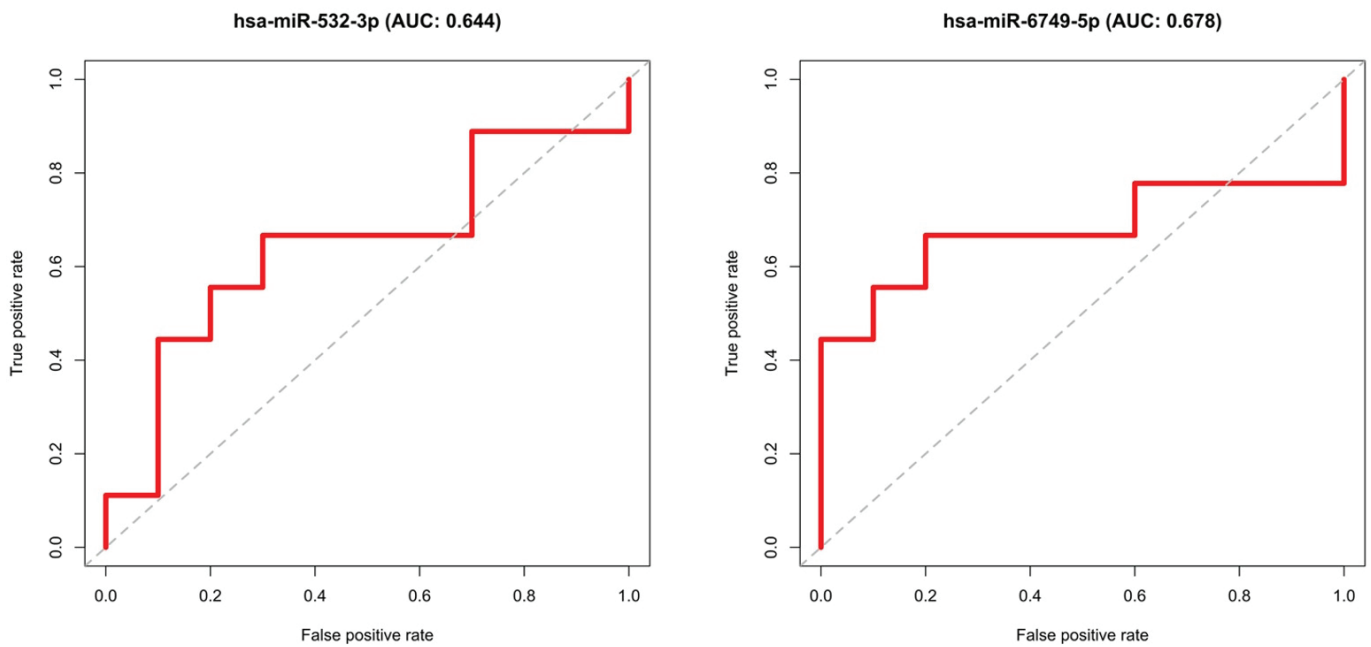


Fig. 3 - Validation of biomarker candidates. Receiver operating characteristic (ROC) curves show the ability of differently expressed exosomal miRNAs (adjusted p-value <0.5) to differentiate PCa and BPH samples of the test dataset.

In the heat map (Fig. 4), the hierarchical clustering based on these eight miRNAs is shown via the dendrograms. Besides, the blocks in black and grey visualize the two patient cohorts. The expression profiles of the miRNAs are graphically represented through different colour intensities. A clear separation of the two groups cannot be concluded, yet three clusters can be identified, of which the leftmost cluster contains only PCa except for one outlier. The middle cluster is split in half between PCa and BPH and the one on the right has a slight tendency towards BPH. A tendency of lower expression values is remarkable in the upper left corner (PCa). In contrast, the upper right corner (BPH) displays higher expression values.

Using a machine learning algorithm is an alternative approach to find a stable diagnostic tool for the differentiation of patients with PCa and those with BPH. Single miRNAs can be variously affected, either in cancer genesis or through other cellular processes. As shown above, some miRNAs are dysregulated, but not over all patients in the same extent. The found panel consists of eight miRNAs, combines highly dysregulated miRNAs (fold change >1.5) with those that were not prominent in the search for single biomarkers. There seem to be certain ranges of values that can be grouped into clusters. From this, it could be suggested that a patient falling within the left value range is very likely to have a diagnosis of PCa. If a patient is categorized in the middle or right cluster a statement cannot be made with certainty and the currently performed diagnostics should be carried out.

The detected panel of eight miRNAs was further validated on the training and test dataset and visualized in ROC curves (Fig. 4). On the training dataset, the AUC of >0.8 indicates

a high distinguishing potential. A decline of the AUC based on the test dataset was expectable, although a clear distinction of the patient cohorts cannot be stated in this case (AUC < 0.7). A reason might be the relatively small sample size in this study.

Nonetheless, the use of miRNA panels is a promising approach, as it is not as susceptible to interference as an individual biomarker, whose expression depends on various factors.

Limitations

We are aware that this study is limited by the currently still high costs for high-throughput processes. The sample selection was influenced by the availability of the required amount of urine volume and the quality of the samples collected, as the protein concentration or the presence of blood cells may also affect the concentration of small RNAs (40). Due to the number of samples, a correlation between clinicopathological parameters such as the Gleason score and individual miRNAs could not be determined. The comparability with other studies is also limited due to a lack of standardized protocols and quality standards. The results of this study for both the search for single biomarkers and the miRNA panel certainly depend on the underlying data quality, especially the UMI read count. Furthermore, we tried to consider the conditions in everyday clinical practice and therefore used a low possible initial urine volume. A higher starting volume might have led to an increased output of small RNA reads.

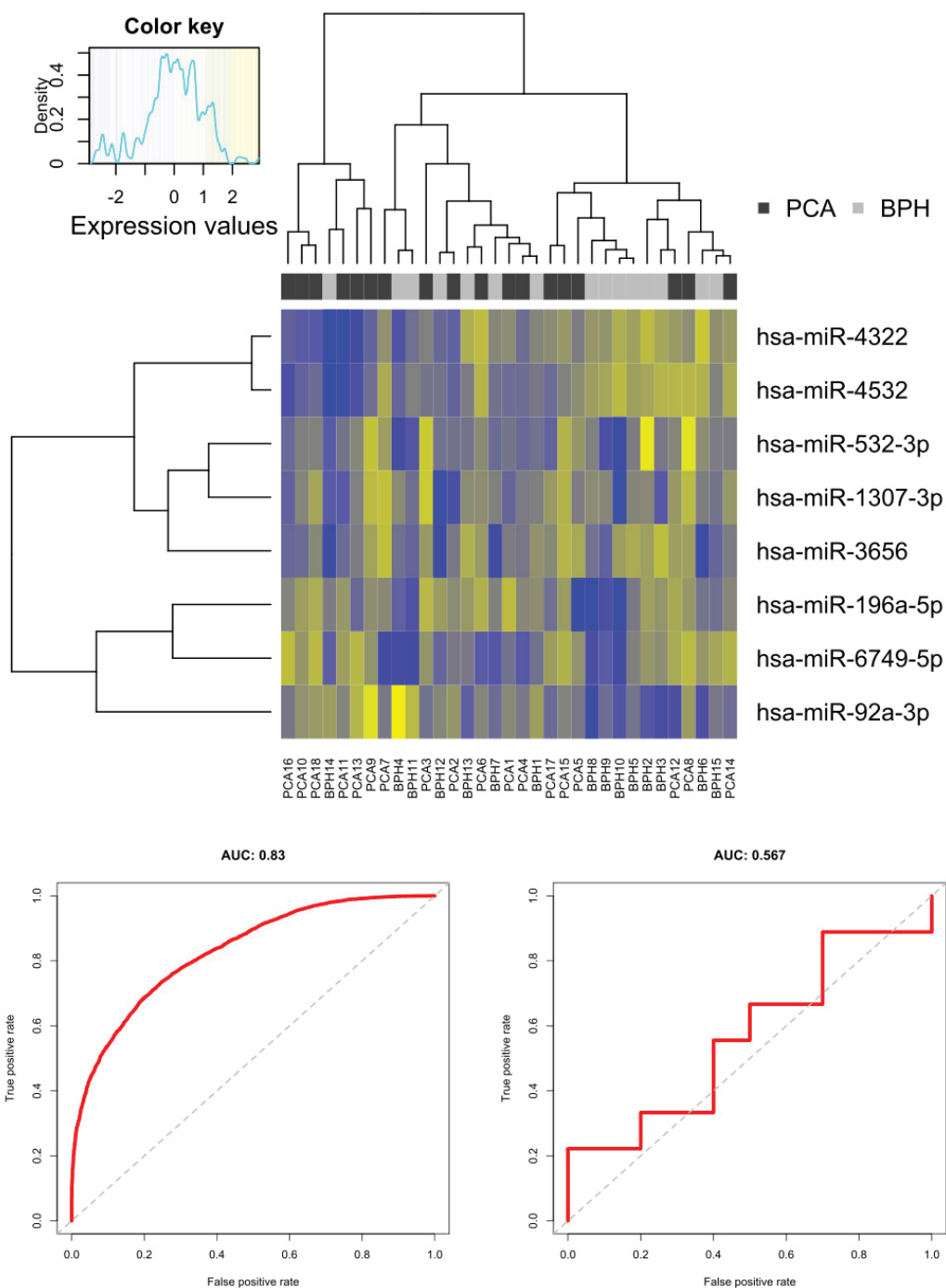


Fig. 4 - Heat map and validation of the miRNA panel. Heat map (using Z scores) of miRNA pattern detection with dendrograms from hierarchical clustering for the identified panel of exosomal miRNAs (top). ROC curves of miRNA panel (bottom): left = ROC curve based on training dataset, right = validation of test dataset.

Conclusion

PCa is a serious disease with far-reaching consequences for the patient, whereas BPH is a benign disease that affects a large proportion of the male population at an advanced age. Further diagnostic tools are needed to improve the current differentiation standards, since the PSA is not cancer specific and may be elevated in BPH and other non-malignant conditions of the prostate as well (6).

The possibility of using miRNAs from urinary exosomes to differentiate benign and malignant prostate diseases is demonstrated in this study. In particular, two promising biomarker candidates for the diagnosis of PCa have been identified. Since their exact molecular effects are not known yet, their biological function should be investigated in follow-up studies for a better understanding. The results of this work should also be validated and confirmed in, at best, multicentre study



cohorts with a larger sample size. The search for biomarker panels using a machine learning algorithm is a promising and robust approach by which previously overlooked miRNAs might increase the assay accuracy when additional data from a larger study will be available. To date, the transrectal biopsy remains the gold standard in the diagnosis of PCa. However, if the current development of high-throughput methods continues in terms of efficiency and cost-effectiveness, we believe that a non-invasive urine test based on miRNAs from urinary exosomes is a promising future option.

Acknowledgements

Many thanks to Fatemeh Gholamrezaei for teaching all the laboratory practical skills and supervising us, also to Prof. Dr. Florian Kreppel and colleagues for the intellectual support and exchange within the journal club. For the helpful and friendly provision of their equipment in the laboratory in Wuppertal, we would also like to thank Prof. Dr. Jan Postberg and Dr. Patrick Weil. For the financial support, we would like to thank the Paul-Kuth foundation.

Data availability

Supporting data are available online at <https://www.ebi.ac.uk/biostudies/studies/S-BSST683>

Disclosures

Conflict of interest: The authors declare no conflict of interest.
 Financial support: The work of KS and MT was supported by de.NBI (FKZ 031 A 534A), a project of the German Federal Ministry of Education and Research (BMBF). The funding of ME relates to PURE and VALIBIO, projects of Northrhine-Westphalia.
 LM, JH and AS were supported by the Paul-Kuth-Foundation, Wuppertal, Germany.
 SD, NMD and SR were supported by the Helios Kliniken GmbH, Berlin, Germany (Grant ID 000030).
 Author contributions statement: AS was the principal investigator. AS, MK and CK provided the original concept for the research questions and the study design. CK was responsible for the study protocol and ethics approval. JH and LM were responsible for the laboratory implementation of the study. SD, NMD and SR enrolled all patients in this study and collected the urine samples and the clinical data. KS and MT were responsible for the statistical planning and bioinformatic analysis of the data. They also generated the tables and figures. JH and LM wrote the first draft of the article and AS, MK, CK, and KS, MT, reviewed later versions of the article. ME reviewed the last draft of the article. JH and LM contributed equally.

References

- McNeal JE. Normal histology of the prostate. *Am J Surg Pathol.* 1988;12(8):619-633. [CrossRef PubMed](#)
- Garraway WM, Collins GN, Lee RJ. High prevalence of benign prostatic hypertrophy in the community. *Lancet.* 1991;338(8765):469-471. [CrossRef PubMed](#)
- Egan KB. The epidemiology of benign prostatic hyperplasia associated with lower urinary tract symptoms: prevalence and incident rates. *Urol Clin North Am.* 2016;43(3):289-297. [CrossRef PubMed](#)
- Sung H, Ferlay J, Siegel RL, et al. Global cancer statistics 2020: GLOBOCAN estimates of incidence and mortality worldwide for 36 cancers in 185 countries. *CA Cancer J Clin.* 2021;71(3):209-249. [CrossRef PubMed](#)
- Jemal A, Bray F, Center MM, Ferlay J, Ward E, Forman D. Global cancer statistics. *CA Cancer J Clin.* 2011;61(2):69-90. [CrossRef PubMed](#)
- European Association of Urology Guidelines. 2020 Edition. Arnhem, The Netherlands: European Association of Urology Guidelines Office; 2020. [Online](#)
- Loeb S, Vellekoop A, Ahmed HU, et al. Systematic review of complications of prostate biopsy. *Eur Urol.* 2013;64(6):876-892. [CrossRef PubMed](#)
- Sharma S, Zapatero-Rodríguez J, O'Kennedy R. Prostate cancer diagnostics: clinical challenges and the ongoing need for disruptive and effective diagnostic tools. *Biotechnol Adv.* 2017;35(2):135-149. [CrossRef PubMed](#)
- Buschow SI, Liefhebber JM, Wubbolts R, Stoorvogel W. Exosomes contain ubiquitinated proteins. *Blood Cells Mol Dis.* 2005;35(3):398-403. [CrossRef PubMed](#)
- Valadi H, Ekström K, Bossios A, Sjöstrand M, Lee JJ, Lötvall JO. Exosome-mediated transfer of mRNAs and microRNAs is a novel mechanism of genetic exchange between cells. *Nat Cell Biol.* 2007;9(6):654-659. [CrossRef PubMed](#)
- Nilsson J, Skog J, Nordstrand A, et al. Prostate cancer-derived urine exosomes: a novel approach to biomarkers for prostate cancer. *Br J Cancer.* 2009;100(10):1603-1607. [CrossRef PubMed](#)
- Friedman RC, Farh KK-H, Burge CB, Bartel DP. Most mammalian mRNAs are conserved targets of microRNAs. *Genome Res.* 2009;19(1):92-105. [CrossRef PubMed](#)
- Bartel DP. MicroRNAs: genomics, biogenesis, mechanism, and function. *Cell.* 2004;116(2):281-297. [CrossRef PubMed](#)
- Marton S, Garcia MR, Robello C, et al. Small RNAs analysis in CLL reveals a deregulation of miRNA expression and novel miRNA candidates of putative relevance in CLL pathogenesis. *Leukemia.* 2008;22(2):330-338. [CrossRef PubMed](#)
- Mitchell PS, Parkin RK, Kroh EM, et al. Circulating microRNAs as stable blood-based markers for cancer detection. *Proc Natl Acad Sci USA.* 2008;105(30):10513-10518. [CrossRef PubMed](#)
- Mall C, Rocke DM, Durbin-Johnson B, Weiss RH. Stability of miRNA in human urine supports its biomarker potential. *Biomarkers Med.* 2013;7(4):623-631. [CrossRef PubMed](#)
- Markert L, Holdmann J, Klinger C, et al. Small RNAs as biomarkers to differentiate benign and malign prostate diseases: an alternative for transrectal punch biopsy of the prostate? *PLoS One.* 2021;16(3):e0247930. [CrossRef PubMed](#)
- R Core Team. R: A Language and Environment for Statistical Computing. 2019. [Online](#)
- Turewicz M, Kohl M, Ahrens M, et al. BioInfra.Prot: a comprehensive proteomics workflow including data standardization, protein inference, expression analysis and data publication. *J Biotechnol.* 2017;261:116-125. [CrossRef PubMed](#)
- Walker A. openxlsx: Read, Write and Edit XLSX Files. 2019. [Online](#)
- Kuhn M. caret: Classification and Regression Training. 2019. [Online](#)
- Love MI, Huber W, Anders S. Moderated estimation of fold change and dispersion for RNA-seq data with DESeq2. *Genome Biol.* 2014;15(12):550. [CrossRef PubMed](#)
- Wickham H. ggplot2: Elegant Graphics for Data Analysis. 2016. [Online](#)
- Wilke CO. cowplot: Streamlined Plot Theme and Plot Annotations for 'ggplot2'. 2019. [Online](#)
- Slowikowski K. ggrepel: Automatically Position Non-Overlapping Text Labels with 'ggplot2'. 2019. [Online](#)



26. Robin X, Turck N, Hainard A, et al. pROC: an open-source package for R and S+ to analyze and compare ROC curves. *BMC Bioinformatics*. 2011;12(1):77. [CrossRef PubMed](#)
27. Breiman L. Random Forests. *Mach Learn*. 2001;45(1):5-32. [CrossRef](#)
28. Liaw A, Wiener M. Classification and regression by randomForest. *R News*. 2002;2(3):18-22.
29. Griffiths-Jones S. The microRNA Registry. *Nucleic Acids Res*. 2004;32(Database issue)(suppl 1):D109-D111. [CrossRef PubMed](#)
30. Yamada Y, Arai T, Kato M, et al. Role of pre-miR-532 (*miR-532-5p* and *miR-532-3p*) in regulation of gene expression and molecular pathogenesis in renal cell carcinoma. *Am J Clin Exp Urol*. 2019;7(1):11-30. [PubMed](#)
31. Han J, Wang F, Lan Y, et al. KIFC1 regulated by miR-532-3p promotes epithelial-to-mesenchymal transition and metastasis of hepatocellular carcinoma via gankyrin/AKT signaling. *Oncogene*. 2019;38(3):406-420. [CrossRef PubMed](#)
32. Gu C, Cai J, Xu Z, et al. MiR-532-3p suppresses colorectal cancer progression by disrupting the ETS1/TGM2 axis-mediated Wnt/ β -catenin signaling. *Cell Death Dis*. 2019;10(10):739. [CrossRef PubMed](#)
33. Jiang W, Zheng L, Yan Q, Chen L, Wang X. MiR-532-3p inhibits metastasis and proliferation of non-small cell lung cancer by targeting FOXP3. *J BUON*. 2019;24(6):2287-2293. [PubMed](#)
34. Andl T, Ganapathy K, Bossan A, Chakrabarti R. MicroRNAs as guardians of the prostate: those who stand before cancer. What do we really know about the role of microRNAs in prostate biology? *Int J Mol Sci*. 2020;21(13):4796. [CrossRef PubMed](#)
35. Guo J, Liu C, Wang W, et al. Identification of serum miR-1915-3p and miR-455-3p as biomarkers for breast cancer. *PLoS One*. 2018;13(7):e0200716-e. [CrossRef PubMed](#)
36. Li K, Zhu X, Li L, et al. Identification of non-invasive biomarkers for predicting the radiosensitivity of nasopharyngeal carcinoma from serum microRNAs. *Sci Rep*. 2020;10(1):5161. [CrossRef PubMed](#)
37. Zou X, Li M, Huang Z, et al. Circulating miR-532-502 cluster derived from chromosome X as biomarkers for diagnosis of breast cancer. *Gene*. 2020;722:144104. [CrossRef PubMed](#)
38. Pospisilova S, Pazourkova E, Horinek A, et al. MicroRNAs in urine supernatant as potential non-invasive markers for bladder cancer detection. *Neoplasma*. 2016;63(5):799-808. [CrossRef PubMed](#)
39. Liang Y, Ridzon D, Wong L, Chen C. Characterization of microRNA expression profiles in normal human tissues. *BMC Genomics*. 2007;8(1):166. [CrossRef PubMed](#)
40. Thomas CE, Sexton W, Benson K, Sutphen R, Koomen J. Urine collection and processing for protein biomarker discovery and quantification. *Cancer Epidemiol Biomarkers Prev*. 2010;19(4):953-959. [CrossRef PubMed](#)

The role of microRNAs in COVID-19 with a focus on miR-200c

Hadi Sodagar¹, Shahriar Alipour^{1,2}, Sepideh Hassani¹, Shiva Gholizadeh-Ghaleh Aziz¹, Mohammad Hasan Khadem Ansari¹, Rahim Asghari^{3,4}

¹Department of Biochemistry, Faculty of Medicine, Urmia University of Medical Sciences, Urmia - Iran

²Student Research Committee, Urmia University of Medical Sciences, Urmia - Iran

³Department of Internal Medicine, School of Medicine, Urmia University of Medical Sciences, Urmia - Iran

⁴Hematology, Immune Cell Therapy and Stem Cells Transplantation Research Center, Clinical Research Institute, Urmia University of Medical Sciences, Urmia - Iran

ABSTRACT

Objective: Epigenetics is a quickly spreading scientific field, and the study of epigenetic regulation in various diseases such as infectious diseases is emerging. The microribonucleic acids (miRNAs) as one of the types of epigenetic processes bind to their target messenger RNAs (mRNAs) and regulate their stability and/or translation. This study aims to evaluate non-coding RNAs (ncRNAs) with a focus on miR-200c in COVID-19. In this review, we first define the epigenetics and miRNAs, and then the role of miRNAs in diseases focusing on lung diseases is explained. Finally, in this study, we will investigate the role and position of miRNAs with a focus on miR-200c in viral and severe acute respiratory syndrome-related coronavirus (SARS-CoV2) infections.

Methods: Systematic search of MEDLINE, PubMed, Web of Science, Embase, and Cochrane Library was conducted for all relative papers from 2000 to 2021 with the limitations of the English language. Finally, we selected 128 articles which fit the best to our objective of study, among which 5 articles focused on the impact of miR-200c.

Results: Due to the therapeutic results of various drugs in different races and populations, epigenetic processes, especially miRNAs, are important. The overall results showed that different types of miRNAs can be effective on the process of various lung diseases through different target pathways and genes. It is likely that amplified levels of miR-200c may lead to decreased angiotensin-converting enzyme-2 (ACE2) expression, which in turn may increase the potential of infection, inflammation, and the complications of coronavirus disease.

Conclusion: miR-200c and its correlation with ACE2 can be used as early prognostic and diagnostic markers.

Keywords: Covid-19, Epigenetic, Lung diseases, miR-200c, miRNAs

Received: November 5, 2021

Accepted: February 22, 2022

Published online: March 21, 2022

Corresponding author:

Shahriar Alipour
Department of Biochemistry, Faculty of Medicine
Urmia University of Medical Sciences
11km SERO Road
0098 Urmia - Iran
alipour.sh@umsu.ac.ir

Shiva Gholizadeh-Ghaleh Aziz
Department of Biochemistry, Faculty of Medicine
Urmia University of Medical Sciences
11km SERO Road
0098 Urmia - Iran
gholizadeh.sh@umsu.ac.ir

Introduction

Epigenetics is defined as hereditary changes in gene expression without altering the deoxyribonucleic acid (DNA) sequence (1). Methylation of cytosine in the DNA sequence and the biochemical changes of histones are two critical mechanisms in the epigenetics that play an important role in gene regulation, differentiation, and carcinogenicity (2-5). Another mechanism that affects epigenetics and the gene expression is microribonucleic acids (miRNAs). miRNAs are non-coding endogenous RNAs with a length of 20 to 25 nucleotides. These molecules can bind to untranslated 3' regions (UTRs) and suppress the expression of messenger RNAs (mRNAs) at the posttranscriptional level by pairing a specific base sequence (6,7). miRNAs bind to their target mRNAs and regulate their stability and/or translation. If miRNAs bind completely to their target sequence on the



mRNA, they can lead to degradation; but in case of binding incorrectly, translational suppression of their target genes occurs by a mechanism that has not yet been fully understood (8). Each miRNA is predicted to have multiple gene targets and each mRNA may be regulated by more than one miRNA (9,10). The miRNAs play a vital role in many important biological processes, including cell proliferation (11), growth (12), differentiation (13), apoptosis (14), metabolism (15), aging (16), signal transduction (17), and viral infections (18). It is estimated that about one-third of genes and their pathways are regulated and controlled by miRNAs. Briefly, miRNAs have a remarkable effect on the genomic and epigenetic mechanisms (19,20).

The role of miRNAs in diseases focusing on lung diseases

The miRNAs involve in the development, progression, prognosis, diagnosis, and evaluation of therapeutic response in human diseases (21). In recent years, altered expression of the miRNAs has been identified in many human cancers (22),

cardiac hypertrophy and failure (23), metabolic disorders (24), immune system-related diseases, and inflammation (9). Also, the miRNAs have been studied in lung homeostasis, functional development, and various pulmonary diseases including asthma, chronic obstructive pulmonary disease (COPD), cystic fibrosis (CF), idiopathic pulmonary fibrosis (IPF), and lung cancer (25) (Tab. I).

In recent years, an increasing amount of research has shown the impact of miRNAs in the progress of pulmonary diseases (43). Our knowledge of the role of miRNAs in lung diseases has developed step by step. The role of miRNAs in the unique pulmonary cells is thought to be essential in understanding the mechanism of lung function and disease pathogenesis (25). More recently, many studies have begun to report the effects of miRNA transfer via extracellular vesicles. In lung diseases, this transfer was indicated to be facilitated via the intercellular communication between many types of cells in the respiratory system including endothelial cells (44), bronchial epithelial cells (45), mesenchymal stem cells, and others (46).

TABLE I - Relationship between miRNA types and their target genes in different lung diseases

Disease	miRNA	Gene target	Expression in disease	Sample	Measurement type	Ref
Asthma	miR-145	RUNX3	Up	PB	Quantitative PCR	(26,27)
	miR-21	IL-12	Up	Serum	qRT-PCR	(49)
	miR-133a	RhoA	Down	hBSMCs	qRT-PCR	(50)
	mir-19a	TGF β R2	Up	BEC	RT-PCR	(28)
	miR-155	IL-13Ra1	Up	Macrophages—monocytes	RT-PCR	(48)
COPD	miR-15b	SMAD7	Up	Lung	qRT-PCR	(29)
	miR-146a	COX-2	Down	PLF	RT-PCR/Northern Blot	(30)
	miR-24-3p	BIM	Down	Lung	RT-PCR	(31)
	miR-93-5	NFKBIA	Up	PBMCs	High-throughput microarray	(32)
CF	miR-126	TOM1	Down	Lung	RT-PCR	(33)
	miR-145	CFTR	Up	Cell line	qRT-PCR	(34)
	miR-138	SIN3A	Down	Cell culture	Quantitative PCR	(61)
	miR-9	ANO1	Up	Bronchial tissues	RT-PCR	(35)
IPF	let-7d	HMG2A	Down	Lung	Microarrays	(36)
	miR-21	Smad, Smad7	Up	Lung	miRNA array/Northern blotting	(37)
	miR-200c	TGF- β 1	Down	HLT	miR Array	(38)
	miR-199a-5p	TGF- β	Up	Serum	TaqMan miRNA assay	(39)
Lung cancer	miR-137	SLC22A18	Down	Lung	Bioinformatics analysis and luciferase reporter assay	(40)
	mirRNA-34a	TGF β R2	Down	Tissues	qRT-PCR and Western blot	(41)
	miR-449a	E2F3	Down	Lung cancer tissue	RT-PCR	(42)
	miR-200	ZEB1	Down	Tissue	RT-PCR	(55)

BEC = human bronchial epithelial cells; CF = cystic fibrosis; CFTR = Cystic Fibrosis Transmembrane Channel; COPD = chronic obstructive pulmonary disease; HLT = human lung tissue; IPF = idiopathic pulmonary fibrosis; miRNA = microribonucleic acid; PB = peripheral blood; PLF = primary lung fibroblast; qRT-PCR = quantitative reverse transcription polymerase chain reaction; PBMC = peripheral blood mononuclear cell; hBSMC = Human Bronchial Smooth Muscle Cells.

The miRNAs in Asthma

Asthma is a chronic inflammatory disease of the lungs that is often associated with clinical features such as airway hyperresponsiveness (AHR), airflow obstruction, excessive mucus secretion, and airway wall structural changes (remodeling) (47). Interleukin (IL)-13 and transcription factor signal transducer-and-activation-of-transcription-6 (STAT6)-operated pathways have been shown to play a significant role in regulating the prominent asthma features, for example, AHR and remodeling. miR-155 has been shown to be upregulated in order to target directly the transcription of the IL-13 receptor $\alpha 1$ (IL13Ra1) in human macrophages, reducing the levels of IL13Ra1 protein and decreasing the levels of activated STAT6, which is vital in regulating the IL-13 signaling pathway (48). Inhibition of miR-21 leads to a decrease in Th2 cytokine levels (IL-4, IL-5, and IL-13), the number of inflammatory airway leukocytes and AHR (49). Downregulation of miR-133a was followed by an increased expression of RhoA and subsequently increased bronchial hyperactivity in a murine model of asthma (50). Elevated expression of the miR-155 has also been indicated in murine models of asthma. Additionally, by using antagomir against miR-145, the mucus secretion, Th2 cytokine production, and eosinophil infiltration in the airways decreased (51).

The miRNAs in lung cancer

Dysfunction of miRNAs is often identified in malignancies, including lung tumor. Lung cancer is the leading cause of cancer-related mortality worldwide and to date the roles of miRNAs in lung cancer have been specified and reviewed widely along with the other diseases. Histologically, lung cancer can be mostly divided into small cell (SCLC) and non-small cell lung cancer (NSCLC). The latter is more common and is subclassified into squamous, adenocarcinoma, and large-cell carcinoma (52). Recent sequencing studies have exposed a very large number of targets for each single miRNA. By regulating the posttranscriptional gene expression, miRNAs strongly involved in wide-ranging pathways with the main effect are on the progressive and carcinogenesis routes (53,54). Concisely, various miRNAs that are recognized as either oncogenes or tumor suppressors in lung cancer are also involved in the immune system response, for instance, the miR-200 family. The low expression of the miR-200 family members in human early-stage lung adenocarcinomas has been correlated with upregulation of PD-L1 (55) and CD8⁺ T-cell immunosuppression and metastasis, which resulted in the reduction of tumor load. This finding greatly supported the role of miR-200 as a tumor suppressor.

The miRNAs in COPD

COPD is an inflammatory progressive lung disease that is prompted by chronic inflammation exposure of the airways to stimuli including cigarette smoking and other noxious gases. An increasing number of studies have demonstrated that injured cells such as endothelial and epithelial cells participate seriously in the pathogenesis of COPD (56). The

exposure of the respiratory epithelial cells to the harmful agents like cigarette smoke leads to the release of proinflammatory and inflammatory cytokines such as IL-1, IL-6, IL-8, and tumor necrosis factor (TNF)- α (57,58).

The miRNAs and CF

In the Caucasian community, CF is the most frequent deadly hereditary disease. It is caused by a recessive mutation in the CFTR (Cystic Fibrosis Transmembrane Channel) gene, which codes for a chloride channel (59). miRNAs can target CFTR directly or indirectly for regulating CF. Several miRNAs can complementarily and directly regulate CFTR expression such as miR-145 (via SMAD3 and TGF- β), miR-223 (via CFTR mRNA), miR-9 (via Anoctamin 1), and miR-494 (via Solute Carrier family 12Member 2 (SLC12A2)), alone or together. However, miR-509-3p and miR-494 downregulate CFTR expression (60). Some miRNAs like miR-138 can also repress the biosynthesis intermediary actors, such as the transcription factor SIN3A (SIN3 transcription regulator family member A) and CFTR (61).

The miRNAs and infections

Recent advances in molecular mechanisms point to the importance of miRNAs in the lung and respiratory infections. Acute viral respiratory infections (AVRIs) are the most common causes of acute respiratory symptoms (62). Changes in the regulation of miRNA expression in the epithelial cells of human rhinovirus (hRV), influenza (IV), human metapneumovirus, human coronavirus, and respiratory syncytial virus infections are associated with the pathogenesis of acute respiratory diseases (63). For example, the expression of host miRNAs changes in response to IV stimulation. These miRNAs directly or indirectly target viral and host genes to regulate virus replication, stimulate or suppress innate immune responses and cell apoptosis during the viral infection (64,65). IV increases the expression of miR-4276 by upregulating two proteins involved in the apoptotic pathway, Cas9 and Cdc6c (74), and eventually leads to increased virus replication and apoptosis. Furthermore, a number of specific cellular miRNAs in IV-infected cells including miR-323, miR-491, and miR-654 target the protected region of viral PB1 gene to prevent the virus from replicating in MDCK cells (76).

Another mechanism in IV infection is the altered expression of cellular miRNAs and their effect on important signaling pathways associated with the immune system (66). In hRV infections, miRNAs result in antiviral responses by modulating the immune response (miR-128 and miR-155) as well as controlling virus entry into the infected lung cells (miR-23b) (67).

RSV causes viral respiratory disease in infants and young children (68), modulating the expression of host cell miRNAs for antiviral responses and virus replication similar to the miRNAs mentioned above (69,70). For instance, miR-125a regulates nuclear factor kappa B (NF- κ B) signaling pathway by suppressing A20 inhibitor protein (CCL5) as an important cytokine in both innate and compatible immune systems (71). Coronaviruses cause a wide range of respiratory infections, from mild upper respiratory tract infections to severe lower respiratory tract infections (72). Table II shows the four major



TABLE II - Relationship between different types of miRNAs and their target genes in well-known viral lung infections

Viral disease	miRNA	Gene target	Effects on gene regulation	Pathways	Ref
Influenza virus	– <i>miRNA-4276</i>	– COX6C	– Up	– Inhibits COX6C and caspase-9 and promoting viral replication	(74)
	– <i>miR-323, miR-491</i>	– PB1	– Up	– Inhibits replication of virus	(75)
	– <i>let-7c</i>	– M1	– Up	– Reduces virus replication by degrading M1 mRNA	(76)
	– <i>miR-146a-5</i>	– TRAF6	– Up	– Negatively regulates innate immune and inflammatory responses	(77)
	– <i>miR-576-3p</i>	– AP1G1	– Down	– Regulates virus entry	(78)
	– <i>miR-21-3p</i>	– HDAC8	– Down	– Suppresses IAV replication	(79)
	– <i>miR-132, miR-200c</i>	– MAPK3, IRAK1	– Up	– Regulates antiviral response	(64)
Rhinoviruses	– <i>miR-128, miR-155</i>	– SMAD2, EGFR	– Up	– Regulates the immune response against RV-1B and inhibits virus replication	(80)
	– <i>miR-23b</i>	– VLDLR	– Up	– Prevents viral infection by decreasing the VLDLR	(81)
RSV	▪ <i>let-7f</i>	CCL7, SOCS3	– Up	– Antiviral host response	(82)
	▪ <i>miR-30, let-7i</i>	– IL-13, TLR4, RUNX2	– Up	– Induces miRNAs to involve in the immune response pathways such as NF-κB and type I IFNs	(83-85)
	▪ <i>miR-221</i>	– NGF, TrkA	– Down	– Promotes viral replication	(86)
	▪ <i>miR-125a</i>	– TNFAIP3	– Down	– Inhibits NF-κB signaling pathway and results in reducing macrophage activation	(87)
Coronavirus	OC43 <i>miR-9</i>	– NF-κB	Up	N protein of virus binds to miR-9 and modulates NF-κB expression	(88)
	SARS <i>miR-17, miR-574-5p, miR-214</i>	– Virulent proteins, including N, S, M, and E	Up	– Suppresses viral replication that may aid evasion of immune surveillance until successful infection of other cells	(89,90)
	MERS ▪ <i>miR-16-1-3p, miR-26a-1-3p, miR-425-5p, miR-1275, miR-2277-5p, miR-500b-5p, miR627-5p, miR-1257, miR-1275</i>	– MAP3K9, MYO15B, SPOCK1	Up	– miRNA-mRNA network significantly impacts MERS-CoV replication	(91)
	MERS <i>miR628-5p, miR-18a-3p, hsa-miR332-3p</i>	– Viral mRNA	Up	– These miRNAs may downregulate viral gene expression resulting in the inhibition of viral replication	(92)
	SARS-CoV2 ▪ <i>miR-146a-5p</i>	IL-6	Down	– Acts as a negative regulator of NF-κB as the transcription factor of the IL-6 gene	(93)
	▪ <i>miR-200c</i>	ACE2	Up	– Overexpression of miR-200c induces downregulation of ACE2 in human cells	
	▪ <i>miR-1202</i>	SARS-CoV2 ORF1a/b	Up	– Targets SARS-CoV2 genome	(94)
<i>let-7d-5p</i>	– TMPRSS2	Up	– Expression of let-7d-5p negatively correlates with TMPRSS2 expression	(95)	

IL = interleukin; MERS = Middle East respiratory syndrome; miRNA = microribonucleic acid; NF-κB = nuclear factor kappa B; RSV = respiratory syncytial virus; SARS-CoV = severe acute respiratory syndrome-related coronavirus; IAV = Influenza A viruses.

categories of the pulmonary virus families and some of the most important miRNAs that change the expression of the genes involved in infections with these viruses. Severe acute respiratory syndrome coronaviruses (SARS-CoV) use host cell miRNAs to escape removal by the immune system (89).

In Middle East respiratory syndrome coronavirus (MERS-CoV) infection, cellular miRNAs act as an antiviral therapeutic agent (92). The functional mechanisms of miRNAs in SARS-CoV2 as the causative agent of COVID-19 are diverse. For example, increased miR-200c expression in the disease downregulates the expression of angiotensin-converting enzyme (ACE2) protein that is the receptor essential for the virus entry into the cell (73).

Association of miR-200c with the genes involved in inflammation (ACE2, IL-6)

miR-200c-3p is a member of the miR-200 family with two clusters miR-200a/b/429 and miR-200c/141. The miR-200c-3p is one of the most important miRNAs of the second cluster. Studies on the miR-200 family have shown that it has a variety of roles in cancer progression, drug resistance, and oxidative stress (96,97). The results of various studies have revealed the crucial role of the miR-200c epithelial-mesenchymal transmission, proliferation, metastasis, apoptosis, autophagy, and therapeutic resistance in several types of cancer (98). The miR-200c is also measured as a biomarker to predict disease progression, diagnosis, and response to therapy in several cancers, both in tissues and in body fluids (blood, urine) (96).

Studies using miRNAs can contribute not only to the understanding of virus-host interactions but also to the stratification of the different severities of COVID-19. In this sense, miR-200c-3p, which has been associated with viral infections, including influenza A, offers itself as a candidate for the study of COVID-19. The analysis of its expression in groups of patients presenting different levels of disease aggressiveness could contribute to a better screening of patients affected by SARS-CoV2. Thus, in Pimenta's study, which aimed to analyze the expression of miR-200c-3p in saliva samples from patients with COVID-19, the results showed that the expression pattern of miR-200c-3p increased with disease severity (99).

Furthermore, the significant impact of miR-200c-3p in acute respiratory distress syndrome (ARDS) was discovered, which proposes it as a potential factor in SARS-CoV-2 research and is considered as a potential diagnostic agent for SARS-CoV-2 studies (100). In a study of the H5N1 avian influenza virus (AIV) ACE, serum levels of miRNA-200c-3p were found to increase in the virus causing acute pulmonary injury and ARDS. This miRNA binds to the 3'-UTR locus of the ACE2 gene, and inhibits the expression of this protein and thus exacerbates the disease (100-102).

The ACE2 gene was first identified from complementary DNA in the left ventricle of the human heart (102). ACE2 inactivates angiotensin II (Ang II) by cleavage and produces Ang 1-7 (103).

Ang II binds to type 1 and type 2 Ang II receptors with high affinity and is involved in regulating blood pressure, body fluid balance, inflammation, cell proliferation, hypertrophy, and fibrosis (104-106). ACE2 has been shown to neutralize

the development of severe ARDS caused by AIV, coronavirus, and sepsis in mice (106). ACE2 has also been reported as a receptor for the SARS-CoV2 virus to enter the pneumocytes (107).

The role of miR-200c in lung inflammation and lung diseases

MiR-200c, alongside with miR-141, is placed in the intragenic zone of chromosome 12. MiR-200c family has beneficial effects on preventing drug resistance, cancer development, and oxidative stress. It consists of two clusters: (1) miR-200c/141 cluster including miR-141-3p and miR-141-5p, miR-200c-3p, miR-200c-5p on chromosome 12p13.31; (2) miR-200a/b/429 cluster including miR-200a-3p, miR-200a-5p, miR-200b-3p, miR-200b-5p, and miR-429 on chromosome 1p36.33 (108).

miR-200, like ACE2, is greatly expressed in the epithelial cells of the pneumocytes, mainly in type II alveolar epithelial cells. The expression of miR-200 has a crucial role in the differentiation of type II alveolar epithelial cells in fetal lungs, which are important components of the renin-angiotensin system signaling pathway all over the body. miR-200 displays several important effects in the body such as anti-remodeling, anti-inflammatory, and anti-proliferative through reduction of angiotensin II levels (Fig. 1) (109). Remarkable points in this issue are about controlling COVID-19 patients' mortality rates and disease severity, by upregulating ACE2 levels with using angiotensin receptor blockers or ACE2 blockers (110). miR-200 is the exact and direct target of ACE2 at 3'-UTR of ACE2 mRNA which by binding to its locus results in the depression of ACE2 expression as a receptor responsible for ARDS incidence. Normally, ACE2 catalyzes the conversion of AgII to Ag1-7. Later, Ag1-7 binds to mitochondrial assembly (MAS) receptors resulting in Ag1-7 protective effects including anti-proliferation, anti-necrotic and anti-hypertrophic as well as vasodilation and declining of proinflammatory cytokine secretion. SARS-CoV2 inhibits this pathway and worsens AgII adverse effects on lung tissue during the acute phase of the disease. It was reported that SARS-CoV2 induces the secretion of IL-6, TNF- α , IL-1 β (102,111-113). Activation of NF- κ B pathway, an important factor in ARDS pathogenesis, is one of the noticeable pathways leading to the upregulation of miR-200c-3p. Increased expression of miR-200c-3p occurred when the ACE2 expression decreased (100) (Fig. 1).

These mechanisms include increased miR-200c expression, inhibition of ACE2 expression, by affecting ACE2 protein outside the cell, and by inhibition of other anti-inflammatory functions, all of which are shown in the figure. (1) increased miR-200c expression that SARS-CoV-2 inhibit ACE2 indirectly by regulating miR-200c and directly inhibiting ACE2 expression, (2) by affecting the ACE2 gene, (3) ACE2 protein outside the cell, and (4) by inhibiting other anti-inflammatory functions, all of which are shown in the figure. In addition, miR-200c can also reduce ace2 expression, thereby reducing ACE2 expression and reducing its function. According to research results, the reduction in disease severity in COVID-19 patients associates with the correlation between low expression of ACE2 and high levels of miR-200c-3p in the lungs and the upper respiratory tract (114,115).



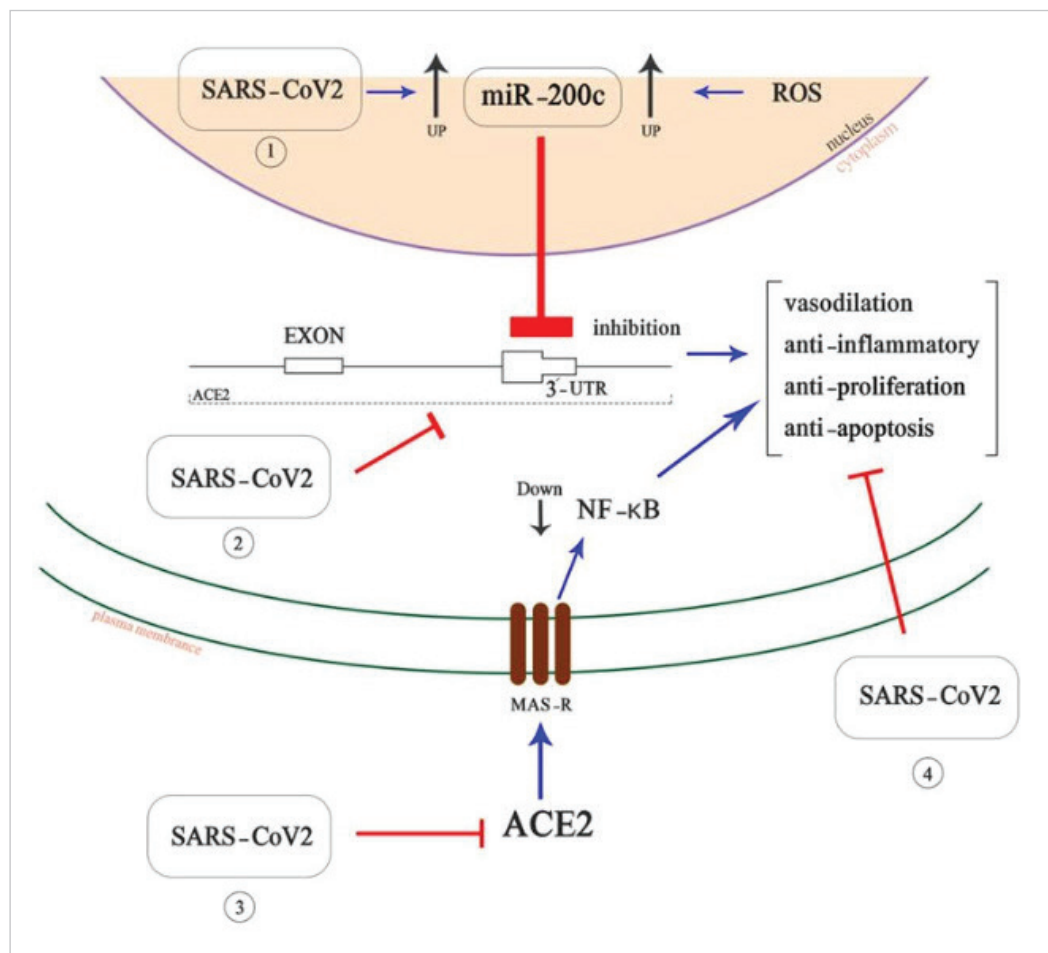


Fig. 1 - MiR-200c and ACE2 mechanism of function in the pathogenesis of COVID-19. SARS-CoV2 induces inflammation and severe ARDS through four mechanisms: (1) virus indirectly leads to ACE2 downregulation by enhancing miR-200c expression. (2) Virus directly inhibits ACE2 gene expression. (3) SARS-CoV2 inhibits binding of ACE2 protein to its receptor on the lung cells. (4) SARS-CoV2 inhibits the anti-inflammatory effects of ACE2. ACE2 = angiotensin-converting enzyme-2; ARDS = acute respiratory distress syndrome; COVID = coronavirus; SARS-CoV = severe acute respiratory syndrome-related coronavirus.

Recent studies about the entrance of SARS-CoV-2 to the host cells imply that some miRNAs can actually control the expression of ACE2 and TMPRSS2, which are potentially of high effect in SARS-COV-2 pathogenesis (116).

Several pathways have been studied about the effect of epigenetics on the regulation of ACE2/TMPRSS2 expression levels in respiratory diseases. The epigenetic repression of miRNA transcription can control their regulatory regions. For instance, Lysine-specific demethylase 5B (JARID1B, encoded by the KDM5B gene) was displayed to suppress the transcription of miR-200 family including miR-141, miR-200a, miR-200b, miR-200c, and miR-429. Hsa-miR-125a/hsa-let-7e miRNAs inhibit the transcription of miR-200 family through stimulating H3K4me3 histone, which demethylates the miRNAs of this family. Therefore, hsa-miR-125a-5p via binding to miR-200 family pursues 3'-UTR of ACE2 mRNA and results in the enhancement of ACE2 gene expression while 3'-UTR of the TMPRSS2 is targeted by hsa-let-7e-5p. Concludingly, JARID1B epigenetic activity doesn't directly regulate the expression of ACE2 and TMPRSS2 (116). Scientists have investigated if promoting H3K4me3 demethylation is caused by repression of the transcription of the let-7e and miR-125a via JARID1B gene (117); for example, the upregulation of

JARID1B in lung cancer cell line A549 concluded threefold depression of miR-200a and miR-200c expression, while JARID1B knockdown enhanced 1.5-fold their conserved and stable levels (118).

The experimental data show the presence of controlling network containing miR-125a/let-7e/miR-200 families, ACE2/TMPRSS2 as well as histone demethylase JARID1B, and further point a new way for signaling pathway for ACE2 expression. In one report, the single-cell RNA sequencing data analysis sharply indicated that in the majority of human cells ACE2 and TMPRSS2 are not expressed without JARID1B. So, for better understanding, the viral infection pathogenesis needs to be investigated in the regulatory network related to the expression of JARID1B, ACE2, and TMPRSS2 in human respiratory epithelial cells (116).

According to cellular ontologies research on 24 miRNAs, for evaluating the miRNAs targeting SARS-CoV-2 host cell receptor ACE2, it was revealed that miR-429, miR-200a-3p, miR-210-3p, miR-200b-3p, and miR-200c-3p were highly expressed in the respiratory epithelial cells and miR-200c-3p exists abundantly in the cells including endo-epithelial cell, epithelial cells, respiratory epithelial cells, leukocytes, hematopoietic cells, and myeloid leukocytes. Also, miR-200b

and miR-200c were discovered to be extremely conserved (119).

In clinical trials, miR-200 and its correlation with ACE2 can be used as early prognostic and diagnostic markers. Its location on the upstream of ARDS signaling pathways may reduce the morbidity and mortality rates of COVID-19 via epigenetic procedures, which can be so beneficial for human survival.

Conclusion

At present, there is no exact treatment for COVID-19. Due to the importance of miRNAs in pulmonary diseases, mainly the infectious viral diseases as well as SARS-COV-2, they can be potential candidates of targeted therapy in SARS-COV-2 in order to reduce the morbidity and mortality rates of this disease as miR-200c and its correlation with ACE2 can be used as early prognostic and diagnostic markers. However, further research must be carried out to reveal the exact effect of miR-200c in the pathogenesis of COVID-19 in order to be used clinically.

Authors' contributions

HS was responsible for the largest share in writing the article. SA and SG-GA conceptualized and wrote the article and article design. However, SA share has been higher. SA contributed in review and editing of final submitted version. MHKA and RA contributed in Methodology, Data validation and Writing original draft of this article.

Acknowledgments

The authors would like to thank the officials of Urmia University of Medical Sciences and the Student Research Committee for their support of this project.

Disclosures

Conflict of interest: The authors declare no conflict of interest. Financial support: This review article was partly supported by Urmia University of Medical Sciences.

References

- Egger G, Liang G, Aparicio A, Jones PA. Epigenetics in human disease and prospects for epigenetic therapy. *Nature*. 2004; 429(6990):457-463. [CrossRef PubMed](#)
- Jones PA, Baylin SB. The fundamental role of epigenetic events in cancer. *Nat Rev Genet*. 2002;3(6):415-428. [CrossRef PubMed](#)
- Klose RJ, Bird AP. Genomic DNA methylation: the mark and its mediators. *Trends Biochem Sci*. 2006;31(2):89-97. [CrossRef PubMed](#)
- Baylin SB, Ohm JE. Epigenetic gene silencing in cancer – a mechanism for early oncogenic pathway addiction? *Nat Rev Cancer*. 2006;6(2):107-116. [CrossRef PubMed](#)
- Jones PA, Laird PW. Cancer epigenetics comes of age. *Nat Genet*. 1999;21(2):163-167. [CrossRef PubMed](#)
- Ambros V. The functions of animal microRNAs. *Nature*. 2004;431(7006):350-355. [CrossRef PubMed](#)
- Jadideslam G, Ansarin K, Sakhinia E, Alipour S, Pouremamali F, Khabbazi A. The microRNA-326: autoimmune diseases, diagnostic biomarker, and therapeutic target. *J Cell Physiol*. 2018;233(12):9209-9222. [CrossRef PubMed](#)
- Kolahi S, Farajzadeh M-J, Alipour S, et al. Determination of mir-155 and mir-146a expression rates and its association with expression level of TNF- α and CTLA4 genes in patients with Behcet's disease. *Immunol Lett*. 2018;204:55-59. [CrossRef PubMed](#)
- Shahriar A, Ghaleh-Aziz Shiva G, Ghader B, Farhad J, Hosein A, Parsa H. The dual role of mir-146a in metastasis and disease progression. *Biomed Pharmacother*. 2020;126:110099. [CrossRef PubMed](#)
- Rajewsky N. microRNA target predictions in animals. *Nat Genet*. 2006;38(6)(suppl):S8-S13. [CrossRef PubMed](#)
- Cheng AM, Byrom MW, Shelton J, Ford LP. Antisense inhibition of human miRNAs and indications for an involvement of miRNA in cell growth and apoptosis. *Nucleic Acids Res*. 2005;33(4):1290-1297. [CrossRef PubMed](#)
- Karp X, Ambros V. Developmental biology. Encountering microRNAs in cell fate signaling. *Science*. 2005;310(5752):1288-1289. [CrossRef PubMed](#)
- Miska EA. How microRNAs control cell division, differentiation and death. *Curr Opin Genet Dev*. 2005;15(5):563-568. [CrossRef PubMed](#)
- Xu P, Guo M, Hay BA. MicroRNAs and the regulation of cell death. *Trends Genet*. 2004;20(12):617-624. [CrossRef PubMed](#)
- Alshalalfa M, Alhadj R. Using context-specific effect of miRNAs to identify functional associations between miRNAs and gene signatures. *BMC Bioinformatics*. 2013;14(12)(suppl 12):S1. [CrossRef PubMed](#)
- Bartel DP. MicroRNAs: target recognition and regulatory functions. *Cell*. 2009;136(2):215-233. [CrossRef PubMed](#)
- Cui Q, Yu Z, Purisima EO, Wang E. Principles of microRNA regulation of a human cellular signaling network. *Mol Syst Biol*. 2006;2(1):46. [CrossRef PubMed](#)
- Barbu MG, Condrat CE, Thompson DC, et al. MicroRNA involvement in signaling pathways during viral infection. *Front Cell Dev Biol*. 2020;8:143. [CrossRef PubMed](#)
- Yang N, Ekanem NR, Sakyi CA, Ray SD. Hepatocellular carcinoma and microRNA: new perspectives on therapeutics and diagnostics. *Adv Drug Deliv Rev*. 2015;81:62-74. [CrossRef PubMed](#)
- Nana-Sinkam SP, Geraci MW. MicroRNA in lung cancer. *J Thorac Oncol*. 2006;1(9):929-931. [CrossRef PubMed](#)
- Yang N, Coukos G, Zhang L. MicroRNA epigenetic alterations in human cancer: one step forward in diagnosis and treatment. *Int J Cancer*. 2008;122(5):963-968. [CrossRef PubMed](#)
- Blenkiron C, Miska EA. miRNAs in cancer: approaches, aetiology, diagnostics and therapy. *Hum Mol Genet*. 2007;16(Spec No 1):R106-R113. [CrossRef PubMed](#)
- Divakaran V, Mann DL. The emerging role of microRNAs in cardiac remodeling and heart failure. *Circ Res*. 2008;103(10):1072-1083. [CrossRef PubMed](#)
- Rottiers V, Näär AM. MicroRNAs in metabolism and metabolic disorders. *Nat Rev Mol Cell Biol*. 2012;13(4):239-250. [CrossRef PubMed](#)
- Sessa R, Hata A. Role of microRNAs in lung development and pulmonary diseases. *Pulm Circ*. 2013;3(2):315-328. [CrossRef PubMed](#)
- Qiu Y-Y, Zhang Y-W, Qian X-F, Bian T. miR-371, miR-138, miR-544, miR-145, and miR-214 could modulate Th1/Th2 balance in asthma through the combinatorial regulation of Runx3. *Am J Transl Res*. 2017;9(7):3184-3199. [PubMed](#)
- Yu Y, Wang L, Gu GJCCA. The correlation between Runx3 and bronchial asthma. *Clin Chim Acta*. 2018;487:75-79. [CrossRef](#)
- Haj-Salem I, Fakhfakh R, Bérubé JC, et al. MicroRNA-19a enhances proliferation of bronchial epithelial cells by



- targeting TGF β R2 gene in severe asthma. *Allergy*. 2015;70(2): 212-219.
29. Ezzie ME, Crawford M, Cho J-H, et al. Gene expression networks in COPD: microRNA and mRNA regulation. *Thorax*. 2012;67(2):122-131. [CrossRef](#)
 30. Sato T, Liu X, Nelson A, et al. Reduced miR-146a increases prostaglandin E2 in chronic obstructive pulmonary disease fibroblasts. *Am J Respir Crit Care Med*. 2010;182(8):1020-1029.
 31. Nouws J, Wan F, Finnemore E, et al. MicroRNA miR-24-3p reduces DNA damage responses, apoptosis, and susceptibility to chronic obstructive pulmonary disease. *JCI Insight*. 2021;6(2). [CrossRef](#)
 32. Dang X, Qu X, Wang W, et al. Bioinformatic analysis of microRNA and mRNA Regulation in peripheral blood mononuclear cells of patients with chronic obstructive pulmonary disease. *Respir Res*. 2017;18(1):1-13. [CrossRef](#)
 33. Oglesby IK, Bray IM, Chotirmall SH, et al. miR-126 is down-regulated in cystic fibrosis airway epithelial cells and regulates TOM1 expression. *J Immunol*. 2010;184(4):1702-1709.
 34. Gillen AE, Gosalia N, Leir S-H, Harris A. MicroRNA regulation of expression of the cystic fibrosis transmembrane conductance regulator gene. *Biochem J*. 2011;438(1):25-32. [CrossRef](#)
 35. Sonnevile F, Ruffin M, Coraux C, et al. MicroRNA-9 down-regulates the ANO1 chloride channel and contributes to cystic fibrosis lung pathology. *Nat Commun*. 2017;8(1):1-11.
 36. Pandit KV, Corcoran D, Yousef H, et al. Inhibition and role of let-7d in idiopathic pulmonary fibrosis. *Am J Respir Crit Care Med*. 2010;182(2):220-229. [CrossRef](#)
 37. Liu G, Friggeri A, Yang Y, et al. miR-21 mediates fibrogenic activation of pulmonary fibroblasts and lung fibrosis. *J Exp Med*. 2010;207(8):1589-1597.
 38. Yang S, Banerjee S, de Freitas A, et al. Participation of miR-200 in pulmonary fibrosis. *Am J Pathol*. 2012;180(2):484-493. [CrossRef](#)
 39. Yang G, Yang L, Wang W, Wang J, Wang J, Xu Z. Discovery and validation of extracellular/circulating microRNAs during idiopathic pulmonary fibrosis disease progression. *Gene*. 2015; 562(1):138-144.
 40. Zhang B, Liu T, Wu T, Wang Z, Rao Z, Gao J. microRNA-137 functions as a tumor suppressor in human non-small cell lung cancer by targeting SLC22A18. *Int J Biol Macromol*. 2015;74:111-118.
 41. Ma Z-L, Hou P-P, Li Y-L, et al. MicroRNA-34a inhibits the proliferation and promotes the apoptosis of non-small cell lung cancer H1299 cell line by targeting TGF β R2. *Tumour Biol*. 2015; 36(4):2481-2490.
 42. Ren X-S, Yin M-H, Zhang X, et al. Tumor-suppressive microRNA-449a induces growth arrest and senescence by targeting E2F3 in human lung cancer cells. *Cancer Lett*. 2014;344(2): 195-203. [CrossRef](#)
 43. Chen J, Hu C, Pan P. Extracellular vesicle microRNA transfer in lung diseases. *Front Physiol*. 2017;8:1028. [CrossRef PubMed](#)
 44. Aliotta JM, Pereira M, Wen S, et al. Exosomes induce and reverse monocrotaline-induced pulmonary hypertension in mice. *Cardiovasc Res*. 2016;110(3):319-330. [CrossRef PubMed](#)
 45. Fujita Y, Araya J, Ito S, et al. Suppression of autophagy by extracellular vesicles promotes myofibroblast differentiation in COPD pathogenesis. *J Extracell Vesicles*. 2015;4(1):28388. [CrossRef PubMed](#)
 46. Lee C, Mitsialis SA, Aslam M, et al. Exosomes mediate the cytoprotective action of mesenchymal stromal cells on hypoxia-induced pulmonary hypertension. *Circulation*. 2012;126(22): 2601-2611. [CrossRef PubMed](#)
 47. Fanta CH. Asthma. *N Engl J Med*. 2009;360(10):1002-1014. [CrossRef PubMed](#)
 48. Martinez-Nunez RT, Louafi F, Sanchez-Elsner T. The interleukin 13 (IL-13) pathway in human macrophages is modulated by microRNA-155 via direct targeting of interleukin 13 receptor α 1 (IL13R α 1). *J Biol Chem*. 2011;286(3): 1786-1794. [CrossRef PubMed](#)
 49. Elbehidy RM, Youssef DM, El-Shal AS, et al. MicroRNA-21 as a novel biomarker in diagnosis and response to therapy in asthmatic children. *Mol Immunol*. 2016;71:107-114. [CrossRef PubMed](#)
 50. Chiba Y, Tanabe M, Goto K, Sakai H, Misawa M. Down-regulation of miR-133a contributes to up-regulation of RhoA in bronchial smooth muscle cells. *Am J Respir Crit Care Med*. 2009;180(8):713-719. [CrossRef PubMed](#)
 51. Collison A, Mattes J, Plank M, Foster PS. Inhibition of house dust mite-induced allergic airways disease by antagonism of microRNA-145 is comparable to glucocorticoid treatment. *J Allergy Clin Immunol*. 2011;128(1):160-167. e4. [CrossRef](#)
 52. Wu K-L, Tsai Y-M, Lien C-T, Kuo P-L, Hung AJ. The roles of microRNAs in lung cancer. *Int J Mol Sci*. 2019;20(7):1611. [CrossRef PubMed](#)
 53. Lin PY, Yu SL, Yang PC. MicroRNA in lung cancer. *Br J Cancer*. 2010;103(8):1144-1148. [CrossRef PubMed](#)
 54. He L, Thomson JM, Hemann MT, et al. A microRNA polycistron as a potential human oncogene. *Nature*. 2005;435(7043):828-833.
 55. Chen L, Gibbons DL, Goswami S, et al. Metastasis is regulated via microRNA-200/ZEB1 axis control of tumour cell PD-L1 expression and intratumoral immunosuppression. *Nat Commun*. 2014;5(1):5241. [CrossRef PubMed](#)
 56. Osei ET, Florez-Sampedro L, Timens W, Postma DS, Heijink IH, Brandsma C-A. Unravelling the complexity of COPD by microRNAs: it's a small world after all. *Eur Respir J*. 2015;46(3): 807-818. [CrossRef PubMed](#)
 57. Hobbs BD, Tantisira KG. MicroRNAs in COPD: small molecules with big potential. *Eur Respir J*. 2019;53:1900515.
 58. Wang Y, Lyu X, Wu X, Yu L, Hu K. Long non-coding RNA PVT1, a novel biomarker for chronic obstructive pulmonary disease progression surveillance and acute exacerbation prediction potentially through interaction with microRNA-146a. *J Clin Lab Anal*. 2020;34(8):e23346. [CrossRef PubMed](#)
 59. Riordan JR, Rommens JM, Kerem B, et al. Identification of the cystic fibrosis gene: cloning and characterization of complementary DNA. *Science*. 1989;245(4922):1066-1073. [CrossRef PubMed](#)
 60. Oglesby IK, Chotirmall SH, McElvaney NG, Greene CM. Regulation of cystic fibrosis transmembrane conductance regulator by microRNA-145, -223, and -494 is altered in Δ F508 cystic fibrosis airway epithelium. *J Immunol*. 2013;190(7): 3354-3362. [CrossRef PubMed](#)
 61. Ramachandran S, Karp PH, Jiang P, et al. A microRNA network regulates expression and biosynthesis of wild-type and Δ F508 mutant cystic fibrosis transmembrane conductance regulator. *Proc Natl Acad Sci USA*. 2012;109(33): 13362-13367. [CrossRef PubMed](#)
 62. Poy MN, Eliasson L, Krutzfeldt J, et al. A pancreatic islet-specific microRNA regulates insulin secretion. *Nature*. 2004; 432(7014):226-230. [CrossRef PubMed](#)
 63. Moschos SA, Williams AE, Perry MM, Birrell MA, Belvisi MG, Lindsay MA. Expression profiling in vivo demonstrates rapid changes in lung microRNA levels following lipopolysaccharide-induced inflammation but not in the anti-inflammatory action of glucocorticoids. *BMC Genomics*. 2007;8(1):240. [CrossRef PubMed](#)
 64. Buggele WA, Johnson KE, Horvath CM. Influenza A virus infection of human respiratory cells induces primary microRNA expression. *J Biol Chem*. 2012;287(37):31027-31040. [CrossRef PubMed](#)
 65. Lam W-Y, Yeung AC-M, Ngai KL-K, et al. Effect of avian influenza A H5N1 infection on the expression of microRNA-141



- in human respiratory epithelial cells. *BMC Microbiol.* 2013;13(1):104. [CrossRef PubMed](#)
66. Li Y, Li J, Belisle S, Baskin CR, Tumpey TM, Katze MG. Differential microRNA expression and virulence of avian, 1918 reassortant, and reconstructed 1918 influenza A viruses. *Virology.* 2011;421(2):105-113. [CrossRef PubMed](#)
 67. Baulina NM, Kulakova OG, Favorova OO. MicroRNAs: the role in autoimmune inflammation. *Acta Nat (Engl Ed).* 2016;8(1):21-33. [PubMed](#)
 68. Birkhaug IM, Inchley CS, Aamodt G, Ånestad G, Nystad W, Nakstad B. Infectious burden of respiratory syncytial virus in relation to time of birth modifies the risk of lower respiratory tract infection in infancy: the Norwegian Mother and Child Cohort. *Pediatr Infect Dis J.* 2013;32(6):e235-e241. [CrossRef PubMed](#)
 69. Rossi GA, Silvestri M, Colin AA. Respiratory syncytial virus infection of airway cells: role of microRNAs. *Pediatr Pulmonol.* 2015;50(7):727-732. [CrossRef PubMed](#)
 70. Głobińska A, Pawełczyk M, Kowalski ML. MicroRNAs and the immune response to respiratory virus infections. *Expert Rev Clin Immunol.* 2014;10(7):963-971. [CrossRef PubMed](#)
 71. Leon-Icaza SA, Zeng M, Rosas-Taraco AG. microRNAs in viral acute respiratory infections: immune regulation, biomarkers, therapy, and vaccines. *ExRNA.* 2019;1(1):1-7. [CrossRef PubMed](#)
 72. Gralinski LE, Baric RS. Molecular pathology of emerging coronavirus infections. *J Pathol.* 2015;235(2):185-195. [CrossRef PubMed](#)
 73. Lu D, Chatterjee S, Xiao K, et al. MicroRNAs targeting the SARS-CoV-2 entry receptor ACE2 in cardiomyocytes. *J Mol Cell Cardiol.* 2020;148:46-49. [CrossRef PubMed](#)
 74. Othumpangat S, Noti JD, Beezhold DH. Lung epithelial cells resist influenza A infection by inducing the expression of cytochrome c oxidase VIc which is modulated by miRNA 4276. *Virology.* 2014;468-470:256-264. [CrossRef PubMed](#)
 75. Song L, Liu H, Gao S, Jiang W, Huang WJ. Cellular microRNAs inhibit replication of the H1N1 influenza A virus in infected cells. *J Virol.* 2010;84(17):8849-8860.
 76. Ma YJ, Yang J, Fan XL, et al. Cellular microRNA let-7c inhibits M1 protein expression of the H1N1 influenza A virus in infected human lung epithelial cells. *J Cell Mol Med.* 2012;16(10):2539-2546. [CrossRef PubMed](#)
 77. Deng Y, Yan Y, Tan KS, et al. MicroRNA-146a induction during influenza H3N2 virus infection targets and regulates TRAF6 levels in human nasal epithelial cells (hNECs). *Exp Cell Res.* 2017;352(2):184-192.
 78. Tambyah PA, Sepramaniam S, Ali JM, et al. microRNAs in circulation are altered in response to influenza A virus infection in humans. *PLoS One.* 2013;8(10):e76811.
 79. Xia B, Lu J, Wang R, et al. miR-21-3p regulates influenza A virus replication by targeting histone deacetylase-8. *Front Cell Infect Microbiol.* 2018;8:175.
 80. Bondanese VP, Francisco-Garcia A, Bedke N, Davies DE, Sanchez-Elsner T. Identification of host miRNAs that may limit human rhinovirus replication. *World J Biol Chem.* 2014;5(4):437.
 81. Ouda R, Onomoto K, Takahasi K, et al. Retinoic acid-inducible gene I-inducible miR-23b inhibits infections by minor group rhinoviruses through down-regulation of the very low density lipoprotein receptor. *J Biol Chem.* 2011;286(29):26210-26219. [CrossRef](#)
 82. Bakre A, Mitchell P, Coleman JK, et al. Respiratory syncytial virus modifies microRNAs regulating host genes that affect virus replication. *J Gen Virol.* 2012;93(Pt 11):2346-2356. [CrossRef](#)
 83. Thornburg NJ, Hayward SL, Crowe Jr. Respiratory syncytial virus regulates human microRNAs by using mechanisms involving beta interferon and NF-κB. *mBio.* 2012;3(6):e00220-12. [CrossRef](#)
 84. Chen X-M, Splinter PL, O'Hara SP, LaRusso NF. A cellular micro-RNA, let-7i, regulates Toll-like receptor 4 expression and contributes to cholangiocyte immune responses against *Cryptosporidium parvum* infection. *J Biol Chem.* 2007;282(39):28929-28938.
 85. Vergoulis T, Vlachos IS, Alexiou P, et al. TarBase 6.0: capturing the exponential growth of miRNA targets with experimental support. *Nucleic Acids Res.* 2012;40(D1):D222-D229.
 86. Othumpangat S, Walton C, Piedimonte G. MicroRNA-221 modulates RSV replication in human bronchial epithelium by targeting NGF expression. *PLoS One.* 2012;7(1):e30030.
 87. Inchley CS, Sonerud T, Fjærli HO, Nakstad B. Nasal mucosal microRNA expression in children with respiratory syncytial virus infection. *BMC Infect Dis.* 2015;15(1):1-11.
 88. Lai FW, Stephenson KB, Mahony J, Lichty BD. Human coronavirus OC43 nucleocapsid protein binds microRNA 9 and potentiates NF-κB activation. *J Virol.* 2014;88(1):54-65.
 89. Mallick B, Ghosh Z, Chakrabarti J. MicroRNome analysis unravels the molecular basis of SARS infection in bronchoalveolar stem cells. *PLoS One.* 2009;4(11):e7837.
 90. Tahamtan A, Inchley CS, Marzban M, et al. The role of microRNAs in respiratory viral infection: friend or foe? *Rev Med Virol.* 2016;26(6):389-407. [CrossRef](#)
 91. Zhang X, Chu H, Wen L, et al. Competing endogenous RNA network profiling reveals novel host dependency factors required for MERS-CoV propagation. *Emerg Microbes Infect.* 2020;9(1):733-746. [CrossRef](#)
 92. Hasan MM, Akter R, Ullah M, Abedin M, Ullah G, Hossain M. A computational approach for predicting role of human microRNAs in MERS-CoV genome. *Adv Bioinformatics.* 2014;2014:967946.
 93. Sabbatinelli J, Giuliani A, Matacchione G, et al. Decreased serum levels of the inflammaging marker miR-146a are associated with clinical non-response to tocilizumab in COVID-19 patients. *Mech Ageing Dev.* 2021;193:111413. [CrossRef](#)
 94. Chow JT-S, Salmena LJG. Prediction and analysis of SARS-CoV-2-targeting microRNA in human lung epithelium. *Genes (Basel).* 2020;11(9):1002. [CrossRef](#)
 95. Mukhopadhyay D, Mussa BM. Identification of novel hypothalamic microRNAs as promising therapeutics for SARS-CoV-2 by regulating ACE2 and TMPRSS2 expression: an in silico analysis. *Brain Sci.* 2020;10(10):666.
 96. Mutlu M, Raza U, Saatci Ö. miR-200c: a versatile watchdog in cancer progression, EMT, and drug resistance. *J Mol Med (Berl).* 2016;94(6):629-644. [CrossRef PubMed](#)
 97. Filios SR, Xu G, Chen J, Hong K, Jing G, Shalev A. MicroRNA-200 is induced by thioredoxin-interacting protein and regulates Zeb1 protein signaling and beta cell apoptosis. *J Biol Chem.* 2014;289(52):36275-36283. [CrossRef PubMed](#)
 98. Shao X-L, Chen Y, Gao L. MiR-200c suppresses the migration of retinoblastoma cells by reversing epithelial mesenchymal transition. *Int J Ophthalmol.* 2017;10(8):1195-1202. [CrossRef PubMed](#)
 99. Pimenta R, Viana NI, Dos Santos GA, et al. MiR-200c-3p expression may be associated with worsening of the clinical course of patients with COVID-19. *Mol Biol Res Commun.* 2021;10(3):141-147. [PubMed](#)
 100. Liu Q, Du J, Yu X, et al. miRNA-200c-3p is crucial in acute respiratory distress syndrome. *Cell Discov.* 2017;3(1):17021. [CrossRef PubMed](#)
 101. Zou Z, Yan Y, Shu Y, et al. Angiotensin-converting enzyme 2 protects from lethal avian influenza A H5N1 infections. *Nat Commun.* 2014;5(1):3594. [CrossRef PubMed](#)
 102. Imai Y, Kuba K, Rao S, et al. Angiotensin-converting enzyme 2 protects from severe acute lung failure. *Nature.* 2005;436(7047):112-116. [CrossRef PubMed](#)
 103. Vickers C, Hales P, Kaushik V, et al. Hydrolysis of biological peptides by human angiotensin-converting enzyme-related



- carboxypeptidase. *J Biol Chem.* 2002;277(17):14838-14843. [CrossRef PubMed](#)
104. Michel MC, Brunner HR, Foster C, Huo Y. Angiotensin II type 1 receptor antagonists in animal models of vascular, cardiac, metabolic and renal disease. *Pharmacol Ther.* 2016;164:1-81. [CrossRef PubMed](#)
105. Chow BS, Allen TJ. Angiotensin II type 2 receptor (AT2R) in renal and cardiovascular disease. *Clin Sci (Lond).* 2016;130(15):1307-1326. [CrossRef PubMed](#)
106. Patel VB, Zhong J-C, Grant MB, Oudit GY. Role of the ACE2/angiotensin 1–7 axis of the renin–angiotensin system in heart failure. *Circ Res.* 2016;118(8):1313-1326. [CrossRef PubMed](#)
107. Andersen KG, Rambaut A, Lipkin WI, Holmes EC, Garry RF. The proximal origin of SARS-CoV-2. *Nat Med.* 2020;26(4):450-452. [CrossRef PubMed](#)
108. Humphries B, Yang C. The microRNA-200 family: small molecules with novel roles in cancer development, progression and therapy. *Oncotarget.* 2015;6(9):6472-6498. [CrossRef PubMed](#)
109. Benhabib H, Guo W, Pierce BM, Mendelson CR. The miR-200 family and its targets regulate type II cell differentiation in human fetal lung. *J Biol Chem.* 2015;290(37):22409-22422. [CrossRef PubMed](#)
110. Fosbøl EL, Butt JH, Østergaard L, et al. Association of angiotensin-converting enzyme inhibitor or angiotensin receptor blocker use with COVID-19 diagnosis and mortality. *JAMA.* 2020;324(2):168-177. [CrossRef PubMed](#)
111. Papannarao JB, Schwenke D, Manning PJ, Katare R. Upregulated miR-200c may increase the risk of obese individuals to severe COVID-19. *medRxiv.* 2021. [CrossRef](#)
112. Li W, Moore MJ, Vasileva N, et al. Angiotensin-converting enzyme 2 is a functional receptor for the SARS coronavirus. *Nature.* 2003;426(6965):450-454. [CrossRef PubMed](#)
113. Qin C, Zhou L, Hu Z, et al. Dysregulation of immune response in patients with coronavirus 2019 (COVID-19) in Wuhan, China. *Clin Infect Dis.* 2020;71(15):762-768. [CrossRef PubMed](#)
114. Yang C, Li Y, Xiao S-Y. Differential expression of ACE2 in the respiratory tracts and its relationship to COVID-19 pathogenesis. *EBioMedicine.* 2020;60:103004. [CrossRef PubMed](#)
115. Soltani S, Zandi M. miR-200c-3p upregulation and ACE2 downregulation via bacterial LPS and LTA as interesting aspects for COVID-19 treatment and immunity. *Mol Biol Rep.* 2021;48(7):5809-5810. [CrossRef](#)
116. Nersisyan S, Shkurnikov M, Turchinovich A, Knyazev E, Tonevitsky A. Integrative analysis of miRNA and mRNA sequencing data reveals potential regulatory mechanisms of ACE2 and TMPRSS2. *PLoS One.* 2020;15(7):e0235987-e. [CrossRef](#)
117. Mitra D, Das PM, Huynh FC, Jones FE. Jumonji/ARID1 B (JARID1B) protein promotes breast tumor cell cycle progression through epigenetic repression of microRNA let-7e. *J Biol Chem.* 2011;286(47):40531-40535. [CrossRef PubMed](#)
118. Enkhbaatar Z, Terashima M, Oktyabri D, et al. KDM5B histone demethylase controls epithelial-mesenchymal transition of cancer cells by regulating the expression of the microRNA-200 family. *Cell Cycle.* 2013;12(13):2100-2112. [CrossRef PubMed](#)
119. Bozgeyik I. Therapeutic potential of miRNAs targeting SARS-CoV-2 host cell receptor ACE2. *Meta Gene.* 2021;27:100831. [CrossRef PubMed](#)

Assessment of background levels of autoantibodies as a prognostic marker for severe SARS-CoV-2 infection

Frank M. Sullivan¹, Agnes Tello^{1,2}, Petra Rauchhaus³, Virginia Hernandez Santiago¹, Fergus Daly¹

¹Division of Population and Behavioural Sciences, St Andrews University Medical School, St Andrews - United Kingdom

²Edinburgh Clinical Trials Unit, Usher Institute, University of Edinburgh, Edinburgh - United Kingdom

³Tayside Clinical Trials Unit, University of Dundee, Dundee - United Kingdom

ABSTRACT

Background: Patients with more severe forms of SARS-CoV-2 exhibit activation of immunological cascades. Participants (current or ex-smokers with at least 20 years pack history) in a trial (Early Diagnosis of Lung Cancer, Scotland [ECLS]) of autoantibody detection to predict lung cancer risk had seven autoantibodies measured 5 years before the pandemic. This study compared the response to Covid infection in study participants who tested positive and negative to antibodies to tumour-associated antigens: p53, NY-ESO-1, CAGE, GBU4-5, HuD, MAGE A4 and SOX2.

Methods: Autoantibody data from the ECLS study was deterministically linked to the EAVE II database, a national, real-time prospective cohort using Scotland's health data infrastructure, to describe the epidemiology of SARS-CoV-2 infection, patterns of healthcare use and outcomes. The strength of associations was explored using a network algorithm for exact contingency table significance testing by permutation.

Results: There were no significant differences discerned between SARS-CoV-2 test results and EarlyCDT-Lung test results ($p = 0.734$). An additional analysis of intensive care unit (ICU) admissions detected no significant differences between those who tested positive and negative. Subgroup analyses showed no difference in COVID-19 positivity or death rates amongst those diagnosed with chronic obstructive pulmonary disease (COPD) with positive and negative EarlyCDT results.

Conclusions: This hypothesis-generating study demonstrated no clinically valuable or statistically significant associations between EarlyCDT positivity in 2013-15 and the likelihood of SARS-CoV-2 positivity in 2020, ICU admission or death in all participants (current or ex-smokers with at least 20 years pack history) or in those with COPD or lung cancer.

Keywords: COVID-19, Current or ex-smokers, Lung cancer, Mortality prediction, Serum biomarkers

Introduction

Patients infected with Covid-19 show a range of immune responses, from weaker immune responses in asymptomatic individuals, to symptomatic patients showing a varying degree of immune dysregulation. These may be manifested by increased levels of interleukins, C-reactive protein and D-dimer, along with lymphopenia, monocytosis and neutrophilia. Extremely high levels of proinflammatory cytokines can lead to a cytokine storm and macrophage activation

syndrome in patients with severe SARS-CoV-2. This may cause harmful tissue damage, multiple organ failure and hypercoagulability, and is associated with poor clinical outcomes (1). Conversely it is known that people with immune deficiency have an increase in mortality when admitted to hospital with Covid-19 (2). A range of serum autoantibodies, such as nucleolar antinuclear antibodies (ANAs), antineutrophil cytoplasmic antibody (ANCA), anti-cyclic citrullinated peptide, and antiphospholipid autoantibodies, have already been detected in severe SARS-CoV-2 patients and linked to disease severity, reflecting immune system dysregulation in patients with severe SARS-CoV-2 lung disease (3-5). It is not yet clear, however, whether patients who exhibit such robust immune response to SARS-CoV-2 have higher background levels of antibody and autoantibody responsiveness when compared to patients who develop mild disease (6), and for how long the level of autoantibodies persist. One form of antibody response to the development of abnormal cell surface characteristics is tumour-associated autoantibodies. These proteins are produced early in tumorigenesis, being measurable up to 5 years before the development of clinical symptoms (7). They represent biologically amplified markers,

Received: September 7, 2021

Accepted: April 20, 2022

Published online: May 3, 2022

Corresponding author:

Frank M. Sullivan
Division of Population and Behavioural Sciences
St Andrews University Medical School
St Andrews - United Kingdom
fms20@st-andrews.ac.uk



increasing the detectable signal for the corresponding level of antigen (8). They persist in the circulation with half-lives of typically up to 30 days (9).

The EarlyCDT-Lung test is an enzyme-linked immunosorbent assay (ELISA) that measures seven autoantibodies, each with individual specificity for the following tumour-associated antigens (TAAs): p53, NY-ESO-1, CAGE, GBU4-5, HuD, MAGE A4 and SOX2 (10). A sample is positive if at least one autoantibody is elevated above a predetermined cut-off (11). The test has been developed throughout the pre-clinical, clinical assay validation and retrospective biomarker development pathway stages. In cohort studies, it has demonstrated a specificity of 91% and sensitivity of 41%. The Early Diagnosis of Lung Cancer Scotland (ECLS) study was a phase IV biomarker trial using EarlyCDT-Lung followed by imaging in 12,208 smokers and ex-smokers aged 50-75 at risk of developing lung cancer recruited from General Practices in Scotland (12,13). A total of 6,088 participants in the intervention arm received the EarlyCDT-Lung test at the baseline visit and 598 (9.8%) had a positive autoantibody result. In the 2-year analysis of the ECLS trial, EarlyCDT-Lung was shown to reduce late stage presentations of lung cancer.

We have investigated whether the production of autoantibodies in response to cell surface abnormalities in cancer, as measured by the baseline EarlyCDT-Lung test in the ECLS trial, was associated with more severe disease in at-risk participants (current and former smokers) who then developed a SARS-CoV-2 infection 5-6 years later.

Methods

Participants aged 50-75 who were current or ex-smokers with at least 20 years pack history were recruited to ECLS between December 2013 and April 2015, and all baseline assessments of plasma antibody levels occurred during this time (14). SARS-CoV-2 status and outcome data for ECLS participants during 2020 were obtained from the EAVE II database, which is a national, real-time prospective cohort using Scotland's health data infrastructure, to describe the epidemiology of SARS-CoV-2 infection, patterns of healthcare use and outcomes (15,16). Data from both sources was linked using Scotland's Community Health Index (CHI) number at the University of Dundee's Health Informatics Centre (HIC) (17,18).

The strength of associations was explored using a network algorithm for exact contingency table significance testing by permutation. This approach is appropriate for the sparseness of the data here, where an approximate chi-squared analysis would provide severely discrepant outputs. (For 2 × 2 contingency tables, the network algorithm reduces identically to Fisher's exact test.)

Results

There were no significant differences discerned between SARS-CoV-2 test results and EarlyCDT-Lung test results (positive/negative) ($p = 0.734$); or likewise between SARS-CoV-2 test results and EarlyCDT-Lung test results (positive/negative/control) ($p = 0.779$); or finally between SARS-CoV-2 test results and Treatment (tested/not tested) ($p = 0.587$). An additional

analysis of intensive care unit (ICU) admissions detected no significant differences between those who tested positive and negative.

There was no difference in COVID-19 positivity or death rates amongst those diagnosed with lung cancer with positive and negative EarlyCDT-Lung test results (Tab. I).

Table I - SARS-CoV-2 test results by EarlyCDT-Lung test result

Result of SARS-CoV-2 test	Positive		Negative		Control	
	N	%	N	%	N	%
Positive	9	6.7	86	7.8	84	7.0
Negative	126	93.3	1021	92.2	1110	93.0
Total	135	100	1107	100	1194	100
<i>Patient deceased</i>						
No	131	97.0	1072	96.8	1155	96.7
Yes	4	3.0	35	3.2	39	3.3
Total	135	100	1107	100	1194	100

In Table II, nil significance was found.

Table II - Outcomes in at-risk participants (current and former smokers) with lung cancer

Stage	EarlyCDT-Lung test result						Total	
	Test-positive		Test-negative		Not tested		N	%
	N	%	N	%	N	%	N	%
Stage 3	0	(0.0)	1	(14.3)	4	(44.4)	5	(27.8)
Stage 4	0	(0.0)	1	(14.3)	0	(0.0)	1	(5.6)
Other	2	(0.0)	5	(71.4)	5	(55.6)	12	(66.7)
Total	2	(100)	7	(100)	9	(100)	18	(100)
Covid result	N	%	N	%	N	%	N	%
Test-positive	0	(0.0)	1	(14.3)	1	(11.1)	2	(11.1)
Test-negative	2	(100.0)	6	(85.7)	8	(88.9)	16	(88.9)
Total	2	(100)	7	(100)	9	(100)	18	(100)
OR** = 0.00 (0.00, 66.5) $p = 1.0$								
Hospitalized*	N	%	N	%	N	%	N	%
No	0	(0.0)	4	(57.1)	3	(33.3)	7	(38.9)
Yes	2	(100.0)	3	(42.9)	6	(66.7)	11	(61.1)
Total	2	(100)	7	(100)	9	(100)	18	(100)
OR** = 0.00 (0.00, 4.20) $p = 0.44$								
Death*	N	%	N	%	N	%	N	%
No	2	(100.0)	6	(85.7)	9	(100.0)	17	(94.4)
Yes	0	(0.0)	1	(14.3)	0	(0.0)	1	(5.6)
Total	2	(100)	7	(100)	9	(100)	18	(100)
OR** = 9999 (0.015, 9999) $p = 1.0$								

*Event within 28 days of a Covid test.

**Odds ratio (Test-positive vs Test-negative).

Table III shows no difference in COVID-19 positivity or death rates amongst those diagnosed with chronic obstructive pulmonary disease (COPD) with positive and negative EarlyCDT results.

Table III - Outcomes in at-risk participants (current and former smokers) with COPD

Covid result	EarlyCDT-Lung test result							
	Test-positive		Test-negative		Not tested		Total	
	N	%	N	%	N	%	N	%
Positive	1	(6.6)	3	(2.6)	9	(8.3)	13	(5.4)
Negative	15	(93.8)	113	(97.4)	100	(91.7)	228	(94.6)
Total	16	(100)	116	(100)	109	(100)	241	(100)
OR** = 2.51 (0.0913, 24.13) p = 0.407								
Hospitalized*	N	%	N	%	N	%	N	%
No	9	(56.3)	68	(58.6)	58	(53.2)	135	(56.0)
Yes	7	(43.8)	48	(41.4)	51	(46.8)	106	(44.0)
Total	16	(100)	116	(100)	109	(100)	241	(100)
OR** = 0.908 (0.312, 2.858) p = 1.0								
Death*	N	%	N	%	N	%	N	%
No	16	(100.0)	110	(94.8)	105	(96.3)	231	(95.9)
Yes	0	(0.0)	6	(5.2)	4	(3.7)	10	(4.1)
Total	16	(100)	116	(100)	109	(100)	241	(100)
OR** = 9999 (0.176, 9999) p = 1.0								

*Event within 28 days of a Covid test.

**Odds ratio (Test-positive vs Test-negative).

Discussion and conclusions

No clinically valuable or statistically significant associations between EarlyCDT-Lung positivity in 2013-15 and the likelihood of SARS-CoV-2 positivity in 2020, ICU admission or death were found. This was true for the entire study cohort and in subgroup analyses of at-risk participants (current and former smokers) with lung cancer and COPD. This is in contrast to those exhibiting the nucleolar immunofluorescence pattern where a significant association with interstitial lung SARS-CoV-2 disease has been demonstrated (19).

Strengths of the study include the community-based sampling of the ECLS cohort, large numbers of the cohort who had a Covid test validated by laboratory and outcome assessment. Weaknesses include the time which had elapsed between the initial trial and the onset of the pandemic, as well as small numbers of study subjects who were in the subgroup analyses.

Some studies have shown that some routine clinical laboratory tests, such as lymphocyte count, lactate dehydrogenase and D-dimer are known to be affected in patients with COVID-19 (20), with lymphopenia, raised lactate dehydrogenase and elevated D-dimer being associated with worse disease severity and outcomes (21-23). Other studies have

shown significant differences in inflammatory markers amongst patients who required ICU admission compared to patients who have not, and markers of infection and inflammation such as C-reactive protein, procalcitonin, and ferritin which are, as expected, correlated with severe disease (24-27).

This hypothesis-generating study did not find a clear association between the expression of tumour-associated antibodies in the ECLS cohort of at-risk participants (all current and former smokers) and the development of SARS-CoV-2 infection and its complications 5 years later.

Author disclosures

This project was funded by The Lung Foundation. The funder had no role in the design, conduct or analysis of the study. The authors have no other financial conflicts to disclose.

The authors confirm that all appropriate ethical guidelines for the use of human subjects have been followed and ethics committee review has been obtained. The authors confirm that all necessary patient/participant consent or assent has been obtained, and the appropriate institutional forms have been archived.

A version of the article appears as a preprint on ResearchSquare (DOI: 10.21203/rs.3.rs-842075/v1)

Institutional approval was provided by the University of St Andrews.

References

1. Jamal M, Bangash HI, Habiba M, et al. Immune dysregulation and system pathology in COVID-19. *Virulence*. 2021;12(1): 918-936. [CrossRef PubMed](#)
2. Geretti AM, Stockdale AJ, Kelly SH, et al. Outcomes of COVID-19 related hospitalization among people with HIV in the ISARIC WHO Clinical Characterization Protocol (UK): a prospective observational study. *Clin Infect Dis*. 2021 Oct 23:ciaa1605. [CrossRef PubMed](#)
3. Chang SH, Minn D, Kim YK. Autoantibodies in moderate and critical cases of COVID-19. *Clin Transl Sci*. 2021;14(5):1625-1626. [CrossRef PubMed](#)
4. Chauvineau-Grenier A, Bastard P, Servajean A, et al. Autoantibodies neutralizing type I interferons in 20% of COVID-19 deaths in a French hospital. *J Clin Immunol*. 2022 Apr;42(3): 459-470. [CrossRef PubMed](#)
5. Pascolini S, Vannini A, Deleonardi G, et al. COVID-19 and immunological dysregulation: can autoantibodies be useful? *Clin Transl Sci*. 2021;14(2):502-508. [CrossRef PubMed](#)
6. Widjaja G, Turki Jalil A, Sulaiman Rahman H, et al. Humoral immune mechanisms involved in protective and pathological immunity during COVID-19. *Hum Immunol*. 2021 Jul 1:S0198-8859(21)00174-9. [CrossRef PubMed](#)
7. Zhong L, Coe SP, Stromberg AJ, Khattar NH, Jett JR, Hirschowitz EA. Profiling tumor-associated antibodies for early detection. [CrossRef PubMed](#)
8. Chu GCW, Lazare K, Sullivan F. Serum and blood based biomarkers for lung cancer screening: a systematic review. *BMC Cancer*. 2018;18(1):181. [CrossRef PubMed](#)
9. Anderson KS, LaBaer J. The sentinel within: exploiting the immune system for cancer biomarkers. *J Proteome Res*. 2005; 4(4):1123-1133. [CrossRef PubMed](#)
10. Lam S, Boyle P, Healey GF, et al. EarlyCDT-Lung: an immunobio-marker test as an aid to early detection of lung cancer. *Cancer Prev Res (Phila)*. 2011;4(7):1126-1134. [CrossRef PubMed](#)
11. Murray A, Chapman CJ, Healey G, et al. Technical validation of an autoantibody test for lung cancer. *Ann Oncol*. 2010;21(8): 1687-1693. [CrossRef PubMed](#)



12. Pepe MS, Etzioni R, Feng Z, et al. Phases of biomarker development for early detection of cancer. *J Natl Cancer Inst.* 2001 Jul;93(14):1054-1061. [CrossRef PubMed](#)
13. Sullivan FM, Mair FS, Anderson W, et al; Early Diagnosis of Lung Cancer Scotland (ECLS) Team. Earlier diagnosis of lung cancer in a randomised trial of an autoantibody blood test followed by imaging. *Eur Respir J.* 2020;57:2000670. [CrossRef PubMed](#)
14. Sullivan FM, Farmer E, Mair FS, et al. Detection in blood of autoantibodies to tumour antigens as a case-finding method in lung cancer using the EarlyCDT®-Lung Test (ECLS): study protocol for a randomized controlled trial. *BMC Cancer.* 2017;17(1):187. [CrossRef PubMed](#)
15. Kendrick S, Clarke J. The Scottish record linkage system. *Health Bull (Edinb).* 1993;51(2):72-79. [PubMed](#)
16. Mulholland RH, Vasileiou E, Simpson CR, et al. Cohort profile: early pandemic evaluation and enhanced surveillance of COVID-19 (EAVE II) database. *Int J Epidemiol.* 2021;50(4):1064-1065. [CrossRef PubMed](#)
17. National Health Service (NHS). Community Health Index (CHI). [Online](#) (last accessed August 2021).
18. Data Service, Data Team Linkage Options, University of Dundee [Online](#) (last accessed April 2022).
19. Muratori P, Lenzi M, Muratori L, Granito A. Antinuclear antibodies in COVID 19. *Clin Transl Sci.* 2021;14(5):1627-1628. [CrossRef PubMed](#)
20. Qi X, Liu C, Jiang Z, et al. Multicenter analysis of clinical characteristics and outcomes in patients with COVID-19 who develop liver injury. *J Hepatol.* 2020;73(2):455-458. [CrossRef PubMed](#)
21. Lee J, Park SS, Kim TY, Lee DG, Kim DW. Lymphopenia as a biological predictor of outcomes in COVID-19 patients: a nationwide cohort study. *Cancers (Basel).* 2021;13(3):471. [CrossRef PubMed](#)
22. Martha JW, Wibowo A, Pranata R. Prognostic value of elevated lactate dehydrogenase in patients with COVID-19: a systematic review and meta-analysis. *Postgrad Med J.* 2021 Jan 15:postgradmedj-2020-139542. [CrossRef PubMed](#)
23. Poudel A, Poudel Y, Adhikari A, et al. D-dimer as a biomarker for assessment of COVID-19 prognosis: d-dimer levels on admission and its role in predicting disease outcome in hospitalized patients with COVID-19. *PLoS One.* 2021;16(8):e0256744. [CrossRef PubMed](#)
24. Shen B, Yi X, Sun Y, et al. Proteomic and metabolomic characterization of COVID-19 patient sera. *Cell.* 2020;182(1):59-72. e15. [CrossRef PubMed](#)
25. Yitbarek GY, Walle Ayehu G, Asnakew S, et al. The role of C-reactive protein in predicting the severity of COVID-19 disease: a systematic review. *SAGE Open Med.* 2021;9:20503121211050755. [CrossRef PubMed](#)
26. Tong-Minh K, van der Does Y, Engelen S, et al. High procalcitonin levels associated with increased intensive care unit admission and mortality in patients with a COVID-19 infection in the emergency department. *BMC Infect Dis.* 2022;22(1):165. [CrossRef PubMed](#)
27. Kaushal K, Kaur H, Sarma P, et al. Serum ferritin as a predictive biomarker in COVID-19. A systematic review, meta-analysis and meta-regression analysis. *J Crit Care.* 2022 Feb;67:172-181. [CrossRef PubMed](#)

Soluble IL-33 receptor predicts survival in acute kidney injury

Stefan Erfurt¹, Meike Hoffmeister^{2,3}, Stefanie Oess^{2,3}, Katharina Asmus¹, Susann Patschan^{1,3}, Oliver Ritter^{1,3}, Daniel Patschan^{1,3}

¹Department of Internal Medicine I – Cardiology, Nephrology and Internal Intensive Medicine, Brandenburg University Hospital, Brandenburg Medical School (Theodor Fontane), Brandenburg an der Havel - Germany

²Institute of Biochemistry, Brandenburg Medical School (Theodor Fontane), Brandenburg an der Havel - Germany

³Faculty of Health Sciences (FGW), joint faculty of the University of Potsdam, the Brandenburg Medical School Theodor Fontane and the Brandenburg Technical University Cottbus-Senftenberg, Cottbus - Germany

ABSTRACT

Introduction: The prediction of acute kidney injury (AKI)-related outcomes remains challenging. Herein we prospectively quantified soluble ST2 (sST2), the circulating isoform of the IL-33 receptor, in hospitalized patients with AKI.

Methods: In-hospital subjects with AKI of various etiology were identified through the in-hospital AKI alert system of the Brandenburg University hospital. sST2 was measured within a maximum of 48 hours from the time of diagnosis of AKI. The following endpoints were defined: in-hospital death, dialysis, recovery of kidney function until demission.

Results: In total, 151 individuals were included in the study. The in-hospital mortality was 16.6%, dialysis therapy became mandatory in 39.7%, no recovery of kidney function occurred in 27.8%. sST2 was significantly higher in nonsurvivors ($p = 0.024$) but did not differ in the two other endpoints. The level of sST2 increased significantly with the severity of AKI. Further differences were detected in subjects with heart insufficiency (lower sST2), and in patients that required ICU treatment, or ventilatory therapy, or vasopressors (all higher).

Conclusions: The current study suggests sST2 as biomarker of “acute distress”: it predicts post-AKI survival and substantially increases in subjects with a higher degree of cumulative morbidity under acute circumstances (e.g., ICU therapy, vasopressor administration).

Keywords: Acute kidney injury, IL-33, Soluble ST2, Mortality, Biomarker

Introduction

Acute kidney injury (AKI) occurs with increasing frequencies at hospitals in central Europe and the United States. It is being estimated that up to 18% of all hospitalized subjects develop AKI during the treatment course (1). The in-hospital mortality of hospital-acquired AKI has been reported to vary from 10% to 20% (1-3), with exceptionally low survival rates under intensive care conditions (4).

Interleukin-33 (IL-33) belongs to the Interleukin-1 family of cytokines (5). The cytokine was initially found within endothelial cell nuclei of so-called human high endothelial venules (HEV). Pichery and colleagues (6) detected the protein within the nuclei of murine cells in various tissues, such as epithelial cells, lymphoid organs, brain, and embryonic tissue. Within nuclei, IL-33 binds to chromatin (7); in the extracellular space however, it interacts with ST2. The latter exists as membrane-bound and soluble isoform (sST2), respectively (8). IL-33 has been shown to modulate the activity of several immunocompetent cells such as mast cells, group 2 innate lymphoid cells (ILC2s), T helper 2 cells, eosinophils, basophils, dendritic cells, macrophages, and others (9).

Early AKI recognition remains difficult, although new biomarkers have been identified in recent years (10). Future diagnostic criteria will most likely include markers of structural kidney damage (11). Until then, AKI is being diagnosed according to the 2012 published “KDIGO clinical practice guidelines for acute kidney injury” (12).

Experimental data suggest a critical role for IL-33 in the pathogenesis of AKI (13,14). Also, several studies evaluated IL-33 and sST2 as biomarkers in inflammatory and

Received: February 17, 2022

Accepted: May 16, 2022

Published online: June 6, 2022

Corresponding author:

Daniel Patschan

Zentrum für Innere Medizin 1, Kardiologie,
Angiologie, Nephrologie Klinikum Brandenburg,
Medizinische Hochschule Brandenburg

Hochstraße 29

14770 Brandenburg - Germany

d.patschan@gmail.com



noninflammatory diseases. The literature on IL-33 reveals heterogeneous findings, including protein elevation or suppression, or constant serum IL-33, depending on etiology and course of the disease (15-17). Also, IL-33 quantification has been associated with substantial difficulties. Lately we summarized the literature on the topic (18). For instance, Ketelaar et al. (19) used 4 different ELISA kits (Quantikine and DuoSet - R&D systems, respectively; ADI-900-201 - Enzo Life Sciences; SKR038 - GenWay Biotech Inc San Diego USA) for analyzing serum samples from asthma patients. The percentages of samples above the lower detection limit (LLD) were 0 (zero) in two kits (ADI-900-201 and SKR038). Also, the Quantikine kit showed only 2% of all samples above the LLD, the DuoSet kit in contrast was successful in at least 76%. Similar observations were made by Asaka et al. (20), who also employed the Quantikine kit. Finally, Riviere and colleagues (18) reported difficulties in IL-33 quantification as well. Regarding IL-33 and sST2 in conjunction, two studies were performed in AKI subjects so far. The first study revealed sST2 as an early predictor of acute kidney injury in patients with myocardial infarction (21). The second investigation showed sST2 to be AKI predictive in subjects undergoing cardiac surgery (22).

Herein, we prospectively analyzed serum sST2 levels in patients with newly onset AKI of various etiology. Three endpoints were defined: in-hospital death, the need for dialysis, and recovery of kidney function until demission.

Methods

Setting

This prospective observational study was conducted at the Brandenburg University Hospital in Brandenburg an der Havel, Germany. The hospital is part of the Brandenburg Medical School.

Study population and design

The study was approved by the local ethics committee of the Brandenburg Medical School Theodor Fontane in October 2019 (file no. E-01-20190820). All recruited participants were hospitalized patients of the University Hospital Brandenburg. Patients of multiple medical departments with newly onset AKI were included from May 2020 to June 2021. AKI was defined according to criteria 1 or 2 of 2012 revised KDIGO classification (23). The third criterion (urine output of below 0.5 mL/kg/h for at least 6 hours) was not applied since information on urine production was not available in all subjects. Serum IL-33 and sST2 levels were determined once at the time of initial diagnosis of AKI. All patients were over 18 years of age, were not previously receiving renal replacement therapy at the time of blood collection, and signed written informed consent. Preexisting chronic renal failure requiring dialysis, terminal disease with a strictly palliative treatment regimen, suspected or active COVID-19 disease, and age less than 18 years resulted in exclusion from the study. The AKI etiology was identified according to respective criteria for sepsis (24), cardiorenal syndrome types 1 or 3 (25), and hepatorenal syndrome (26). The diagnosis of

obstruction was made by ultrasound analysis, the diagnoses of drug-induced, contrast-associated, and postsurgery AKI were made according to the history. Volume depletion or prerenal AKI was diagnosed if other causes were unlikely and if the patient presented clinical symptoms of volume depletion (e.g., dry skin in conjunction with low blood pressure and tachycardia).

Blood sampling and preanalytics

An automated AKI alert system has been implemented at the Brandenburg University Hospital in 2018. Elevated serum creatinine levels (according to the KDIGO criteria 1 or 2) that are measured during daily laboratory checks are registered by an electronic algorithm and transmitted to the nephrologist in charge. The messages exclusively contain a patient-related number and do not allow to identify individuals without the in-hospital database. After written informed consent was obtained, a standardized venous blood sample was collected in two 3.5 mL serum tubes (BD Vacutainer® SST™ II Advance). Blood was collected in the supine position with as little venous congestion as possible to avoid hemolysis. In patients with central venous line, blood was collected from that catheter. The filled blood tubes were stored upright for 30 minutes to maintain the clotting time specified by the manufacturer. This was followed by centrifugation at 1,400 g for 10 minutes at room temperature. Samples were stored in plastic tubes at constant -22°C until analysis.

Quantification of serum sST2

The quantification of sST2 was performed by using a commercially available kit: Human ST2/IL-33R Quantikine ELISA Kit (DST 200, R&D). The assay detects free and IL-33-complexed ST2. Analyses were performed in duplicates according to the manufacturer's instructions. Sample predilution was adjusted individually to the concentrations. The range of assay sensitivity was 2.45-13.5 pg/mL. Reference blood samples from healthy adults were used for comparison.

Endpoints

Three primary endpoints were defined: in-hospital death, the need for dialysis, and recovery of kidney function until demission. The second criterion (need for dialysis) was fulfilled if one or more dialysis treatment sessions became mandatory. Dialysis was performed as hemodialysis, or hemodiafiltration, or slow extended daily dialysis (SLEDD), or as continuous veno-venous hemodiafiltration (CVVHD(F)). The respective procedure was chosen by the nephrologist in charge. Renal recovery was defined according to the criteria published by Fiorentino et al (27). It was diagnosed, if the last serum creatinine concentration did not differ from the initial value by more than 50%.

Statistics

Initially, results of sST2 quantification were tested for normality with the Kolmogorov-Smirnov test. Since data were not distributed normally, the Mann-Whitney test was applied



for comparisons between two groups. Comparisons between three or more groups were performed with the Kruskal-Wallis test. The results are given as median + the interquartile range (IQR). Correlations were analyzed by calculating the Pearson correlation coefficient. A p-value of below 0.05 was considered as statistically significant. The Youden index (specificity + sensitivity – 1) was employed for the identification of cut-off values, sensitivities and specificities were extracted from ROC (receiver operating characteristic) curves. Statistical analyses were performed with the following applications: WIZARD for MacOS (Version: 2.0.9, developer: Evan Miller, 2021) or Graphpad Prism® (Version 9.3.1).

Results

Baseline characteristics and outcomes

In total, 151 subjects were included in the study (females 62, males 89). The mean age of all individuals was 74.9 ± 13.4 years. The mean in-hospital treatment time was 16.2 ± 10.9 days. In-hospital mortality was 16.6%. Dialysis therapy became mandatory in 39.7%. Renal recovery occurred in 72.2%. All patient characteristics are summarized in Table I.

Etiology and severity of AKI

The most frequent AKI etiology was sepsis with 23.6%. Other etiologies were volume depletion; cardiorenal; contrast-induced (or associated); hepatorenal; drug-induced; obstruction; combined. More than 60% were diagnosed with AKIN (*Acute Kidney Injury Network* (28)) stage III (Tab. I).

Soluble ST2

sST2 was quantified once, at the time of AKI diagnosis plus a maximum of 48 hours in some individuals. Serum ST2 levels correlated negatively with age ($p = 0.004$; $r = -0.233$) but not with the duration of in-hospital treatment ($p = 0.228$) (Fig. 1). Females did not significantly differ from males ($p = 0.407$). Only five patients were younger than 40 years. Out of these, only one subject showed sST2 levels of higher than 2×10^5 pg/mL as opposed to 25% of the individuals with age 60 or higher.

Endpoints

AKI patients with in-hospital death showed significantly higher serum sST2 at the time of diagnosis as compared to surviving subjects ($146,100$ [IQR 97,420-233,700] vs. $74,325$ [IQR 40,030-192,900] pg/mL; $p = 0.024$) (Fig. 2). Additional analysis revealed a sST2 concentration of $>86,110$ pg/mL as cut-off (sensitivity 84%; specificity 55.56%). The risk of in-hospital death was 15.4% in subjects that reached the cut-off (prediction intervals 10.8%-21.4%). Patients requiring dialysis did not differ from those without the need for renal replacement therapy ($123,550$ [IQR 57,050-287,000] vs. $75,890$ [IQR 38,560-189,600] pg/mL; $p = 0.083$) (Fig. 2). Subjects with renal recovery did not differ from patients

Table I - Patients' characteristics

Variable	Result
Age (years \pm SD)	74.9 ± 13.4
Gender (females/males)	62/89
In-hospital treatment (days \pm SD)	16.2 ± 10.9
AKI etiology (%)	
Sepsis	23.6
Volume depletion	23.6
Cardiorenal	20.1
Contrast-induced	12.5
Hepatorenal	2.8
Drug-induced	1.4
Postsurgery	1.4
Obstruction	0.7
Combined	18.5
Morbidities	
Preexisting CKD (%)	73.5
Arterial hypertension (%)	88.4
Diabetes mellitus (%)	48
Coronary artery disease (%)	42.6
Preexisting heart insufficiency (%)	55.6
Pulmonary disease (%)	24.7
Obesity (%)	49
History of neoplasia (%)	27.8
Dialysis initiated (%)	39.7
In-hospital death (%)	16.6
Recovery of kidney function (no/yes in %)	27.8/72.2
ICU treatment (%)	32.5
Ventilatory therapy (%)	17.2
Vasopressor therapy (%)	16.6

without recovery ($78,410$ [IQR 43,520-192,900] vs. $132,900$ [IQR 42,650-258,200] pg/mL; $p = 0.48$) (Fig. 2).

Etiology and AKI stage

sST2 did not differ between all AKI types of a certain etiology ($p = 0.2$). The three most frequent entities (septic AKI; AKI due to volume depletion; cardiorenal AKI) were compared with all other entities combined. However, sST2 did not differ in any of the three analyses (septic AKI, $p = 0.4$; AKI due to volume depletion, $p = 0.6$; cardiorenal AKI, $p = 0.39$). sST2 significantly differed between the AKIN stages (28), the marker gradually increased from stage I to III (I: $51,830$ [IQR 32,310-146,100] vs. II: $73,620$ [IQR 35,650-191,200] vs. III: $128,500$ [IQR 53,060-267,000] pg/mL; $p = 0.014$). The significance levels between AKIN stages I, II, and III were: I vs. II $p = 0.99$; II vs. III $p = 0.35$; I vs. III $p = 0.01$ (Fig. 3).



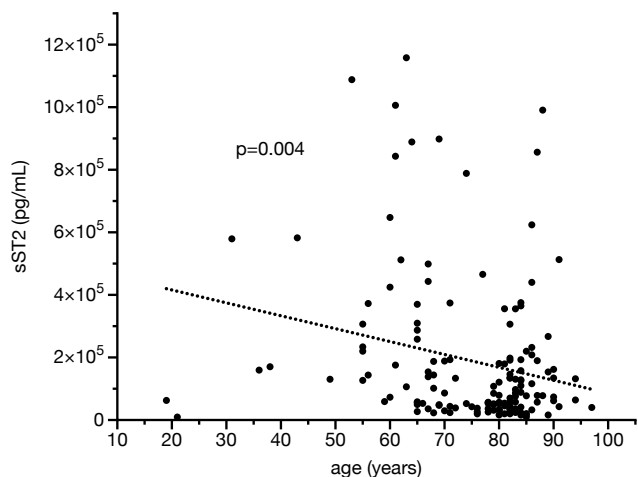


Fig. 1 - Soluble ST2 in relation to the age of all included subjects. Serum levels of the protein correlated negatively with age.

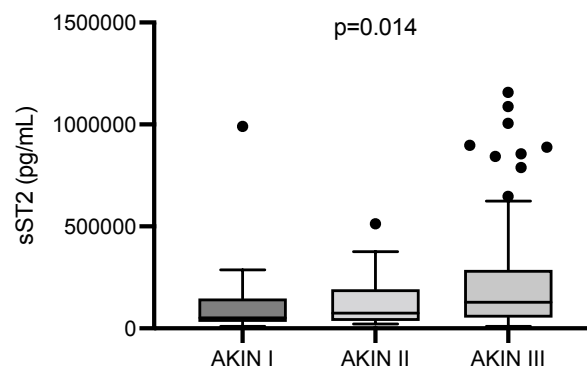


Fig. 3 - Soluble ST2 in relation to the acute kidney injury stage according to AKIN. Serum levels of the protein gradually increased from stages I to III.

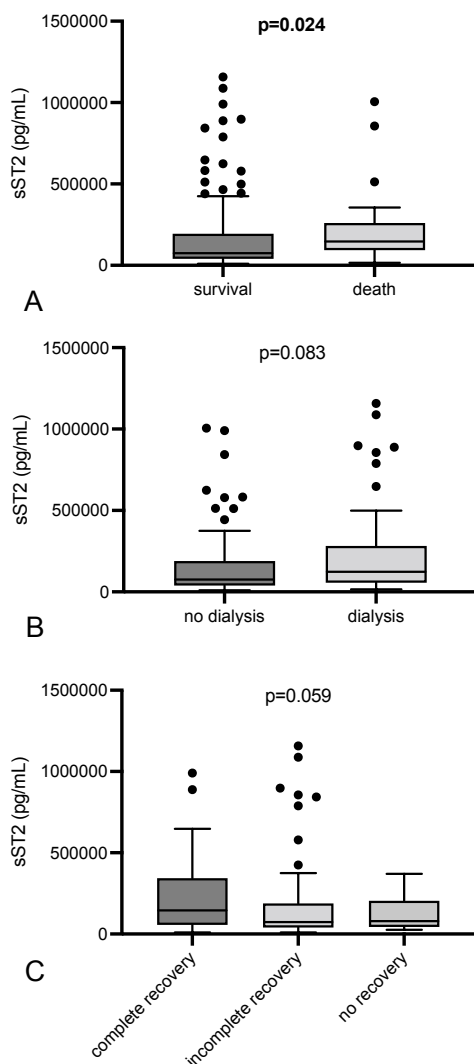


Fig. 2 - Primary endpoints. A) survival; B) dialysis; C) recovery of kidney function. Respective p-values are displayed (the bold p-value in "A" indicates a statistically significant difference).

Morbidities

sST2 did not differ between patients with hypertension or diabetes mellitus as compared to subjects without the respective morbidity ($p = 0.117$ and $p = 0.4$). The same applied for pulmonary disease (one or more of the following diagnoses: chronic obstructive pulmonary disease, asthma, other), obesity, history of neoplasia, and coronary artery disease ($p = 0.934$, $p = 0.247$, $p = 0.738$, and $p = 0.249$). Patients with preexisting heart insufficiency, however, displayed lower serum sST2 than those without heart insufficiency (68,365 [IQR 39,280-134,000] vs. 144,850 [IQR 52,510-309,400] pg/mL; $p = 0.005$) (Fig. 4).

Treatment course

Patients that required treatment at the intensive care unit showed higher sST2 than subjects without ICU therapy (170,200 [IQR 63,970-364,800] vs. 65,745 [IQR 35,620-157,700] pg/mL; $p < 0.001$) (Fig. 3). Subjects that required ventilatory or vasopressor therapy displayed higher sST2 also (181,950 [IQR 107,700-369,800] vs. 73,620 [IQR 40,030-187,200] pg/mL; $p < 0.001$ and 175,500 [IQR 107,700-306,500] vs. 74,755 [IQR 40,030-188,400] pg/mL; $p = 0.004$) (Fig. 5).

Discussion

In the current study, we identified sST2 as novel predictor of survival in subjects with hospital-acquired AKI. To establish new biomarkers in AKI remains a fundamental goal in clinical nephrology. The majority of biomarker studies aimed (and still aim) to find parameters that allow AKI recognition as early as possible. Among the most widely studied molecules are Neutrophil Gelatinase-Associated Lipocalin (NGAL), Kidney Injury Molecule-1 (KIM-1), Liver-Fatty Acid Binding Protein (L-FABP), and the product of urinary Tissue Inhibitor of MetalloProtease-2 (TIMP-2) and Insulin-like Growth Factor-Binding Protein 7 (IGFBP7) (Schrezenmeier and colleagues provided an excellent summary (10)).



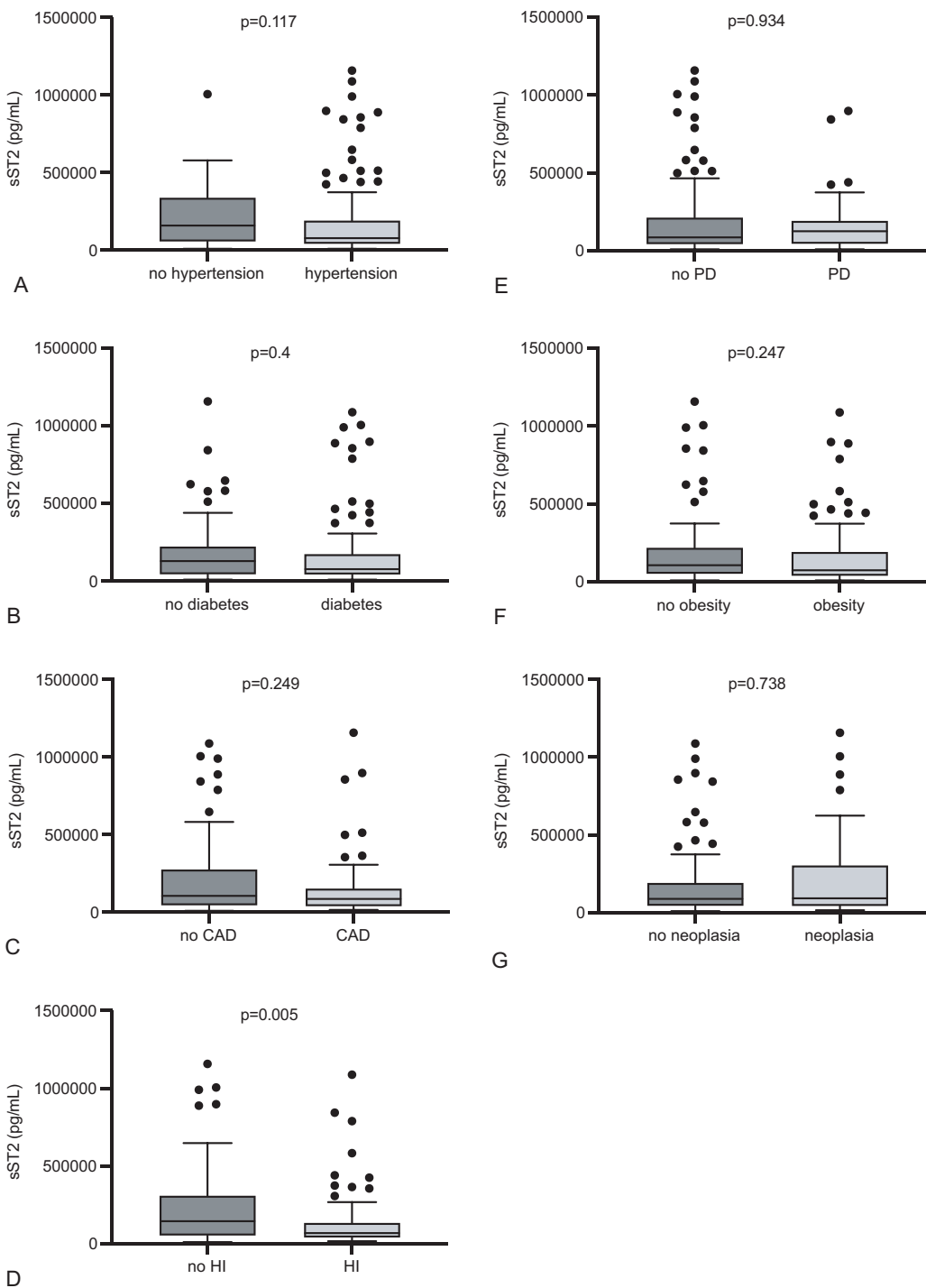


Fig. 4 - Morbidities. In total seven morbidities were analyzed in detail: arterial hypertension (A); diabetes mellitus (B); coronary artery disease (CAD – C); heart insufficiency (HI – D); pulmonary disease (PD – E); obesity (F); history of neoplasia (G). Comparisons were always made between subjects with versus without the respective diagnosis. The only difference in soluble ST2 that reached the level of statistical significance was detected between subjects with versus without preexisting heart insufficiency (higher in subjects without the disease – D).

Several studies additionally evaluated the prognostic value of certain marker molecules, particularly regarding the prediction of in-hospital survival. Hall and colleagues (29) found the urinary concentrations of NGAL, KIM-1, and IL-18 as predictive for the composite endpoint of AKI progression and in-hospital death. All markers were measured instantly if the AKI criteria were fulfilled. A 2011 published study evaluated both the diagnostic and prognostic potency of urinary

NGAL (30). Subjects that reached the primary (composite) endpoint (AKI progression, dialysis, and death) showed higher NGAL levels at the time of inclusion. Survival prediction through both urinary NGAL and KIM-1 was also shown by Nickolas et al (31). Our findings did not only reveal higher sST2 in nonsurvivors but also gradually increased serum levels from AKI stages I to III according to KDIGO (12). Serum ST2 was also higher in subjects that either required vasopressors

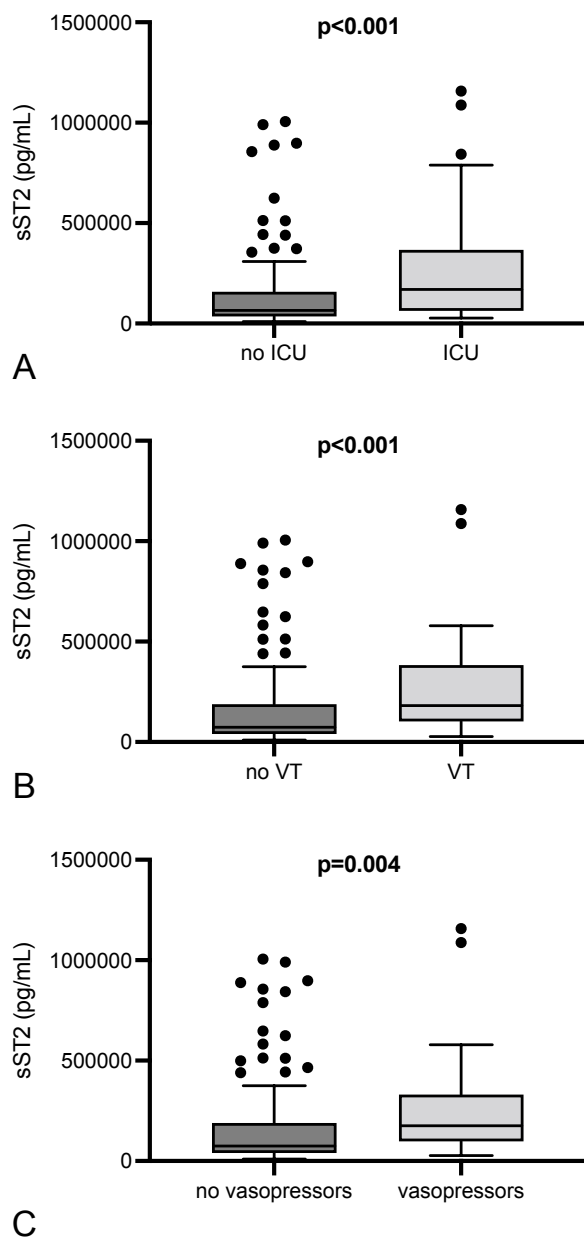


Fig. 5 - Treatment course. sST2 differed in all tested categories: ICU therapy (A), ventilatory (B), and vasopressor therapy (C). The interleukin-33 receptor was detected in significantly higher concentrations if patients received respective measures. ICU = intensive care unit; VT = ventilatory therapy.

or ventilatory therapy or ICU treatment in general. Thus, elevated protein levels are apparently associated with a higher degree of cumulative morbidity under *acute* circumstances. Regarding permanent or preexisting diseases, the only difference occurred between subjects with versus without chronic heart insufficiency. Firouzabadi et al (16) failed to show higher or lower sST2 levels in heart insufficiency as opposed to healthy subjects. The individuals in this particular study did however not suffer from AKI. Regarding cardiac disease, soluble IL-33 receptor (sST2) has been shown to correlate

with myocardial inflammation and fibrosis in rats with acute myocardial infarction (32).

In our study, the predictive value of sST2 was limited to the category survival. Tung and colleagues in contrast identified sST2 to be AKI predictive in patients with ST-segment elevation myocardial infarction (33). In our study cohort, subjects with versus without recovery of kidney function or dialysis did not differ in sST2. The recovery process was only assessed through serum creatinine, a marker that exclusively reflects the amount of glomerular filtration and by no means any adaptive or maladaptive responses within the renal tissue. Several studies included outcome analyses of post-AKI kidney function. Koyner and colleagues (34) identified IL-18, urinary albumin to creatinine ratio, and plasma NGAL to be associated with a higher risk of AKI progression. Comparable to our study, measurements were performed in close timely relation to AKI onset (at the day of AKI diagnosis, at least AKIN stage I). However, subjects exclusively received cardiac surgery. Caironi and colleagues (35) measured plasma proenkephalin A 119-159 (PenKid) in >900 septic subjects in order to identify associations with AKI onset and recovery of kidney (Albumin Italian Outcome Sepsis – ALBIOS – trial). Plasma PenKid was shown as useful not only in AKI but also in post-AKI recovery prediction. The most intriguing difference to our study was the inclusion of subjects with sepsis only. The same applies for the 2018 published Kid-SSS study (Kidney in Sepsis and Septic Shock study), which evaluated the same marker, measured within the first 24 hours after ICU admission (36). More than 580 were included. PenKid levels were associated with major adverse kidney events (MAKES); low levels were suggestive for rapid recovery of kidney function. As opposed to sST2, PenKid reflects the amount of glomerular filtration with high sensitivity. In an observational cohort study, Schunk et al (37) measured the urinary Dickkopf-3 (DKK-3)/creatinine ratio in patients that received cardiac surgery. Some patients participated in the so-called “RenalRIP multicenter trial”. In this particular cohort, a urinary Dickkopf-3 (DKK-3)/creatinine ratio of >471 pg/mg was associated with higher risks for AKI and persistent renal dysfunction. DKK-3 is particularly secreted by stressed tubular epithelial cells (38). In the 2020 published RUBY study finally (39), urinary elevation of the C-C motif chemokine ligand 14 (CCL14) was shown to be predictive for persistent stage III AKI. In the same year, members of the “Acute Disease Quality Initiative Consensus Conference” published “Recommendations on Acute Kidney Injury Biomarkers” (40). Consensus statement number 9 suggests, “... novel biomarkers can be used for prediction of duration and recovery of AKI.” The recommendation received grade C (weak grade). Subsequently, the authors particularly discussed the PenKid and DKK-3 data.

Whether sST2 will presumably serve as marker of recovery prediction in AKI or not still needs to be elucidated more in detail. Herein, a heterogeneous group of AKI subjects was included, suffering from acute kidney dysfunction of various etiology. The data presented in the current study anyhow suggest a role of sST2 as biomarker of “acute distress”: it predicts post-AKI survival and substantially increases in subjects with a higher degree of cumulative morbidity under acute circumstances (e.g., ICU therapy, vasopressor administration). In this respect, two studies

already evaluated the prognostic role of sST2 in sepsis (41,42).

The limitations of the current study shall be mentioned. Prehospital creatinine values were missing in many subjects. The AKI definition according to KDIGO (12) did not consider urine volumes since respective information was missing in too many individuals. Also, follow-up data after hospital demission were not available. Finally, it needs to be evaluated whether or not impaired kidney excretory function potentially modulates circulating sST2 per se. A recently initiated study in sepsis/septic shock will hopefully clarify this particular aspect.

In summary, sST2 may become clinically useful for risk stratification in AKI patients in the future. A respective study should therefore exclusively focus on AKI subjects treated under intensive care conditions. In any case, sST2 has for sure been identified as new candidate for risk prediction in AKI.

Acknowledgment

The authors thank Jana Friedrich for technical assistance.

Disclosures

Conflict of interest: The authors declare that they have no conflict(s) of interest.

Financial support: The study was supported by the *Jackstädt-Stiftung*. Ethics statement: The study was formally approved by the ethics committee of the Medical School of Brandenburg (No.: E-01-20190820).

Author contributions: SE collected all samples and all patient-related clinical data. He also performed all measurements of sST2. He also assisted in writing. MH provided substantial knowledge and experimental expertise regarding quantification of sST2. SO provided substantial knowledge regarding quantification of sST2. KA helped to identify patients and collected patient-related clinical data. SP prepared figures and collected references. OR assisted in data analysis and manuscript writing. DP designed the study, provided funding, analyzed data, and wrote the manuscript. All authors approved the final version of the article.

References

1. Hoste EAJ, Kellum JA, Selby NM, et al. Global epidemiology and outcomes of acute kidney injury. *Nat Rev Nephrol*. 2018;14(10):607-625. [CrossRef PubMed](#)
2. Selby NM, Crowley L, Fluck RJ, et al. Use of electronic results reporting to diagnose and monitor AKI in hospitalized patients. *Clin J Am Soc Nephrol*. 2012;7(4):533-540. [CrossRef PubMed](#)
3. Uchino S, Bellomo R, Bagshaw SM, Goldsmith D. Transient azotaemia is associated with a high risk of death in hospitalized patients. *Nephrol Dial Transplant*. 2010;25(6):1833-1839. [CrossRef PubMed](#)
4. Melo FAF, Macedo E, Fonseca Bezerra AC, et al. A systematic review and meta-analysis of acute kidney injury in the intensive care units of developed and developing countries. *PLoS One*. 2020;15(1):e0226325. [CrossRef PubMed](#)
5. Fields JK, Günther S, Sundberg EJ. Structural basis of IL-1 family cytokine signaling. *Front Immunol*. 2019;10:1412. [CrossRef PubMed](#)
6. Pichery M, Mirey E, Mercier P, et al. Endogenous IL-33 is highly expressed in mouse epithelial barrier tissues, lymphoid organs, brain, embryos, and inflamed tissues: in situ analysis using a novel IL-33-LacZ gene trap reporter strain. *J Immunol*. 2012;188(7):3488-3495. [CrossRef PubMed](#)
7. Roussel L, Erard M, Cayrol C, Girard J-P. Molecular mimicry between IL-33 and KSHV for attachment to chromatin through the H2A-H2B acidic pocket. *EMBO Rep*. 2008;9(10):1006-1012. [CrossRef PubMed](#)
8. Kotsiou OS, Gourgoulanis KI, Zarogiannis SG. IL-33/ST2 axis in organ fibrosis. *Front Immunol*. 2018;9:2432. [CrossRef PubMed](#)
9. Cayrol C, Girard J-P. Interleukin-33 (IL-33): A nuclear cytokine from the IL-1 family. *Immunol Rev*. 2018;281(1):154-168. [CrossRef PubMed](#)
10. Schrezenmeier EV, Barasch J, Budde K, Westhoff T, Schmidt-Ott KM. Biomarkers in acute kidney injury – pathophysiological basis and clinical performance. *Acta Physiol (Oxf)*. 2017;219(3):554-572. [CrossRef PubMed](#)
11. Kellum JA, Romagnani P, Ashuntantang G, Ronco C, Zarbock A, Anders HJ. Acute kidney injury. *Nat Rev Dis Primers*. 2021;7(1):52. [CrossRef PubMed](#)
12. Palevsky PM, Liu KD, Brophy PD, et al. KDOQI US commentary on the 2012 KDIGO clinical practice guideline for acute kidney injury. *Am J Kidney Dis*. 2013;61(5):649-672. [CrossRef PubMed](#)
13. Akcay A, Nguyen Q, He Z, et al. IL-33 exacerbates acute kidney injury. *J Am Soc Nephrol*. 2011;22(11):2057-2067. [CrossRef PubMed](#)
14. Ferhat M, Robin A, Giraud S, et al. Endogenous IL-33 contributes to kidney ischemia-reperfusion injury as an alarmin. *J Am Soc Nephrol*. 2018;29(4):1272-1288. [CrossRef PubMed](#)
15. Chen Z, Hu Q, Huo Y, Zhang R, Fu Q, Qin X. Serum interleukin-33 is a novel predictive biomarker of hemorrhage transformation and outcome in acute ischemic stroke. *J Stroke Cerebrovasc Dis*. 2021;30(2):105506. [CrossRef PubMed](#)
16. Firouzabadi N, Dashti M, Dehshahri A, Bahramali E. Biomarkers of IL-33 and sST2 and lack of association with carvedilol therapy in heart failure. *Clin Pharmacol*. 2020;12:53-58. [CrossRef PubMed](#)
17. Behairy OG, Elsadek AE, Behiry EG, Elhenawy IA, Shalan NH, Sayied KR. Clinical value of serum interleukin-33 biomarker in infants with neonatal cholestasis. *J Pediatr Gastroenterol Nutr*. 2020;70(3):344-349. [CrossRef PubMed](#)
18. Erfurt S, Hoffmeister M, Oess S, et al. Serum IL-33 as a biomarker in different diseases: useful parameter or much need for clarification? *J Circ Biomark*. 2021;10:20-25. [CrossRef PubMed](#)
19. Ketelaar ME, Nawijn MC, Shaw DE, Koppelman GH, Sayers I. The challenge of measuring IL-33 in serum using commercial ELISA: lessons from asthma. *Clin Exp Allergy*. 2016;46(6):884-887. [CrossRef PubMed](#)
20. Asaka D, Yoshikawa M, Nakayama T, Yoshimura T, Moriyama H, Otori N. Elevated levels of interleukin-33 in the nasal secretions of patients with allergic rhinitis. *Int Arch Allergy Immunol*. 2012;158(s1)(suppl 1):47-50. [CrossRef PubMed](#)
21. Vyshnevskaya I, Kopytsya M, Hilova Y, Protchenko E, Petyunina O. Biomarker SST2 as an early predictor of acute renal injury in patients with ST-segment elevation acute myocardial infarction. *Georgian Med News*. 2020;(302):53-58. [PubMed](#)
22. Lobdell KW, Parker DM, Likosky DS, et al. Preoperative serum ST2 level predicts acute kidney injury after adult cardiac surgery. *J Thorac Cardiovasc Surg*. 2018;156(3):1114-1123.e2. [CrossRef PubMed](#)
23. Khwaja A. KDIGO clinical practice guidelines for acute kidney injury. Karger Publishers; 2012. [CrossRef](#)
24. Singer M, Deutschman CS, Seymour CW, et al. The Third International Consensus definitions for sepsis and septic shock (Sepsis-3). *JAMA*. 2016;315(8):801-810. [CrossRef PubMed](#)



25. Ronco C, Haapio M, House AA, Anavekar N, Bellomo R. Cardiorenal syndrome. *J Am Coll Cardiol.* 2008;52(19):1527-1539. [CrossRef PubMed](#)
26. Arroyo V, Ginès P, Gerbes AL, et al. Definition and diagnostic criteria of refractory ascites and hepatorenal syndrome in cirrhosis. *International Ascites Club. Hepatology.* 1996;23(1):164-176. [CrossRef PubMed](#)
27. Fiorentino M, Tohme FA, Wang S, Murugan R, Angus DC, Kellum JA. Long-term survival in patients with septic acute kidney injury is strongly influenced by renal recovery. *PLoS One.* 2018;13(6):e0198269. [CrossRef PubMed](#)
28. Bagshaw SM, George C, Bellomo R; ANZICS Database Management Committee. A comparison of the RIFLE and AKIN criteria for acute kidney injury in critically ill patients. *Nephrol Dial Transplant.* 2008;23(5):1569-1574. [CrossRef PubMed](#)
29. Hall IE, Coca SG, Perazella MA, et al. Risk of poor outcomes with novel and traditional biomarkers at clinical AKI diagnosis. *Clin J Am Soc Nephrol.* 2011;6(12):2740-2749. [CrossRef PubMed](#)
30. Singer E, Elger A, Elitok S, et al. Urinary neutrophil gelatinase-associated lipocalin distinguishes pre-renal from intrinsic renal failure and predicts outcomes. *Kidney Int.* 2011;80(4):405-414. [CrossRef PubMed](#)
31. Nickolas TL, Schmidt-Ott KM, Canetta P, et al. Diagnostic and prognostic stratification in the emergency department using urinary biomarkers of nephron damage: a multicenter prospective cohort study. *J Am Coll Cardiol.* 2012 Jan 17;59(3):246-255. [CrossRef PubMed](#)
32. Sánchez-Más J, Lax A, Asensio-López MC, et al. Modulation of IL-33/ST2 system in postinfarction heart failure: correlation with cardiac remodelling markers. *Eur J Clin Invest.* 2014;44(7):643-651. [CrossRef PubMed](#)
33. Tung YC, Chang CH, Chen YC, Chu PH. Combined biomarker analysis for risk of acute kidney injury in patients with ST-segment elevation myocardial infarction. *PLoS One.* 2015;10(4):e0125282. [CrossRef PubMed](#)
34. Koyner JL, Garg AX, Coca SG, et al; TRIBE-AKI Consortium. Biomarkers predict progression of acute kidney injury after cardiac surgery. *J Am Soc Nephrol.* 2012;23(5):905-914. [CrossRef PubMed](#)
35. Caironi P, Latini R, Struck J, et al; ALBIOS Study Investigators. Circulating proenkephalin, acute kidney injury, and its improvement in patients with severe sepsis or shock. *Clin Chem.* 2018;64(9):1361-1369. [CrossRef PubMed](#)
36. Hollinger A, Wittebole X, François B, et al. Proenkephalin A 119-159 (Penkid) is an early biomarker of septic acute kidney injury: the Kidney in Sepsis and Septic Shock (Kid-SSS) Study. *Kidney Int Rep.* 2018;3(6):1424-1433. [CrossRef PubMed](#)
37. Schunk SJ, Zarbock A, Meersch M, et al. Association between urinary dickkopf-3, acute kidney injury, and subsequent loss of kidney function in patients undergoing cardiac surgery: an observational cohort study. *Lancet.* 2019;394(10197):488-496. [CrossRef PubMed](#)
38. Fang X, Hu J, Chen Y, Shen W, Ke B. Dickkopf-3: current knowledge in kidney diseases. *Front Physiol.* 2020;11:533344. [CrossRef PubMed](#)
39. Hoste E, Bihorac A, Al-Khafaji A, et al; RUBY Investigators. Identification and validation of biomarkers of persistent acute kidney injury: the RUBY study. *Intensive Care Med.* 2020;46(5):943-953. [CrossRef PubMed](#)
40. Ostermann M, Zarbock A, Goldstein S, et al. Recommendations on acute kidney injury biomarkers from the acute disease quality initiative consensus conference: a consensus statement. *JAMA Netw Open.* 2020;3(10):e2019209. [CrossRef PubMed](#)
41. Hur M, Kim H, Kim HJ, et al; GREAT Network. Soluble ST2 has a prognostic role in patients with suspected sepsis. *Ann Lab Med.* 2015;35(6):570-577. [CrossRef PubMed](#)
42. Hoogerwerf JJ, Tanck MWT, van Zoelen MAD, Wittebole X, Laterre P-F, van der Poll T. Soluble ST2 plasma concentrations predict mortality in severe sepsis. *Intensive Care Med.* 2010;36(4):630-637. [CrossRef PubMed](#)

Characterization of extracellular vesicles isolated from different liquid biopsies of uveal melanoma patients

Carmen Luz Pessuti¹, Deise Fialho Costa^{1,2}, Kleber S. Ribeiro^{1,3}, Mohamed Abdouh², Thupten Tsering², Heloisa Nascimento¹, Alessandra G. Commodaro¹, Allexya Affonso Antunes Marcos¹, Ana Claudia Torrecilhas³, Rubens N. Belfort¹, Rubens Belfort Jr¹, Julia Valdemarin Burnier^{2,4,5}

¹Department of Ophthalmology, Federal University of São Paulo, Vision Institute, IPEPO, São Paulo - Brazil

²Cancer Research Program, McGill University Health Centre Research Institute, Montreal, Quebec - Canada

³Department of Pharmaceutical Sciences, Federal University of São Paulo, Diadema, São Paulo - Brazil

⁴Department of Oncology, McGill University, Montreal, Quebec - Canada

⁵Experimental Pathology Unit, Department of Pathology, McGill University, Montreal, Quebec - Canada

ABSTRACT

Purpose: Uveal melanoma (UM) is the most common intraocular malignant tumor in adults. Extracellular vesicles (EVs) have been extensively studied as a biomarker to monitor disease in patients. The study of new biomarkers in melanoma patients could prevent metastasis by earlier diagnosis. In this study, we determined the proteomic profile of EVs isolated from aqueous humor (AH), vitreous humor (VH), and plasma from UM patients in comparison with cancer-free control patients.

Methods: AH, VH and plasma were collected from seven patients with UM after enucleation; AH and plasma were collected from seven cancer-free patients with cataract (CAT; control group). EVs were isolated using the membrane-based affinity binding column method. Nanoparticle tracking analysis (NTA) was performed to determine the size and concentration of EVs. EV markers, CD63 and TSG101, were assessed by immunoblotting, and the EV proteome was characterized by mass spectrometry.

Results: Mean EV concentration was higher in all analytes of UM patients compared to those in the CAT group. In the UM cohort, the mean concentration of EVs was significantly lower in AH and plasma than in VH. In contrast, the mean size and size distribution of EVs was invariably identical in all analyzed analytes and in both studied groups (UM vs. CAT). Mass spectrometry analyses from the different analytes from UM patients showed the presence of EV markers.

Conclusion: EVs isolated from AH, VH, and plasma from patients with UM showed consistent profiles and support the use of blood to monitor UM patients as a noninvasive liquid biopsy.

Keywords: Aqueous humor, Extracellular vesicles, Liquid biopsy, Plasma, Proteomic analysis, Uveal melanoma, Vitreous humor

Introduction

Uveal melanoma (UM) is a primary intraocular tumor in adults that accounts for less than 5% of all melanoma cases (1,2). The incidence of UM has remained stable at ~5.1 per million since the 1970s with subtle differences depending on geographic location, as well as environmental and

occupational factors (1). Despite excellent control of local disease, prognosis remains poor due to metastatic progression affecting ~50% of patients (2-4). Mortality rates for UM are unchanged over the past decades (1).

Extracellular vesicles (EVs) have emerged as biomarkers in various cancers and provide valuable clinical information (5,6). Their use as a biomarker assay has gained interest as a new tool for monitoring of cancer patients; however, standardization and validation of EVs as a biomarker are needed (4,7).

EVs are small lipid bilayer particles released from all types of cells and found in different body fluids, most commonly the blood, but have also been detected in aqueous humor (AH) (8,9). EVs are classified mainly into exosomes (50-100 nm), microvesicles (100-1000 nm), and apoptotic bodies (50 nm-2 µm) based on their biogenesis, number, size, distinct biological functions and markers (10-16). Exosomes are a constitutive and abundant component of the vitreous (17).

EVs are involved in the transfer of biological macromolecules to recipient cells, and modulating various physiological

Received: February 3, 2022

Accepted: May 27, 2022

Published online: June 27, 2022

This article includes supplementary material.

Corresponding author:

Carmen Luz Pessuti
Department of Ophthalmology
Federal University of São Paulo
Porto Street, 69
São Paulo, 09416-020 - Brazil
luz.pessuti@unifesp.br



and pathological processes, such as pathogen dissemination and regulation of the host immune system (18-20). Recent studies have shown that tumor cells release large amounts of EVs that can be uptaken by malignant and stromal cells, inducing tumor progression (21,22). They have been shown to play a major role in mediating metastasis, ranging from oncogenic reprogramming of malignant cells to the formation of pre-metastatic niches (23-25). Furthermore, our group and others have shown that cancer-derived exosomes can transfer bioactive molecules such as proteins, DNA, mRNAs, and miRNAs to recipient cells, thereby changing their function (26-29).

In ocular and cutaneous melanoma, the concentration of EVs and proteins is increased in patients compared to healthy individuals and has been shown to correlate with disease progression (30,31). Moreover, the profile of circulating EV-derived miRNAs is often altered in human cancers, and EVs from UM patients have been shown to contain miR-146, a potential circulating marker in UM (32). Recently, we have reported that the number of EVs produced and the profile of tumor-associated proteins vary between normal melanocytes and UM cell lines, and also between primary and metastatic UM cell lines (33). EVs released by metastatic melanoma cells were enriched in proteins (9,10,23) involved in the pre-metastatic niche formation (25), suggesting their role in preparing the environment for colonization by circulating tumor cells (CTCs).

There is a lack of detailed characterization of EVs in this disease as well as in nonblood-based liquid biopsy. In this study, our aim was to determine the proteomic profile of EVs isolated from AH, vitreous humor (VH), and plasma from patients with UM and to compare with cancer-free control patients.

Materials and methods

Patients

A total of 14 participants were enrolled for this study: 7 patients diagnosed with primary UM, and 7 healthy controls undergoing cataract surgery at the Department of Ophthalmology, Federal University of São Paulo (UNIFESP/EPM), Brazil. The patients were recruited from July 2019 to December 2019 at the Department of Ophthalmology of the UNIFESP/EPM. The clinical characteristics of the study population are described in Table I.

This study was approved by the ethics committee investigational review board (CEP number 2198149) and adhered to the principles of the Declaration of Helsinki and Resolution 196/96 of the Ministry of Health, Brazil. Informed consent was obtained from all participants.

Sample collection

AH and plasma samples were collected from UM patients and controls. Additionally, VH samples were collected from UM patients. Peripheral blood (10 mL) was collected in ethylenediaminetetraacetic acid (EDTA) tubes. The tubes were centrifuged for 10 minutes at $1,900 \times g$, and plasma were collected. VH and AH samples from UM patients were collected from the enucleated eyes after the surgery with a syringe and fine needle. In the control group, AH samples were collected during cataract surgery. All routine surgical procedures were followed. All collected samples were kept at -80°C until the experimental procedure.

TABLE I - Clinical features of patients enrolled in this study

Patients	Sex	Age (years)	Cell Types	Size	TNM
CAT1	Male	70	N/A	N/A	N/A
CAT2	Female	77	N/A	N/A	N/A
CAT3	Female	82	N/A	N/A	N/A
CAT4	Female	77	N/A	N/A	N/A
CAT5	Female	75	N/A	N/A	N/A
CAT6	Male	76	N/A	N/A	N/A
CAT7	Female	63	N/A	N/A	N/A
UM1	Male	72	Mixed UM, predominance of spindle cells affecting the ciliary body and choroid	1.9 × 0.6	pT4E
UM2	Female	86	Epithelioid choroidal melanoma	1.2 × 1.1	pT3B
UM3	Female	53	Mixed choroidal melanoma, predominance of spindle cells	1.3 × 1.0	pT3A
UM5	Male	63	Mixed UM, predominance of spindle cells infiltrating the choroid and ciliary body	1.2 × 1.5	pT3B
UM6	Female	61	Mixed UM, predominance of epithelioid cells	1.0 × 0.8	pT2
UM8	Female	65	Mixed UM, predominance of spindle cells infiltrating the choroid and ciliary body	2.8 × 0.7	pT4B
UM9	Female	39	Mixed choroidal melanoma, predominance of epithelioid cells	1.5 × 1.2	pT3A

Size refers to tumor size (base diameter × thickness [cm × cm]).

CAT = cataract, control group; N/A = not applicable; TNM = tumor, node, metastasis; UM = uveal melanoma.

EV purification and characterization

The protocol for EV isolation was performed according to the guidelines of the International Society for Extracellular Vesicles (ISEV) (10). Samples were centrifuged at $16,000 \times g$ for 10 minutes at 4°C to eliminate cellular debris. Then, EV isolation was performed using the exoEasy Maxi Kit (Qiagen, Valencia, CA, USA) according to the manufacturer's instructions (10,11,34-36). Isolated EVs were diluted $100 \times$ in phosphate-buffered saline (PBS) and analyzed by nanoparticle tracking analysis (NTA) using the NanoSight NS300 instrument (Malvern Analytical, UK). PBS was used as a diluent. Samples and diluent were read in triplicates for 30 seconds at 20 frames per second. The NTA 3.2 software was used to estimate the concentration and size of the particles.

Immunoblotting

EVs isolated from patients and controls were lysed in RIPA buffer containing complete mini protease inhibitors (Sigma) at 4°C for 30 minutes. Samples were sonicated for 2 seconds (three times), and spun at $13,000 \times g$ for 30 minutes at 4°C . Protein concentrations were quantified by the BCA assay (Thermo Fisher Scientific). Protein samples were processed for immunoblotting and mass spectrometry (MS).

EV-derived proteins ($20 \mu\text{g}$) were separated using 12% Mini-PROTEAN[®] precast polyacrylamide gel (Bio-Rad). Proteins were transferred onto polyvinylidene difluoride (PVDF) membranes (Bio-Rad). Membranes were blocked for 1 hour at room temperature with 5% nonfat dry milk in 1X Tris-buffer saline with 0.05% Tween 20 (TBST). Membranes were probed with anti-TSG101 (Abcam; 1:1,000) and anti-CD63 (Abcam; 1:1,000), anti-Alix (ThermoFisher Scientific 1:1,000), anti- β -actin (Sigma 1:1,000), anti-tenascin C (abcam 1:1,000), anti-vimentin (abcam 1:500) primary antibodies, followed by horseradish peroxidase (HRP)-conjugated goat anti-rabbit (Sigma 1:1,000) and goat anti-mouse (Sigma 1:3,000) secondary antibodies. Membranes were washed five times for 10 minutes each time after each incubation and developed using ECL prime Western blot detection (GE Healthcare). Protein signals were visualized using the ChemiDoc XRS + System.

MS analysis

MS analysis was performed in nine samples [AH ($n = 3$), plasma ($n = 3$), and VH ($n = 3$)] from UM-5, UM-6, and UM-8 patients; $20 \mu\text{g}$ of EV proteins from each sample was loaded onto a single stacking gel band to remove contaminants such as lipids, detergents, and salts. Each sample was run in duplicate.

The gel band was reduced with DTT (dithiothreitol), alkylated with iodoacetic acid, and digested with trypsin. Extracted peptides were resolubilized in 0.1% aqueous formic acid and loaded onto a Thermo Scientific Acclaim PepMap (75 μm inner diameter \times 2 cm, C18 3 μm particle size) precolumn and then onto an Acclaim PepMap EASY-Spray (75 μm inner diameter \times 15 cm with 2 μm C18, 2 μm beads) analytical column separation using a Dionex UltiMate 3000 uHPLC at 250 nL/min with a gradient of 2-35% organic (0.1% formic acid in acetonitrile) over 3 hours. Peptides were analyzed

using a Thermo Orbitrap Fusion MS operating at 120,000 resolution (full width at half maximum in MS1) with Higher energy Collisional Dissociation (HCD) sequencing (15,000 resolution) at top speed for all peptides with a charge of 2+ or greater. The MS raw data were converted into *.mgf format (Mascot generic format) for searching using the Mascot 2.6.2 search engine (Matrix Science) against human protein sequences (Uniprot 2019). The database search results were loaded onto Scaffold Q+ Scaffold_4.10.0 (Proteome Sciences) for spectral counting, statistical treatment, data visualization, and quantification. Protein threshold >99%, peptide threshold >95%, and two of a minimum number of unique peptides were applied in Scaffold Q+ to increase the confidence level of identified proteins. Additional filters such as p-value cut-off of 0.05 and a fold-value change of ≥ 2 were used to identify the differential expression of proteins. The identified protein list in Scaffold was exported to Microsoft Excel and uploaded into the DAVID Bioinformatics database (version 6.8) for gene ontology (GO) analyses (i.e., biological process, cellular component, and KEGG pathway). In addition, bioinformatic analysis and Vesiclepedia database (37) search were performed using the FunRich software (version 3.1.3) (37-39).

Statistical analysis

Statistical analysis was performed using the GraphPad software (Prism, version 5.00 for Windows; GraphPad, San Diego, CA). The Mann-Whitney test was used to determine the statistical difference between respective groups. The results are expressed as mean \pm standard deviation (SD). A p-value < 0.05 was considered significant.

Results

Characterization and isolation of EVs from plasma, AH, and VH

EVs were isolated from the plasma, AH, and VH of UM patients, and AH and plasma of cataract patients. Immunoblotting analysis showed the expression of EV markers CD63, TSG101, and Alix with different expression levels depending on the analyzed samples (Fig. 1A, B, and Supplementary Figure A). The expression of CD63 and Alix was higher in UM EVs than in CAT EVs (Fig. 1A, and Supplementary Figure A). Moreover, the expression of both CD63 and TSG101 was higher in EVs isolated from VH and plasma than in EVs isolated from AH (Fig. 1A, B). NTA from all samples showed that EVs ranged from 80 to 442 nm in size, with similar 10 percentile mean (D10) size (133 nm, 135 nm, and 139 nm) in plasma, AH, and VH, respectively (Fig. 1C, D). When analyzing sizes of isolated UM EVs, no difference was observed in all samples: 219 ± 26 nm (range: 168-241) in plasma, 211 ± 37 nm (range: 173-265) in AH, and 216 ± 71 nm (range: 110-314) in VH (Fig. 1D). Also, no difference was observed in the average size of EVs from AH and plasma between the UM and CAT groups (Fig. 1D).

In the UM cohort, the concentration of EVs ranged from 2.6×10^9 to 9×10^{10} particles/mL in AH, VH, and plasma samples (Fig. 1E). The mean concentration of EVs in VH (6.6×10^{10} particles/mL) was significantly higher when compared to AH



(10^{10} particles/mL, $p < 0.01$) and plasma (2.7×10^{10} particles/mL, $p < 0.01$) (Fig. 1E). No difference was observed in the concentration of AH-derived EVs between the UM and CAT groups. In contrast, the concentration of plasma-derived EVs was significantly higher in UM patients than in the CAT control group ($p < 0.001$) (Figs. 1F, G). Notably, we did not find any correlation between the concentrations of EVs isolated from UM patients and ocular tumor size (Fig. 1H, I).

EV protein cargo from plasma AH and VH

To gain an in-depth understanding of the protein cargo in EVs isolated from the different analytes, we performed whole proteomic analysis by MS. For this purpose, we focused our analysis on EVs isolated from three UM patients (UM-5, UM-6, and UM-8). Our goal from this analysis was to determine whether these EVs carried common protein cargo and

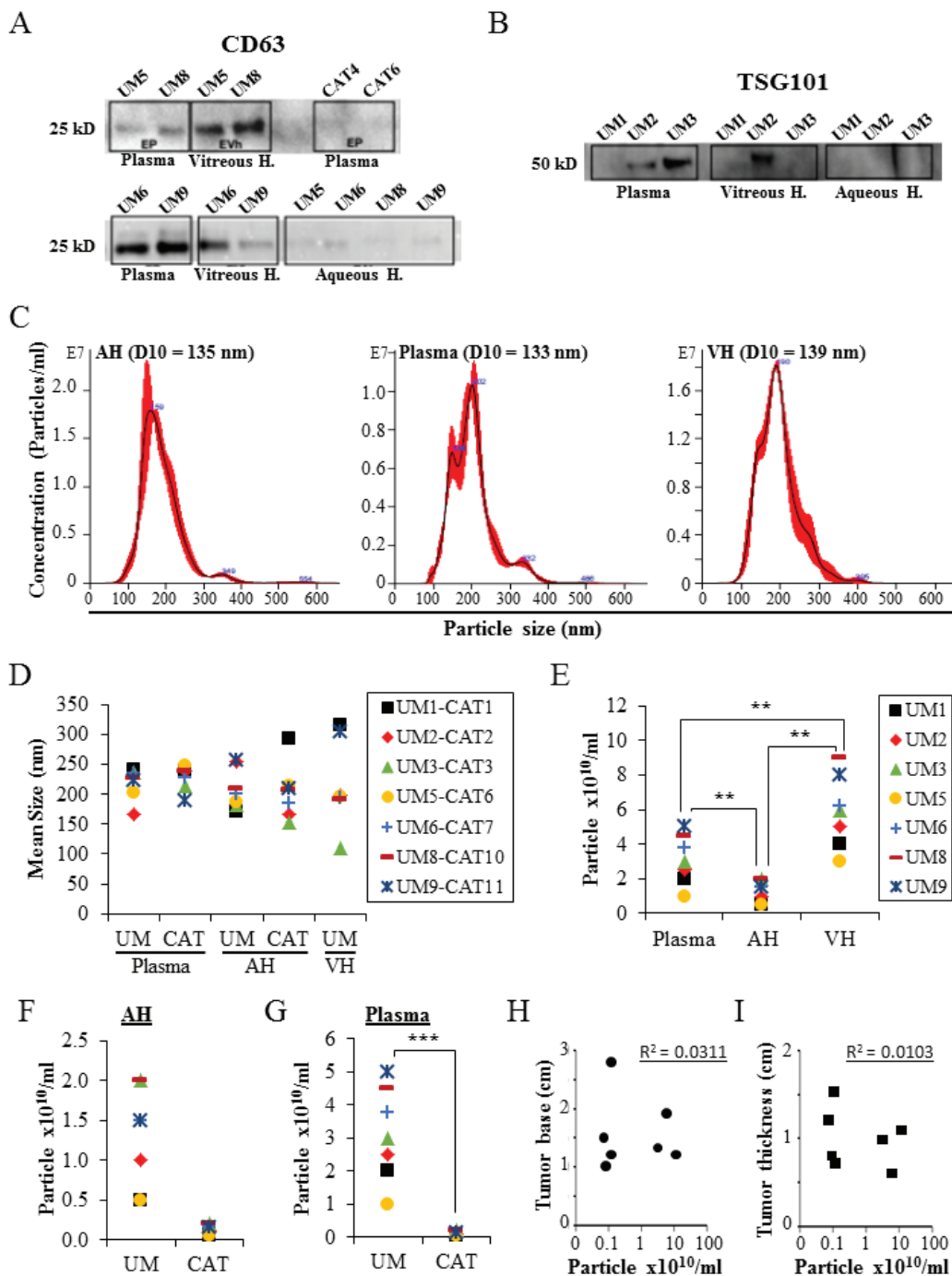


Fig. 1 - Characterization of EVs derived from AH, VH, and plasma. A,B) Proteins isolated from the different assay EVs (seven UM samples and two CAT samples) were analyzed by Western blot for the expression of specific EV markers (i.e., CD63 and TSG101). C) Nanosight analyses of EVs. Representative size distribution histograms showing data of EVs from AH, plasma, and VH. Note that mean EV sizes are similar. Histograms are displayed as averaged EV concentration (black line) and the variation between four repeated measurements indicating ± 1 standard error of the mean (red outline). D) Mean size of EVs isolated from AH and plasma of UM ($n = 7$) and cataract-suffering (CAT, $n = 7$) patients, and from VH of UM patients ($n = 7$). E) Concentrations of EVs isolated from different analytes of seven UM patients. $**p < 0.01$. F,G) Concentrations of EVs isolated from AH (F) and plasma (G) of UM ($n = 7$) and cataract-suffering (CAT, $n = 7$) patients. $***p < 0.001$. H and I) The concentrations of EVs isolated from the plasma of UM patients ($n = 7$) were plotted against ocular tumor size (base diameter (H) and thickness (I)). No correlation was found as shown by the correlation coefficient (R). Legend close to graph D applies to graphs D, F, and G. AH = aqueous humor; CAT = cataract; EV = extracellular vesicle; VH = vitreous humor; UM = uveal melanoma.



also the nature of those proteins. We identified 542 proteins of which 498 (92%) overlap with EV proteins previously reported in the Vesiclepedia database (Supplementary Table A, List of EV-contained proteins identified by MS screening) (Fig. 2A) (37). As a readout for the purity of isolated EVs, we detected proteins that are specific to the tissue of origin (i.e., complement and coagulation factors in EVs from the plasma, melanocyte protein PMEL and HTRA1 in the VH, and beta- and gamma-crystallin in the AH) (Tab. II). In addition, protein cargo detected in isolated EVs included typical EV protein signatures such as ESCRT components CD81, CD63, CD9, HLA, annexins and syntenin (Supplementary Table A, List of EV-contained proteins identified by MS screening). Moreover, herein, we report the presence of 44 novel proteins not previously reported in the Vesiclepedia database (37); 2 are present in all EVs, 4 are present in EVs from plasma and VH, 4 are present in EVs from VH and AH, and the rest are unique to EVs from a single analyte (Tab. III).

Interestingly, 209 (39%) of the identified proteins were shared between EVs from the three assays (Fig. 2B). In addition, when we analyzed each analyte separately, we observed that EVs from the three samples shared 106 (33%) proteins in AH, 181 (44%) in VH, and 247 (73%) in plasma (Fig. 2C-E).

Proteins by GO analysis in specific biological processes

Of the proteins found in our proteomic analyses data from UM patients, 344 proteins were detected from plasma EVs, 334 in EVs from AH, and 421 in EVs from VH (Fig. 2B). To identify the physiological processes to which these proteins were associated, clustering was conducted into GO categories using the DAVID bioinformatics platform (Fig. 3). Characterization by biological process highlighted categories related to retina homeostasis, regulation of apoptosis, cell growth, and the activation of pathways involved in cancer cell biology (i.e., MAPK/ERK cascades). In addition, of the highly expressed proteins, several clustered in the categories of cell-cell adhesion and movement of cell or subcellular component (Fig. 3A). When clustering the proteins based on cellular component, we found they grouped into EV categories (i.e., vesicles) (Fig. 3B). Molecular functions clustering using KEGG pathway analysis revealed that isolated EVs were enriched for proteins related to immune escape from cancer, such as those involved in complement and coagulation cascades, and proteins involved in cell metabolic activities and interaction with extracellular matrix (ECM). Particularly, a panel of proteins clustered in the PI3k-Akt signaling pathway and the proteoglycan group were exclusively present in plasma-isolated EVs (Fig. 3C).

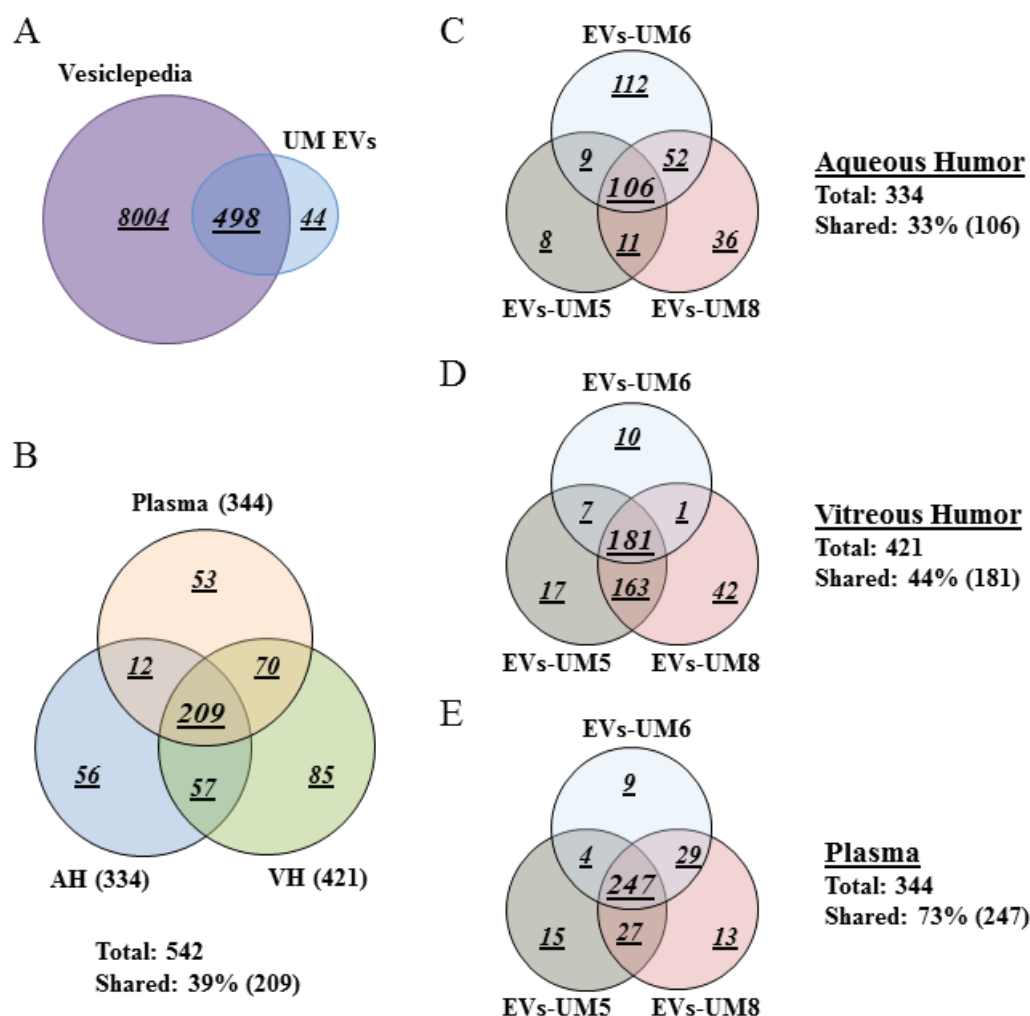


Fig. 2 - Plasma-derived EV protein cargo mirrored that of EVs isolated from AH and VH of UM patients. Venn diagram analyses. A) The majority of proteins isolated from EVs derived from the different analytes were shared with data published in Vesiclepedia database. B) EVs isolated from the three analytes shared 209 proteins (39%). C-E) Analyses of EV protein cargo in the same analytes from different donors. Note that these EVs shared 106 proteins (33%, C) in the aqueous humor, 181 proteins (44%, D) in the vitreous humor and 247 proteins (73%, E), which is in the same range of those shared between EVs from the three analytes (39%, see B). Data were collected from three UM patient analytes repeated twice each (UM5-1, UM5-2, UM6-1, UM6-2, UM8-1, and UM8-2). AH = aqueous humor; EV = extracellular vesicle; VH = vitreous humor; UM = uveal melanoma.



TABLE II - Protein readout for the purity of isolated EVs

	Identified Proteins	ID	Spectrum Count		
			AH	VH	P
Plasma	Coagulation factor V	FA5	2	0	146
	C4b-binding protein alpha chain	C4BPA	1	7	127
	Coagulation factor IX	FA9	1	16	79
	von Willebrand factor	VWF	0	0	72
	Coagulation factor X	FA10	2	11	70
	Multimerin-1	MMRN1	0	0	33
	Platelet glycoprotein Ib alpha chain	GP1BA	0	2	22
	C4b-binding protein beta chain	C4BPB	0	0	14
	Serum amyloid P-component	SAMP	0	7	14
	C-reactive protein	CRP	1	1	13
	Sushi, von Willebrand factor type A, EGF and pentraxin domain-containing protein 1	SVEP1	0	0	2
Serum amyloid A-1 protein	SAA1	0	0	1	
VH	Pigment epithelium-derived factor	PEDF	37	111	13
	Retinol-binding protein 3	RET3	3	111	0
	Melanocyte protein PMEL	PMEL	0	27	1
	Serine protease HTRA1	HTRA1	0	8	0
	Retinaldehyde-binding protein 1	RLBP1	0	2	0
	Retinoschisin	XLRS1	0	2	0
	Interphotoreceptor matrix proteoglycan 1	IMPG1	0	1	0
AH and VH	Opticin	OPT	12	12	0
AH	Beta-crystallin B1	CRBB1	179	2	1
	Alpha-crystallin A2 chain	CRYA2	146	0	0
	Alpha-crystallin B chain	CRYAB	139	7	0
	Gamma-crystallin S	CRYGS	97	1	0
	Beta-crystallin A3	CRBA1	76	0	0
	Beta-crystallin A4	CRBA4	52	0	0
	Gamma-crystallin C	CRGC	44	0	0
	Gamma-crystallin D	CRGD	42	0	0
	Retinal dehydrogenase 1	AL1A1	41	0	0
	Filensin	BFSP1	2	0	0
	Phakinin	BFSP2	2	0	0

Data are derived from three patients (UM-5, UM-6, and UM-8) and samples were run in duplicates.
 AH = aqueous humor; EV = extracellular vesicle; ID = alternative name; P = plasma; VH = vitreous humor.

UM arises from melanocytes of the uveal tract (25,34). EVs isolated from the AH and VH may contain proteins reflective of UM cells. We pooled our data from intraocular-derived EVs by focusing on proteins that regulate tumor growth and oncogenesis (Tab. IV). This identified a panel of proteins that are mainly involved in protecting cells against apoptosis, controlling cell growth, promoting angiogenesis, and inducing cell spreading (i.e., clusterin, alpha-enolase, fibulin-1, cathepsin, HSP, ECM1, MET, and GAS6). Moreover, vimentin

(an intermediate filament protein that is overexpressed in epithelial tumors such as UMs) was detected in VH-derived EVs (Tab. IV) (36,38-40).

Plasma-isolated EVs were also enriched in proteins involved in the regulation of cell proliferation (i.e., SPARC, tenascin, plexin) and cell survival (i.e., clusterin), and the metastatic process such as metastatic niche organization (i.e., ECM1, ECM2, emilin, C-reactive protein [CRP], oncoprotein-induced transcript 3 [OIT3], and integrins) (Tab. V, and

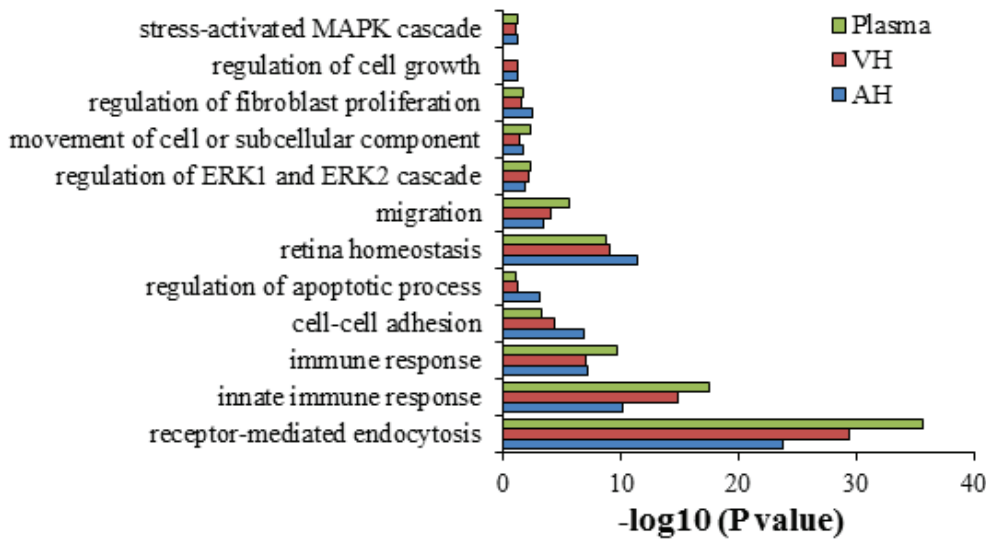
TABLE III - Newly characterized protein from EVs isolated from plasma, aqueous humor, or vitreous humor

Identified Proteins	ID	P	VH	AH
Complement C4-B	CO4B	Y	Y	Y
Beta-crystallin B1	CRBB1	Y	Y	Y
Vitamin K-dependent protein C	PROC	Y	Y	N
Immunoglobulin J chain	IGJ	Y	Y	N
L-selectin	LYAM1	Y	Y	N
Neuropilin-2	NRP2	Y	Y	N
Soluble scavenger receptor cysteine-rich domain-containing protein SSC5D	SRCRL	Y	N	N
Extracellular matrix protein 2	ECM2	Y	N	N
Plexin domain-containing protein 1	PLDX1	Y	N	N
Retinol-binding protein 3	RET3	N	Y	Y
Opticin	OPT	N	Y	Y
Beta-1,4-glucuronyltransferase 1	B4GA1	N	Y	Y
Wnt inhibitory factor 1	WIF1	N	Y	Y
Beta-Ala-His dipeptidase	CNDP1	N	Y	N
Receptor-type tyrosine-protein phosphatase zeta	PTPRZ	N	Y	N
Macrophage colony-stimulating factor 1 receptor	CSF1R	N	Y	N
Serpin E3	SERP3	N	Y	N
Cadherin-related family member 1	CDHR1	N	Y	N
Clusterin-like protein 1	CLUL1	N	Y	N
Retinaldehyde-binding protein 1	RLBP1	N	Y	N
Retinoschisin	XLRS1	N	Y	N
Adipocyte plasma membrane-associated protein	APMAP	N	Y	N
Left-right determination factor 2	LFTY2	N	Y	N
Neuronal cell adhesion molecule	NRCAM	N	Y	N
Interphotoreceptor matrix proteoglycan 1	IMPG1	N	Y	N
Triggering receptor expressed on myeloid cells 2	TREM2	N	Y	N
Cathepsin L1	CATL1	N	Y	N
Endothelial lipase	LIPE	N	Y	N
BPI fold-containing family B member 4	BPIB4	N	Y	N
Semaphorin-3B	SEM3B	N	Y	N
Zinc transporter ZIP12	S39AC	N	Y	N
Tsukushin	TSK	N	Y	N
Beta-crystallin A3	CRBA1	N	N	Y
Beta-crystallin A4	CRBA4	N	N	Y
Gamma-crystallin C	CRGC	N	N	Y
Gamma-crystallin D	CRGD	N	N	Y
Gamma-crystallin B	CRGB	N	N	Y
Beta-crystallin B3	CRBB3	N	N	Y
Filensin	BFSP1	N	N	Y
Protein S100-B	S100B	N	N	Y
Secreted frizzled-related protein 3	SFRP3	N	N	Y
Phakinin	BFSP2	N	N	Y
DNA polymerase theta	DPOLQ	N	N	Y
Protein kinase C-binding protein NELL2	NELL2	N	N	Y

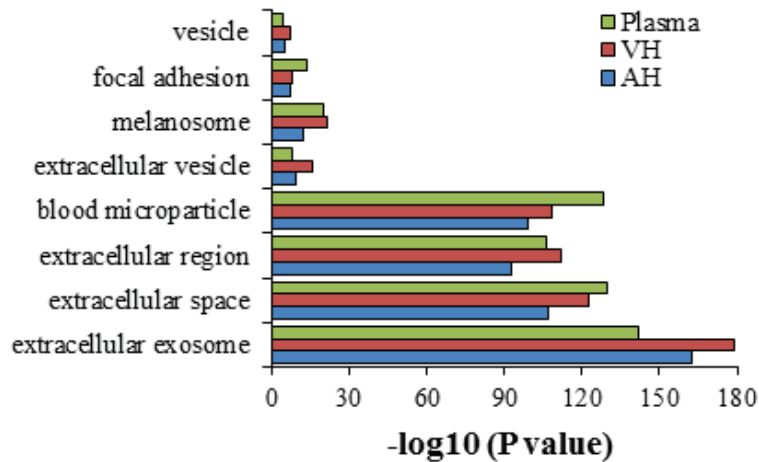
Data are derived from three patients (UM-5, UM-6, and UM-8) and samples were run in duplicates.
 AH = aqueous humor; ID = alternative name; N = absent; P = plasma; VH = vitreous humor; Y = present.



A Biological Process



B Cellular component



C KEEG pathway

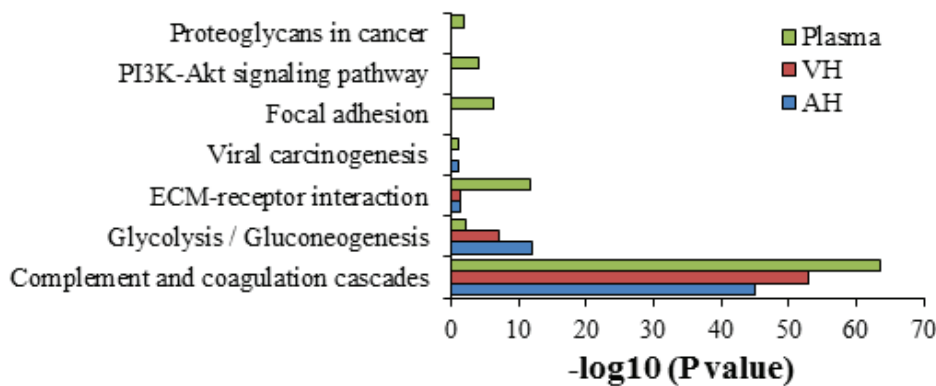


Fig. 3 - Gene ontology classification of EV protein cargo. The most enriched categories in biological process (A), cellular component (B), and molecular function (C) are shown. Data were collected from three UM patient analytes repeated twice (UM5-1, UM5-2, UM6-1, UM6-2, UM8-1, and UM8-2). EV = extracellular vesicle; UM = uveal melanoma.



TABLE IV - Protein cargo from aqueous humor- or vitreous humor-derived EVs involved in cell proliferation, survival, and invasion

Identified Proteins	Alternative Name	Spectrum Count	
		AH	VH
Clusterin	CLUS	50	175
Pigment epithelium-derived factor	PEDF	37	111
Alpha-enolase	ENOA	30	7
Vitronectin	VTNC	29	100
Gamma-enolase	ENOG	7	2
Cathepsin D	CATD	6	64
Fibulin-1	FBLN1	6	4
Myocilin	MYOC	6	
Heat shock protein HSP 90-alpha	HS90A	5	10
Galectin-1	LEG1	3	
Heat shock protein HSP 90-beta	HS90B	3	4
Extracellular matrix protein 1	ECM1	2	5
Growth arrest-specific protein 6	GAS6	2	
CD44 antigen	CD44	2	5
C-reactive protein	CRP	1	1
Plexin domain-containing protein 2	PXDC2		3
Ras-related protein Rab-1A	RAB1A		1
Vimentin	VIME		14
Cathepsin B	CATB		8
Hepatocyte growth factor receptor	MET		6
Cadherin-related family member 1	CDHR1		6
Fibronectin	FINC		38
Periostin	POSTN		4
Legumain	LGMN		3
Cathepsin F	CATF		3

AH = aqueous humor; EV = extracellular vesicle; VH = vitreous humor. Data are derived from three patients (UM-5, UM-6, and UM-8) and samples were run in duplicates.

Supplementary Figure A) (41-44). These data suggest that, while AH- and VH-isolated proteins govern in situ UM growth and motility, those contained in the plasma-derived EVs are more involved in UM cell metastatic organotropism and the maintenance of the metastatic niche.

Discussion

EVs have been reported to regulate many aspects of physiological and pathological processes such as cancer. They carry substances that mirror the content of their cell of origin and have the capability to exhibit different biological functions on recipient cells via trafficking of different factors, that is, nucleic acids, proteins, lipids (10,21,44-52). EVs released from tumor cells promote cell proliferation, migration, invasion,

TABLE V - Protein cargo from UM plasma-derived EVs involved in cell proliferation and survival, and metastatic niche organization

Identified Proteins	Alternative Name	Spectrum Count
Fibronectin	FINC	130
Vitronectin	VTNC	109
Clusterin	CLUS	57
Integrin alpha-IIb	ITA2B	30
Endoplasmic	ENPL	28
Integrin beta-3	ITB3	22
SPARC	SPRC	22
Nidogen-1	NID1	16
Vinculin	VINC	14
Tenascin	TENA	13
Pigment epithelium-derived factor	PEDF	13
C-reactive protein	CRP	13
Heat shock protein HSP 90-alpha	HS90A	10
Fibulin-1	FBLN1	9
Heat shock protein HSP 90-beta	HS90B	7
Endoplasmic reticulum chaperone BiP	BIP	7
CD44 antigen OS = Homo sapiens	CD44	6
Heat shock cognate 71 kDa protein	HSP7C	4
Extracellular matrix protein 1	ECM1	3
Plexin domain-containing protein 2	PXDC2	2
Extracellular matrix protein 2	ECM2	2
Beta-parvin	PARVB	2
Caveolae-associated protein 2	CAVN2	2
Ras-related protein Rab-1A	RAB1A	1
Hepatocyte growth factor activator	HGFA	1
Oncoprotein-induced transcript 3 protein	OIT3	1
EMILIN-1	EMIL1	1
Vascular endothelial growth factor receptor 3	VEGFR3	1
Plexin-B1	PLXB1	1
Integrin beta-1	ITB1	1
Alpha-enolase	ENOA	1
Protein S100-A8	S10A8	1
Protein S100-A9	S10A9	1

Data are derived from three patients (UM-5, UM-6, and UM-8) and samples were run in duplicates.

EV = extracellular vesicle; UM = uveal melanoma.

angiogenesis, and metastases (54,57-63). EV cargo could be used as circulating biomarkers in liquid biopsy, mainly in the context of cancer. In the present study, we determined the proteomic profile of EVs isolated from AH, VH, and plasma from patients with UM in comparison with cancer-free control patients.



The size and distribution of EVs detected in the three samples were consistent with exosomes (10). In the blood samples, a significantly higher concentration of EVs was found in UM patients compared to the control group. This is in agreement with our recent observations that UM cell lines shed more EVs than normal choroidal melanocytes (33). Another study suggests that EV has potential roles in cancer progression and invasion (11). Interestingly, the mean concentration of EVs in VH from UM patients was higher when compared to plasma and AH, which seems normal as UM takes place in the posterior segment of the eye.

We showed that EVs derived from AH, VH, and plasma were positive for CD63 and TSG101 markers. Besides, the expression of CD63 was higher in UM EVs in comparison with EVs isolated from samples of control group. Our data corroborate with a study that demonstrated high levels of CD63 in exosomes isolated from plasma of melanoma patients (53). Also a study showed exosomal marker TSG101 was detected in plasma-derived exosome from ovarian cancer patients (21).

We observed that the plasma EV proteomic cargo resembles that of EVs obtained from AH and VH. Although we found that only 209 proteins (39%) were shared between EVs from the three samples (a value that reached 221 proteins [49%] and 279 proteins [57%] when taking into account only AH vs. plasma and VH vs. plasma, respectively), this is not surprising as the plasma is the common carrier of EVs from different tissues.

Moreover, proteomic mining of isolated EVs from UM group identified a set of proteins involved in oncogenesis (i.e., regulation of cell proliferation and survival, promotion of angiogenesis, and cell invasion) and metastasis (i.e., cell spreading and metastatic niche organization) (36,38-43,54). For example, SPARC abrogation has been reported to reduce cell proliferation in UM (41). Cathepsin, a lysosomal acid proteinase, was reported to be involved in different cancer types, especially in regulating UM invasion potential (36,40). Galectin has been shown to facilitate cell migration, to promote metastasis, and to be a hallmark for cancer aggressiveness (55,56). OIT3 is involved in the development and function of the liver, which is the primary site for UM metastasis (54). In addition, several integrins were detected in the isolated EVs from the UM group. These proteins are involved in adhesion to extracellular matrix components and specific organotropism of metastasizing cancer cells (43,64). The integrins present in the EV preparations demonstrate an upregulation of various signal transduction molecules such as S100-A. It has been shown that exosome-derived integrins are internalized by target cells and activate SRC phosphorylation and proinflammatory S100 gene expression (64). Furthermore, EVs from melanoma were found to upregulate S100 proteins in recipient target cells, resulting in vascular leakiness and promotion of metastasis (31,65).

Other proteins found in the datasets such as heat shock proteins and CRP are indicators of worse prognosis in UM (38,42). In addition, melanocyte-specific type I transmembrane glycoprotein (PMEL) was enriched in EVs from VH and less in EVs from plasma. This protein is released by proteolytic ectodomain shedding and may be used as a melanoma-specific blood marker (5,6,67,68).

Interestingly, the recovered protein cargo contained factors involved in cell proliferation, cell survival, oncogenesis, cell invasion, and metastatic niche organization. Together, these data suggest that plasma from UM patients could be used as liquid biopsy platform for patient diagnosis and non-invasive monitoring.

Using clustering analysis based on GO biological process, categories consistent with retinal homeostasis and activation of intracellular pathways involved in cancer cell biology were identified (i.e., MAPK/ERK cascades). Almost all UMs are characterized by mutations in one of *GNAQ*, *GNA11*, *PLCB4*, or *CYSLTR2* genes, and these are upstream activators of the MAPK/ERK cascade (66).

One limitation of this study is the low number of analyzed samples for the proteomic characterization (three UM samples). However, the consistency of the data between the analyzed samples makes the conclusions valuable. Unfortunately, due to the lack of material, performing differential protein expression analysis is not possible at this stage. Studies including more samples are in progress to address this weakness.

Liquid biopsy is already distinguishing cancer-free individuals from non-small cell lung cancer patients and pancreatic ductal adenocarcinoma by the quantitative analysis of exosomal miR-21 and miR-10b, respectively (67). Intra-EV metabolites from prostate cancer patients before and after prostatectomy revealed novel biomarkers (68). One must remember that not only tumor cells release exosomal RNA to affect biological functions but also many normal cells will secrete the same exosomal RNA physiologically (69). As mentioned before, exosomal integrins could be used to predict organ-specific metastasis (64). Therefore, therapy supported by liquid biopsy could be driven in a premature way in case of early metastasis diagnosis or even somehow by targeting and blocking cancer pre-metastatic EV development. Certainly, this promising new tool has to be used with caution, and further studies are needed.

In conclusion, it has been observed that VH is significantly enriched in EVs when compared to AH and plasma in UM patients. EV concentrations in plasma and AH from UM patients was higher when compared to those in the cataract group. Proteomic analysis demonstrated that EVs from the different samples shared a panel of proteins, suggesting that circulating UM EVs mirrored the in situ shed of EVs (i.e., AH and VH). EVs isolated from AH, VH, and plasma from patients with UM showed consistent profiles and support the use of blood to monitor UM patients as a noninvasive liquid biopsy.

Acknowledgments

The authors would like to acknowledge the technical expertise and scientific support of the Proteomics facility of the MUHC-RI, especially Lorne Taylor and Amy Wong.

Disclosures

Financial support: This work was supported by CNPq process No. 429571/2018-6, FAPESP, and CAPES. RBJ is an investigator for CNPq Brazil.

Conflict of interest: The authors report no conflict of interest.

Data Availability: All data generated and analyzed during this study are included in this manuscript.



References

- Ortega MA, Fraile-Martínez O, García-Hondurilla N, et al. Update on uveal melanoma: translational research from biology to clinical practice. [Review]. *Int J Oncol*. 2020;57(6):1262-1279. [CrossRef PubMed](#)
- Abildgaard SK, Vorum H. Proteomics of uveal melanoma: a minireview. *J Oncol*. 2013;2013:820953. [CrossRef PubMed](#)
- Zuidervaart W, Hensbergen PJ, Wong MC, et al. Proteomic analysis of uveal melanoma reveals novel potential markers involved in tumor progression. *Invest Ophthalmol Vis Sci*. 2006;47(3):786-793. [CrossRef PubMed](#)
- Ramasamy P, Murphy CC, Clynes M, et al. Proteomics in uveal melanoma. *Exp Eye Res*. 2014;118:1-12. [CrossRef PubMed](#)
- Surman M, Hoja-Lukowicz D, Szwed S, et al. An insight into the proteome of uveal melanoma-derived ectosomes reveals the presence of potentially useful biomarkers. *Int J Mol Sci*. 2019;20(15):E3789. [CrossRef PubMed](#)
- Surman M, Stępień E, Przybyło M. Melanoma-derived extracellular vesicles: focus on their proteome. *Proteomes*. 2019;7(2):21. [CrossRef PubMed](#)
- Contreras-Naranjo JC, Wu HJ, Ugaz VM. Microfluidics for exosome isolation and analysis: enabling liquid biopsy for personalized medicine. *Lab Chip*. 2017;17(21):3558-3577. [CrossRef PubMed](#)
- Pessuti CL, Costa DF, Ribeiro KS, et al. Extracellular vesicles from the aqueous humor of patients with uveitis. *Pan-Am J Ophthalmol*. 2019;1(1):1-3. [CrossRef](#)
- Perkumas KM, Hoffman EA, McKay BS, Allingham RR, Stamer WD. Myocilin-associated exosomes in human ocular samples. *Exp Eye Res*. 2007;84(1):209-212. [CrossRef PubMed](#)
- Théry C, Witwer KW, Aikawa E, et al. Minimal information for studies of extracellular vesicles 2018 (MISEV2018): a position statement of the International Society for Extracellular Vesicles and update of the MISEV2014 guidelines. *J Extracell Vesicles*. 2018;7(1):1535750. [CrossRef PubMed](#)
- Zhang H, Freitas D, Kim HS, et al. Identification of distinct nanoparticles and subsets of extracellular vesicles by asymmetric flow field-flow fractionation. *Nat Cell Biol*. 2018;20(3):332-343. [CrossRef PubMed](#)
- Ramirez MI, Amorim MG, Gadelha C, et al. Technical challenges of working with extracellular vesicles. *Nanoscale*. 2018;10(3):881-906. [CrossRef PubMed](#)
- Simpson RJ, Lim JW, Moritz RL, Mathivanan S. Exosomes: proteomic insights and diagnostic potential. *Expert Rev Proteomics*. 2009;6(3):267-283. [CrossRef PubMed](#)
- Devhare PB, Ray RB. Extracellular vesicles: novel mediator for cell to cell communications in liver pathogenesis. *Mol Aspects Med*. 2018;60:115-122. [CrossRef PubMed](#)
- Yáñez-Mó M, Siljander PR, Andreu Z, et al. Biological properties of extracellular vesicles and their physiological functions. *J Extracell Vesicles*. 2015;4(1):27066. [CrossRef PubMed](#)
- Kao CY, Papoutsakis ET. Extracellular vesicles: exosomes, microparticles, their parts, and their targets to enable their biomanufacturing and clinical applications. *Curr Opin Biotechnol*. 2019;60:89-98. [CrossRef PubMed](#)
- Zhao Y, Weber SR, Lease J, et al. Liquid biopsy of vitreous reveals an abundant vesicle population consistent with the size and morphology of exosomes. *Transl Vis Sci Technol*. 2018;7(3):6. [CrossRef PubMed](#)
- Wiklander OPB, Brennan MÁ, Lötvall J, Breakefield XO, El Andaloussi S. Advances in therapeutic applications of extracellular vesicles. *Sci Transl Med*. 2019 May 15;11(492):eaav8521. [CrossRef PubMed](#)
- Campos JH, Soares RP, Ribeiro K, Andrade AC, Batista WL, Torrecilhas AC. Extracellular vesicles: role in inflammatory responses and potential uses in vaccination in cancer and infectious diseases. *J Immunol Res*. 2015;2015:832057. [CrossRef PubMed](#)
- Marcilla A, Martin-Jaular L, Trelis M, et al. Extracellular vesicles in parasitic diseases. *J Extracell Vesicles*. 2014;3(1):25040. [CrossRef PubMed](#)
- Liang B, Peng P, Chen S, et al. Characterization and proteomic analysis of ovarian cancer-derived exosomes. *J Proteomics*. 2013;80:171-182. [CrossRef PubMed](#)
- Andrade LNS, Otake AH, Cardim SGB, et al. Extracellular vesicles shedding promotes melanoma growth in response to chemotherapy. *Sci Rep*. 2019;9(1):14482. [CrossRef PubMed](#)
- Angi M, Kalirai H, Prendergast S, et al. In-depth proteomic profiling of the uveal melanoma secretome. *Oncotarget*. 2016;7(31):49623-49635. [CrossRef PubMed](#)
- Lazar I, Clement E, Ducoux-Petit M, et al. Proteome characterization of melanoma exosomes reveals a specific signature for metastatic cell lines. *Pigment Cell Melanoma Res*. 2015;28(4):464-475. [CrossRef PubMed](#)
- Guo Y, Ji X, Liu J, et al. Effects of exosomes on pre-metastatic niche formation in tumors. *Mol Cancer*. 2019;18(1):39. [CrossRef PubMed](#)
- Plebancik MP, Angeloni NL, Vinokour E, et al. Pre-metastatic cancer exosomes induce immune surveillance by patrolling monocytes at the metastatic niche. *Nat Commun*. 2017;8(1):1319. [CrossRef PubMed](#)
- Milane L, Singh A, Mattheolabakis G, Suresh M, Amiji MM. Exosome mediated communication within the tumor microenvironment. *J Control Release*. 2015;219:278-294. [CrossRef PubMed](#)
- Chennakrishnaiah S, Tsering T, Aprikian S, Rak J. Leukobiopsy—a possible new liquid biopsy platform for detecting oncogenic mutations. *Front Pharmacol*. 2020;10:1608. [CrossRef PubMed](#)
- Abdoun M, Floris M, Gao ZH, Arena V, Arena M, Arena GO. Colorectal cancer-derived extracellular vesicles induce transformation of fibroblasts into colon carcinoma cells. *J Exp Clin Cancer Res*. 2019;38(1):257. [CrossRef PubMed](#)
- Eldh M, Olofsson Bagge R, Lässer C, et al. MicroRNA in exosomes isolated directly from the liver circulation in patients with metastatic uveal melanoma. *BMC Cancer*. 2014;14(1):962. [CrossRef PubMed](#)
- Peinado H, Alečković M, Lavotshkin S, et al. Melanoma exosomes educate bone marrow progenitor cells toward a pro-metastatic phenotype through MET. *Nat Med*. 2012;18(6):883-891. [CrossRef PubMed](#)
- Ragusa M, Barbagallo C, Statello L, et al. miRNA profiling in vitreous humor, vitreal exosomes and serum from uveal melanoma patients: pathological and diagnostic implications. *Cancer Biol Ther*. 2015;16(9):1387-1396. [CrossRef PubMed](#)
- Tsering T, Laskaris A, Abdoun M, et al. Uveal melanoma-derived extracellular vesicles display transforming potential and carry protein cargo involved in metastatic niche preparation. *Cancers (Basel)*. 2020;12(10):E2923. [CrossRef PubMed](#)
- Ding M, Wang C, Lu X, et al. Comparison of commercial exosome isolation kits for circulating exosomal microRNA profiling. *Anal Bioanal Chem*. 2018;410(16):3805-3814. [CrossRef PubMed](#)
- Enderle D, Spiel A, Coticchia CM, et al. Characterization of RNA from exosomes and other extracellular vesicles isolated by a novel spin column-based method. *PLoS One*. 2015;10(8):e0136133. [CrossRef PubMed](#)
- Zhu L, Wada M, Usagawa Y, et al. Overexpression of cathepsin D in malignant melanoma. *Fukuoka Igaku Zasshi*. 2013;104(10):370-375. [PubMed](#)
- Kalra H, Simpson RJ, Ji H, et al. Vesiclepedia: a compendium for extracellular vesicles with continuous community



- annotation. *PLoS Biol.* 2012;10(12):e1001450. [CrossRef PubMed](#)
38. Faingold D, Marshall JC, Anteck E, et al. Immune expression and inhibition of heat shock protein 90 in uveal melanoma. *Clin Cancer Res.* 2008;14(3):847-855. [CrossRef PubMed](#)
 39. Wu X, Zhou J, Rogers AM, et al. c-Met, epidermal growth factor receptor, and insulin-like growth factor-1 receptor are important for growth in uveal melanoma and independently contribute to migration and metastatic potential. *Melanoma Res.* 2012;22(2):123-132. [CrossRef PubMed](#)
 40. Pardo M, García A, Antrobus R, Blanco MJ, Dwek RA, Zitzmann N. Biomarker discovery from uveal melanoma secretomes: identification of gp100 and cathepsin D in patient serum. *J Proteome Res.* 2007;6(7):2802-2811. [CrossRef PubMed](#)
 41. Maloney SC, Marshall JC, Anteck E, et al. SPARC is expressed in human uveal melanoma and its abrogation reduces tumor cell proliferation. *Anticancer Res.* 2009;29(8):3059-3064. [PubMed](#)
 42. Schicher N, Edelhauser G, Harmankaya K, et al. Pretherapeutic laboratory findings, extent of metastasis and choice of treatment as prognostic markers in ocular melanoma—a single centre experience. *J Eur Acad Dermatol Venereol.* 2013;27(3):e394-e399. [CrossRef PubMed](#)
 43. Janik ME, Lityńska A, Przybyło M. Studies on primary uveal and cutaneous melanoma cell interaction with vitronectin. *Cell Biol Int.* 2014;38(8):942-952. [CrossRef PubMed](#)
 44. Lykke-Andersen S, Brodersen DE, Jensen TH. Origins and activities of the eukaryotic exosome. *J Cell Sci.* 2009;122(Pt 10):1487-1494. [CrossRef PubMed](#)
 45. Ratajczak J, Wysoczynski M, Hayek F, Janowska-Wieczorek A, Ratajczak MZ. Membrane-derived microvesicles: important and underappreciated mediators of cell-to-cell communication. *Leukemia.* 2006;20(9):1487-1495. [CrossRef PubMed](#)
 46. Bellingham SA, Coleman BM, Hill AF. Small RNA deep sequencing reveals a distinct miRNA signature released in exosomes from prion-infected neuronal cells. *Nucleic Acids Res.* 2012;40(21):10937-10949. [CrossRef PubMed](#)
 47. Di Vizio D, Morello M, Dudley AC, et al. Large oncosomes in human prostate cancer tissues and in the circulation of mice with metastatic disease. *Am J Pathol.* 2012;181(5):1573-1584. [CrossRef PubMed](#)
 48. Kahlert C, Melo SA, Protopopov A, et al. Identification of double-stranded genomic DNA spanning all chromosomes with mutated KRAS and p53 DNA in the serum exosomes of patients with pancreatic cancer. *J Biol Chem.* 2014;289(7):3869-3875. [CrossRef PubMed](#)
 49. Théry C, Boussac M, Véron P, et al. Proteomic analysis of dendritic cell-derived exosomes: a secreted subcellular compartment distinct from apoptotic vesicles. *J Immunol.* 2001;166(12):7309-7318. [CrossRef PubMed](#)
 50. van Niel G, D'Angelo G, Raposo G. Shedding light on the cell biology of extracellular vesicles. *Nat Rev Mol Cell Biol.* 2018;19(4):213-228. [CrossRef PubMed](#)
 51. Zaborowski MP, Balaj L, Breakefield XO, Lai CP. Extracellular vesicles: composition, biological relevance, and methods of study. *Bioscience.* 2015;65(8):783-797. [CrossRef PubMed](#)
 52. Inamdar S, Nitiyanandan R, Rege K. Emerging applications of exosomes in cancer therapeutics and diagnostics. *Bioeng Transl Med.* 2017;2(1):70-80. [CrossRef PubMed](#)
 53. Logozzi M, De Milito A, Lugini L, et al. High levels of exosomes expressing CD63 and caveolin-1 in plasma of melanoma patients. *PLoS One.* 2009;4(4):e5219. [CrossRef PubMed](#)
 54. Xu ZG, Du JJ, Zhang X, et al. A novel liver-specific zona pellucida domain containing protein that is expressed rarely in hepatocellular carcinoma. *Hepatology.* 2003;38(3):735-744. [CrossRef PubMed](#)
 55. Sindrewicz P, Lian LY, Yu LG. Interaction of the oncofetal Thomsen-Friedenreich antigen with galectins in cancer progression and metastasis. *Front Oncol.* 2016;6:79. [CrossRef PubMed](#)
 56. Ahmed H, ALSadek DM. Galectin-3 as a potential target to prevent cancer metastasis. *Clin Med Insights Oncol.* 2015;9:113-121. [CrossRef PubMed](#)
 57. Al-Nedawi K, Meehan B, Micallef J, et al. Intercellular transfer of the oncogenic receptor EGFRvIII by microvesicles derived from tumour cells. *Nat Cell Biol.* 2008;10(5):619-624. [CrossRef PubMed](#)
 58. Aga M, Bentz GL, Raffa S, et al. Exosomal HIF1 α supports invasive potential of nasopharyngeal carcinoma-associated LMP1-positive exosomes. *Oncogene.* 2014;33(37):4613-4622. [CrossRef PubMed](#)
 59. Abdouh M, Hamam D, Gao ZH, Arena V, Arena M, Arena GO. Exosomes isolated from cancer patients' sera transfer malignant traits and confer the same phenotype of primary tumors to oncosuppressor-mutated cells. *J Exp Clin Cancer Res.* 2017;36(1):113. [CrossRef PubMed](#)
 60. Xu J, Liao K, Zhou W. Exosomes regulate the transformation of cancer cells in cancer stem cell homeostasis. *Stem Cells Int.* 2018;2018:4837370. [CrossRef PubMed](#)
 61. Shen M, Ren X. New insights into the biological impacts of immune cell-derived exosomes within the tumor environment. *Cancer Lett.* 2018;431:115-122. [CrossRef PubMed](#)
 62. Dos Anjos Pultz B, Andrés Cordero da Luz F, Socorro Faria S, et al. The multifaceted role of extracellular vesicles in metastasis: priming the soil for seeding. *Int J Cancer.* 2017;140(11):2397-2407. [CrossRef PubMed](#)
 63. Becker A, Thakur BK, Weiss JM, Kim HS, Peinado H, Lyden D. Extracellular vesicles in cancer: cell-to-cell mediators of metastasis. *Cancer Cell.* 2016;30(6):836-848. [CrossRef PubMed](#)
 64. Hoshino A, Costa-Silva B, Shen TL, et al. Tumour exosome integrins determine organotropic metastasis. *Nature.* 2015;527(7578):329-335. [CrossRef PubMed](#)
 65. Che P, Yang Y, Han X, et al. S100A4 promotes pancreatic cancer progression through a dual signaling pathway mediated by Src and focal adhesion kinase. *Sci Rep.* 2015;5(1):8453. [CrossRef PubMed](#)
 66. Amaro A, Gangemi R, Piaggio F, et al. The biology of uveal melanoma. *Cancer Metastasis Rev.* 2017;36(1):109-140. [CrossRef PubMed](#)
 67. Li S, Yi M, Dong B, Tan X, Luo S, Wu K. The role of exosomes in liquid biopsy for cancer diagnosis and prognosis prediction. *Int J Cancer.* 2021;148(11):2640-2651. [CrossRef PubMed](#)
 68. Puhka M, Takatalo M, Nordberg ME, et al. Metabolomic profiling of extracellular vesicles and alternative normalization methods reveal enriched metabolites and strategies to study prostate cancer-related changes. *Theranostics.* 2017;7(16):3824-3841. [CrossRef PubMed](#)
 69. Vafaei S, Fattahi F, Ebrahimi M, Janani L, Sharifabrizi A, Madjd Z. Common molecular markers between circulating tumor cells and blood exosomes in colorectal cancer: a systematic and analytical review. *Cancer Manag Res.* 2019;11:8669-8698. [CrossRef PubMed](#)

Effectiveness of periodontal intervention on the levels of N-terminal pro-brain natriuretic peptide in chronic periodontitis patients

Ibrahim Fazal¹, Bhavya Shetty¹, Umesh Yadalam², Safiya Fatima Khan², Manjusha Nambiar²

¹Department of Periodontology, Faculty of Dental Sciences, M. S. Ramaiah University of Applied Sciences, Bangalore, Karnataka - India

²Department of Periodontology, Sri Rajiv Gandhi College of Dental Sciences and Hospital, Bangalore, Karnataka - India

ABSTRACT

Background: N-terminal-pro-brain natriuretic peptide (NT-proBNP) is an inactive hormone that is seen during inflammation and is a known biomarker of cardiovascular disease (CVD). Evidence suggests that periodontitis has a bidirectional relationship with CVD and NT-proBNP has a potential role in periodontal disease. However, there is no evidence on the impact of nonsurgical periodontal therapy (NSPT) on the levels of NT-proBNP in gingival crevicular fluid (GCF) and serum in patients with chronic periodontitis. Hence, the aim of this study was to compare the levels of NT-proBNP in GCF and serum in patients with chronic generalized periodontitis.

Materials and methods: GCF and serum samples were collected in 19 patients with chronic periodontitis before and after NSPT after 6 weeks and the cumulative or reduction in values of NT-proBNP in GCF and serum was assessed. NT-proBNP levels in GCF and serum were determined by enzyme-linked immunosorbent assay.

Results: The concentrations of NT-proBNP were significantly reduced in GCF and serum after NSPT. Statistically significant difference of NT-proBNP concentration between pre- and postgroups in GCF was apparent ($p < 0.0001$), whereas statistically nonsignificant results in NT-proBNP serum levels when compared at baseline to postoperative state with mean of 61.77 (22.6 standard deviation [SD]) preoperatively and 72.67 (51.86 SD) postoperatively ($p = 0.0007$) was observed.

Conclusion: Significant reduction of NT-proBNP concentrations in GCF and serum in patients with chronic periodontitis subjected to NSPT was observed. This may account for a significant relation between periodontal disease, bacteremia, and CVD.

Keywords: Brain natriuretic peptide, Cardiovascular biomarker, Nonsurgical periodontal therapy, NT-proBNP, Periodontal disease

Background

Periodontitis is a multifactorial inflammatory disease caused by interactions between periodontal microflora and host immune response (1). Perpetuating periodontal

destruction is an important sequela of periodontitis that can lead to the subsequent loss of teeth. The expression of the disease results from the interaction of host defense mechanisms, microbial agents, and environmental and genetic factors.

Traditional clinical diagnosis of periodontal disease cannot reliably identify the sites of ongoing periodontal destruction and does not provide information about the patient's susceptibility to disease, whether the disease is progressing or not, or the disease in remission, or the response to treatment will be positive or negative. Although specific microorganisms are implicated in periodontitis, many other aspects of tissue changes are known to negatively alter periodontal status. Based on this concept, serum, gingival tissue fluid, saliva, and tissue biopsy samples have now been investigated for periodontal adversities and their association with markers associated with systemic complications.

Received: July 8, 2022

Accepted: August 29, 2022

Published online: October 3, 2022

Corresponding author:

Dr Ibrahim Fazal

Department of Periodontology

Faculty of Dental Sciences

M. S. Ramaiah University of Applied Sciences, Bangalore

560054, Karnataka - India

ibrahim.f.dhinda@gmail.com



Gingival crevicular fluid (GCF) contains a variety of biochemical factors that may be used as biomarkers for the diagnosis or prognosis of periodontal tissue in health and disease. GCF, both stimulated and unstimulated, can be obtained non-invasively from various oral sites and has been shown to be a reliable predictor of disease activity. Due to the increased activity of the disease, many proteins and enzymes in GCF increase. Means obtained for each standard marker activity are observed at GCF, which is 20-fold higher than serum.

The prime objective of scaling and root planing (SRP) is to restore gingival health by completely removing the tooth surface elements that provoke the gingival inflammation, to provide a biologically acceptable root surface, and to facilitate oral hygiene.

Traditional methods for diagnosing periodontal diseases include clinical and radiographic examinations. These traditional measures provide information only about the existing disease and are incapable of predicting disease progression. As a result, advances in oral and periodontal disease diagnostic research are shifting toward methods for identifying and quantifying periodontal risk using objective measures such as biomarkers. One of these biomarkers that can be detected in several inflammatory conditions is N-terminal-pro-brain natriuretic peptide (NT-proBNP).

BNP is a 32 amino acid peptide that is released primarily from the ventricular myocardium in response to increased myocardial wall tension. BNP is produced as a prohormone that is cleaved into two peptides: the active hormone BNP; and a biologically inactive NT-proBNP. Because of its longer half-life compared to active BNP, it has been suggested that serum NT-proBNP may be a viable biomarker for cardiovascular disease (CVD) (1). This peptide is also associated with an increased risk of CV events, cerebral ischemia, and all causes that increase the mortality rate.

In a previous study, patients with periodontitis showed significantly higher NT-proBNP serum levels than subjects without periodontitis. Serum NT-proBNP levels increased as periodontal disease destruction progressed (2). Recent studies have shown an association between periodontitis and elevated serum NT-proBNP levels (1).

To the best of our knowledge, the relationship between GCF and serum levels of NT-proBNP in chronic periodontitis and the effect of SRP on their levels have not been explored. Hence, this study aims to compare the levels of NT-proBNP in serum and GCF in patients with chronic generalized periodontitis before and after SRP.

Materials and methods

The study was conducted at the Department of Periodontology, Faculty of Dental Sciences, M. S. Ramaiah University of Applied Sciences in collaboration with the Department of Microbiology, Ramaiah Medical College and Hospital, Bangalore. Study period was from January 2020 to November 2021.

This study was a nonrandomized comparative interventional study in which serum and GCF samples were collected from 19 patients with chronic periodontitis. The reason for using serum rather than saliva as an indicator for analysis

is that serum is still the best body fluid for evaluating many biomarkers reflecting systemic processes, and substitution should be used with caution. Furthermore, while salivary cortisol levels may be reflective of systemic levels, other immune biomarkers in saliva, particularly cardiac, such as interleukin (IL)-6, soluble IL-6 receptor, and C-reactive protein (CRP) cytokines, have failed to show significant correlations to paired plasma samples. Around 45 days of SRP and cumulative or decreased NT-proBNP levels for both parameters were collected. GCF and serum were evaluated. Because the sensitivity and specificity of cardiac markers are influenced by several factors such as time of presentation, treatment, diagnostic thresholds, kinetic and half-life, the recall period was 45 days. Because NT-proBNP has a shorter half-life and full recovery and reattachment of periodontal apparatus can take up to 6 weeks, 45 days was chosen as the optimal recall interval. Subjects referred to the Department of Periodontology who met the selection criteria were evaluated and included in the study. A total of 19 patients who met the selection criteria were considered sample size for this study. GCF and serum samples were taken before and after SRP. All subjects received nonsurgical periodontal therapy (NSPT), which includes SRP and subgingival debridement.

Inclusion criteria were: Patients within the age 25-50 years, systemically healthy patients, subjects with ≥ 18 completely erupted teeth, subjects with presence of bleeding on probing, probing pocket depth ≥ 5 mm, and clinical attachment level ≥ 6 mm. Exclusion criteria were: atherosclerotic vascular disease (i.e., CVD, stroke, and peripheral artery disease), immunological disorders, arthritis/osteoporosis, history of periodontal intervention within the last 6 months, anti-inflammatory and nonsteroidal anti-inflammatory therapy within 3 months prior to periodontal assessment, and pregnancy or lactation.

The research was performed in accordance with the Declaration of Helsinki of the World Medical Association (2008) and was approved by the Ethics Committee for Human Trials of M. S. Ramaiah University of Applied Sciences with reference no: EC-2020/PG/13. Informed consent was obtained from each patient or their relatives after full explanation of the periodontal examination, GCF, and blood sample withdrawal.

The sample size has been estimated using GPower software v. 3.1.9.4.

Considering the effect size to be measured (dz) at 50%, power of the study at 80%, and the margin of the error at 10%, the total sample size needed was 19.

Collection of serum and GCF NT-proBNP before SRP

NT-proBNP in serum and GCF levels was assessed in patients with periodontitis before SRP. Complete periodontal examination was performed in all subjects (Fig. 1).

The GCF samples from deepest probing depth were collected for NT-proBNP assessment (Fig. 2). The GCF samples from all the patients were collected after 24 hours following baseline examination to avoid contamination of the sample with blood. GCF samples were obtained from the sites with deepest probing depth. Supragingival plaque of the intended



Fig. 1 - Preoperative scaling and root planing.



Fig. 2 - Collection of gingival crevicular fluid samples.

tooth was removed with piezoelectric ultrasonic scaler before sampling. The tooth was dried prior to obtaining the sample. The GCF collection was done using micropipettes with proper isolation of the site with cotton rolls.

Blood samples were obtained in the morning (Fig. 3). This is important because the human body is subjected to variations depending on the time of day; due to this variability of parameters during the day the values are observed to alter, which is reflected in the laboratory results (3), and both the Canadian and US hematology guidelines endorse this view. Although still in debate, fasting before drawing blood is not recommended because the body starts to use its own protein, especially with a small supply of fat. This can lead to glucose levels being too low and even to increased amounts of ketone compounds or a reduction in iron and hemoglobin levels. Subjects should be seated and relaxed and asked not to be anxious as it may cause the body to stimulate and release adrenaline. Therefore, a blood test preceded by physical effort or anxiousness will manifest itself in the form of altered blood serum levels (4). Briefly, 2 mL of venous blood was collected from the antecubital fossa by venipuncture using a 20-gauge needle with a 2 mL syringe. Blood samples



Fig. 3 - Collection of blood sample from antecubital vein.

were allowed to clot at room temperature and, after 1 hour, serum was separated from blood by centrifugation and 0.5 mL of extracted serum was immediately transferred to 1.5-mL aliquots. Each aliquot was stored at -80°C until required for analysis. Ultrasonic SRP procedure was performed.

Collection of serum and GCF NT-proBNP after SRP

NT-proBNP in serum and GCF levels was assessed in patients with chronic generalized periodontitis after SRP after 45 days.

Complete periodontal examination was performed in all subjects and all the clinical parameters were assessed. The procedure for assessing the serum and GCF levels was repeated, blood samples were obtained in the morning. Briefly, 2 mL of venous blood was collected from the antecubital fossa by venipuncture using a 20-gauge needle with a 2 mL syringe. Blood samples were allowed to clot at room temperature and, after 1 hour, serum is separated from blood by centrifugation (Fig. 4) and 0.5 mL of extracted serum was



Fig. 4 - Serum immediately after centrifugation.

immediately transferred to 1.5-mL aliquots. Each aliquot was stored at -80°C until required for analysis.

The GCF samples from the deepest probing depth were collected for NT-proBNP assessment after reevaluating for any local factors postoperatively (Fig. 5). The GCF samples from all the patients were collected after 24 hours following baseline examination to avoid contamination of the sample with blood. GCF samples were obtained from the sites with deepest probing depth (Fig. 6). The tooth was dried prior to obtaining the sample. The GCF collection was done using micropipettes with proper isolation of the site with cotton rolls.



Fig. 5 - Postoperative scaling and root planing.



Fig. 6 - Postoperative gingival crevicular fluid collection.

Comparing the levels of NT-proBNP in serum and GCF

The levels of NT-proBNP in serum and GCF in patients before and after SRP were compared, and the results will determine whether NSPT has an effect on serum and GCF NT-proBNP levels.

Standard preparation

Reconstitution of original BNP standard with 1 mL of sample diluent was done. Standards were kept for 15 minutes with gentle agitation before making further dilutions. Additional standards were prepared by serially diluting the standard stock solutions as given in Table I.

TABLE I - Standard values or concentrates obtained from the serum and GCF samples of BNP, which procures a standard curve as the measure of the values in the samples

Standard Conc. (pg/mL)	Standard Vial	Dilutions
2000	Standard no. 8	Reconstitute with 1 mL sample diluent
1000	Standard no. 7	300 μL Standard no. 8 + 300 μL sample diluent
500	Standard no. 6	300 μL Standard no. 7 + 300 μL sample diluent
250	Standard no. 5	300 μL Standard no. 6 + 300 μL sample diluent
125	Standard no. 4	300 μL Standard no. 5 + 300 μL sample diluent
62.5	Standard no. 3	300 μL Standard no. 4 + 300 μL sample diluent
31.25	Standard no. 2	300 μL Standard no. 3 + 300 μL sample diluent
0	Standard no. 1	300 μL sample diluent

BNP = brain natriuretic peptide; GCF = gingival crevicular fluid.

Table I indicates the standard values or concentrates obtained from the serum and GCF samples of BNP, which procures a standard curve to the measure the values in the samples.

NT-proBNP enzyme-linked immunosorbent assay (ELISA) quantitative assay procedure:

1. Bring all the reagents to room temperature before use (Fig. 7)
2. Pipette standards 1-8 samples – about 100 μL (Fig. 8)
3. Incubate for 90 minutes
4. Wash 1 \times wash buffer; Decant, 4 \times 300 μL
5. Pipette biotinylated anti-BNP 100 μL
6. Incubate 60 minutes (37°C)
7. Wash 1 \times wash buffer; Decant, 4 \times 300 μL
8. Pipette streptavidin: Horseradish peroxidase (HRP) conjugate 100 μL
9. Incubate 30 minutes
10. Wash 1 \times wash buffer; Decant, 4 \times 300 μL
11. Pipette tetramethylbenzidine (TMB) substrate 90 μL
12. Incubate in dark for 10 minutes.
13. NT-proBNP level detection was performed by ELISA in an ELISA plate analyzer.
14. Pipette stop solution 50 μL
15. Measure 450 within 15 minutes

Anti-BNP antibody was precoated in 96-well plates and biotin-conjugated anti-BNP antibody was used as detection antibody. Then, the calibrator, test sample, and biotin-conjugated detection antibody were added to the well and washed with wash buffer. HRP was added and unbound conjugates were washed with wash buffer. TMB substrate will be used to visualize the HRP enzymatic reaction. The TMB will be



Fig. 7 - N-terminal-pro-brain natriuretic peptide enzyme-linked immunosorbent assay kit.

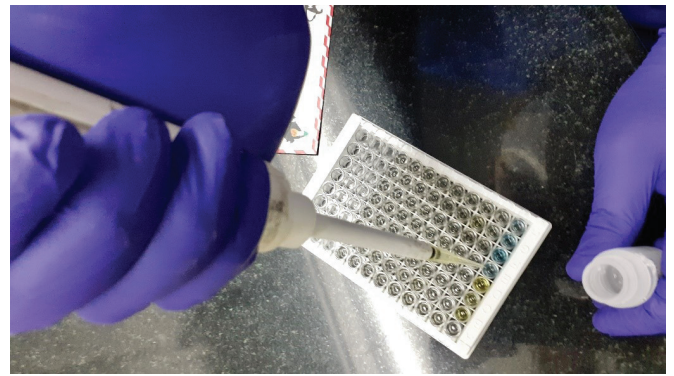


Fig. 9 - Pipetting stop solution – blue to yellow.

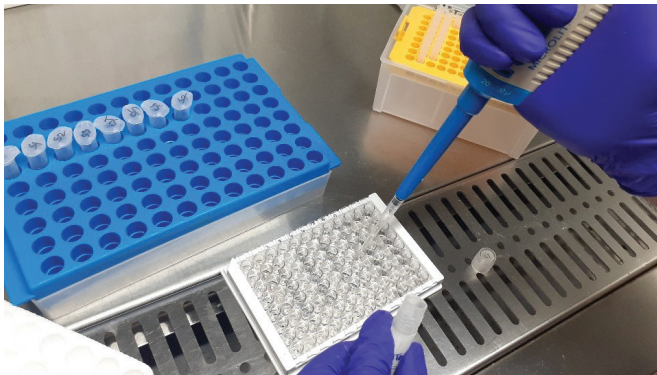


Fig. 8 - (Left) 8 standards in vials. (Right) Adding serum and gingival crevicular fluid samples in the microtiter plate.



Fig. 10 - Screenshot of estimated values obtained.

catalyzed by HRP to give a blue-colored product, which will turn yellow after the addition of the acid solution stops (Fig. 9). The density of the color will be proportional to the amount of NT-proBNP sample collected in the plate. The optical density absorbance (O.D.) reading should be recorded at 450 nm in a microplate reader and then the NT-proBNP concentration should be calculated (Fig. 10). Demographic, clinical, and historical information for certain diseases will also be recorded.

Standard curve was generated using the obtained standard concentration to measure the concentrations of NT-proBNP in GCF and serum (Fig. 11).

Statistical analysis

Statistical Package for the Social Sciences (SPSS) for Windows (Version 22.0, Released 2013; Armonk, NY: IBM Corp.) was used for providing statistical analysis.

Descriptive statistics

Descriptive analysis of all the explanatory and outcome parameters was done using mean and standard deviation for quantitative variables, frequency and proportions for categorical variables.

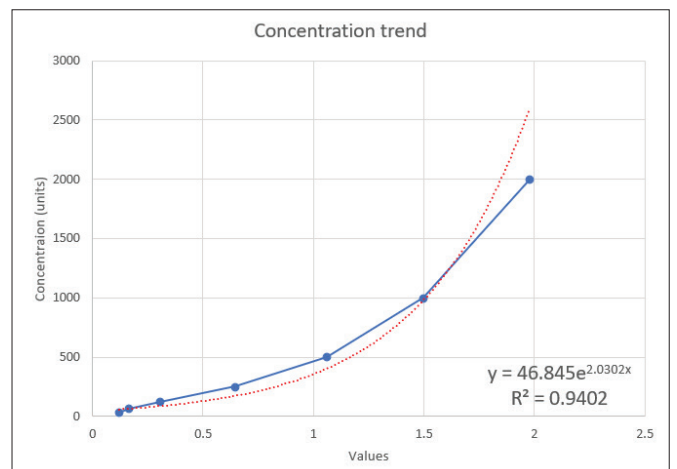


Fig. 11 - Standard curve for concentration trend.

Inferential statistics

Student’s paired t-test was used to compare the mean values of clinical parameters and NT-proBNP levels (GCF and



serum) before and after SRP periods. Pearson correlation test was used to assess the relationship between clinical parameters and NT-proBNP levels (GCF and serum) before and after SRP periods. Stepwise multiple linear regression analysis was performed to predict the variation in the NT-proBNP levels (GCF and serum) in context to clinical parameters before and after SRP periods. The level of significance (p-value) was set at $p < 0.05$ and any other relevant test, if found appropriate during the time of data analysis, were dealt accordingly.

Processing the ELISA kits and estimating the contorted BNP values in GCF and serum were done in the Department of Microbiology, Ramaiah Medical College, Bangalore.

Results

In total, 19 subjects were recruited and treated, and their GCF and serum samples were collected prior to and post-SRP. The sample population comprised of 11 females and 9 males (Fig. 12) and were in the age range of 18 to 50 years (Fig. 13). There was no significant difference between the two groups regarding age and gender.

The purpose of this intervention study was to estimate GCF and serum NT-proBNP levels 45 days before and after the intervention. In this study, nonsurgical periodontal SRP

was selected as the treatment modality and NT-proBNP levels were evaluated 45 days after NSPT.

Table II signifies the pre- and postoperative serum values. Although few subjects showed reduction in concentrations of serum NT-proBNP, however, upon estimation it was found that, in 36.8% of subjects' (n = 7) serum NT-proBNP exhibited higher values even after NSPT. Nevertheless, upon clinical evaluation of periodontal parameters, periodontal status of the subjects was improved. Hence, serum concentration values were not statistically significant ($p > 0.0005$).

Table III signifies the pre- and postoperative NT-proBNP GCF values. The table indicates that there is a significant reduction in GCF post-SRP. Subjects showed drastic reduction in GCF-BNP values, whereas 36.8% subjects (n = 7) showed slight increased concentrations in GCF levels. Clinical evaluation of periodontal parameters showed that periodontal status of the subjects was improved. Hence, GCF concentration values were statistically significant ($p < 0.0001$).

There is a significant increase in NT-proBNP serum levels when compared at baseline to postoperative state with the mean of 61.77 (22.6 standard deviation [SD]) preoperatively and 72.67 (51.86 SD) postoperatively ($p = 0.0007$) (Tab. IV).

Table V shows that there is a significant decrease in GCF levels of NT-proBNP when compared at baseline to

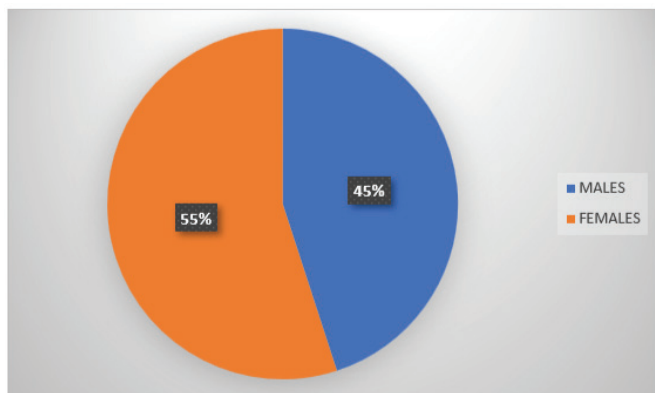


Fig. 12 - Graphical presentation of subjects' gender distribution taken from collection of gingival crevicular fluid and serum samples.

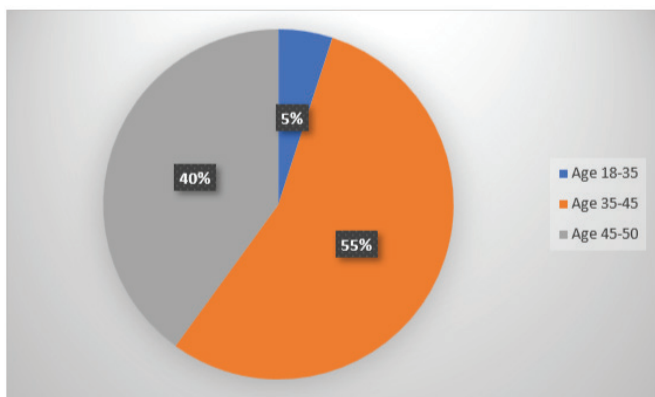


Fig. 13 - Graphical representation of age distribution of subjects for collection of gingival crevicular fluid and serum.

TABLE II - Preoperative and postoperative BNP serum values

Sample ID	BNP Serum Samples	
	Preoperative	Postoperative
D129	56.58	56.81
D584	56.69	56.47
D570	56.58	55.67
D569	57.27	55.44
D557	56.01	55.33
D124	55.22	55.33
D048	55.78	52.91
D045	57.27	56.24
D541	56.24	59.53
D397	56.35	58.45
D099	57.74	279.69
D569	57.62	56.35
D875	59.04	56.01
D868	57.39	57.04
D587	55.89	57.74
D035	56.35	79.74
D577	55.44	57.98
D453	158.05	133.81
D273	58.21	55.78

BNP = brain natriuretic peptide.



TABLE III - Preoperative and postoperative BNP GCF values

Sample ID	BNP GCF Samples	
	Preoperative	Postoperative
D129	59.16	56.81
D584	76.26	58.45
D570	56.81	58.09
D569	58.57	59.40
D557	69.18	58.21
D124	56.81	57.21
D048	57.51	57.16
D045	58.21	50.5
D541	57.86	58.21
D397	56.69	58.21
D099	57.27	62.50
D569	57.16	57.98
D875	58.92	55.11
D868	59.40	50.81
D587	58.09	49.48
D035	67.37	50.40
D577	56.58	50.09
D453	57.62	50.29
D273	685.93	49.79

BNP = brain natriuretic peptide; GCF = gingival crevicular fluid.

TABLE IV - Statistical and numerical analysis of the values obtained for serum NT-proBNP

Serum	Mean (\pm SD)	p-Value
Preoperative	61.77 (\pm 22.6)	0.0007
Postoperative	72.67 (\pm 51.86)	

NT-proBNP = N-terminal-pro-brain natriuretic peptide; SD = standard deviation.

TABLE V - Statistical and numerical analysis of the values obtained for GCF NT-proBNP

Serum	Mean (\pm SD)	p-Value
Preoperative	90.11 (\pm 140.11)	<0.0001
Postoperative	54.93 (\pm 4.23)	

GCF = gingival crevicular fluid; NT-proBNP = N-terminal-pro-brain natriuretic peptide; SD = standard deviation.

postoperative state; this could indicate GCF as a promising indicator for assessing NT-proBNP levels in patients with periodontitis.

Analysis was done by Fischer's analysis test because the significance of the deviation from p-value can be calculated

exactly, rather than relying on an approximation that becomes exact in the limit as the sample size grows to infinity, as with many statistical tests. Significant difference of BNP concentration between pre- and postgroups in GCF was apparent and the mean concentration in the pre-SRP group was high when compared to post-SRP group, which had evidently reduced postintervention ($p < 0.0001$).

Statistically nonsignificant difference of BNP concentration between pre- and postgroups in serum was observed and similarly the mean concentration of BNP in serum was seen to be increased postintervention as compared to preintervention ($p = 0.0007$).

Discussion

Chronic periodontitis is a common condition, affecting 45.9% of the US adult population aged 30 years and older (5). Chronic periodontitis causes loss of connective tissue that supports teeth and alveolar bone, which, if left untreated, is a major cause of tooth loss in adults (6). According to the case definitions of the Centers for Disease Control and Prevention and the American Academy of Periodontology, the estimated prevalence of early/moderate and severe periodontitis is 37.1% and 8.9% in adults, respectively, in the United States (5).

In addition, since diabetes has a great impact on periodontal disease and treatment, we excluded patients with such systemic diseases (7). NT-proBNP also has an indirect effect on pancreatic insulin-producing β -cells through the accumulation of intracellular iron. Patients with CVD, neurodegenerative disease, chronic infections (e.g., tuberculosis and degenerative disease), cancer, and liver disease were also excluded as these diseases impair the onset, progression, and outcome of periodontal disease and may affect the NT-proBNP concentration levels (8).

This study shows that patients with periodontitis have higher serum and GCF NT-proBNP levels. Moreover, as periodontal disease progresses, serum and GCF NT-proBNP levels increase, which reduce adequately after SRP. BNP is a vital cardiovascular biomarker that is actively detected in periodontal diseases; SRP aids in the improvement in clinical parameters, which may be due to resolution of the inflammatory response and the cessation of periodontal destruction, which makes a direct impact on this biomarker and reduces its potential pathogenicity and leads to their lowered concentrations in GCF and serum (9). This could be explained by invasion of periodontal pathogen into vascular endothelial cells in order to evade the immune cells. Endothelial invasion by *Porphyromonas gingivalis* is facilitated by hemagglutinin A, hemagglutinin B, and fimbriae A. Fimbriae A increases expression of different adhesion molecules on the endothelial cells of blood vessels and expression of inflammatory mediators such as IL-6, IL-8, and cyclooxygenase-2. In fact, lipopolysaccharide (LPS) and fimbriae A could coordinate in the proinflammatory stimulation of arterial endothelium by *P. gingivalis*. *Aggregatibacter actinomycetemcomitans* also upregulates the formation of adhesion molecules, however, in lesser amount (10). This suggests that CVD and periodontal disease have a bidirectional relationship (11) and periodontal

intervention has vital influence on periodontal and CVD parameters, which may perhaps decrease the risk of CVD.

In this study, during the estimation of NT-proBNP concentrations in GCF we found that there is substantial decrease in the levels post-SRP when compared at baseline. Significant difference of NT-proBNP concentration between pre- and poststate in GCF was apparent and the mean concentration in the pre-SRP group was high when compared to post-SRP group, which had evidently reduced postintervention ($p < 0.0001$). However, when concentration of NT-proBNP in serum was estimated, few subjects did not show significant reduction. Upon estimation it was found that the serum levels in NT-proBNP with subjects having periodontitis revealed increased values. However, upon clinical evaluation of periodontal parameters, periodontal status of the subjects was improved. This would be because of elimination of local factors and patient education along with maintenance. Hence, serum concentration values were not statistically significant ($p = 0.0007$).

In accordance with the present study, Mahendra Mohan et al assessed CRP levels after SRP evaluated at baseline, 1 month and 45 days in patients with diabetes mellitus and chronic periodontitis (DM-CP) and nondiabetic chronic periodontitis (NDM-CP) patients and showed similar results, suggesting that the CRP levels in both GCF and serum were higher in DM-CP patients than in NDM-CP patients (12). Although there was a significant improvement in both the groups, greater improvement was observed in both GCF and serum samples of DM-CP patients. Our results are consistent with the results of this study, showing a significant reduction in GCF and serum NT-proBNP levels after SRP compared to baseline and 45 days. Both showed a decrease, but a greater decrease in BNP concentration was observed with GCF compared to serum.

However, Paschalina Goutoudi et al concluded that periodontal therapy reduced IL-8 levels in GCF (13). This finding is consistent with our study where NT-proBNP levels decreased in GCF after SRP. However, there is a result contrary to our study that the concentration of NT-proBNP before and after periodontal intervention is not statistically significant. A close association was observed between periodontal destruction and NT-proBNP levels. Patients with periodontitis initially presented with higher periodontal inflammation with high NT-proBNP levels while when SRP was performed, these values decreased after 45 days; NT-proBNP levels decreased significantly in GCF and serum, because there is an inflammatory response and it stops the destruction of periodontal disease affecting NT-proBNP, thereby reducing their levels.

Samah H. Elmeadawy et al have shown that NSPT significantly reduces serum VCAM1 levels. The VCAM1 protein mediates the adhesion of lymphocytes, monocytes, eosinophils, and basophils to the vascular endothelium and may be involved in the development of atherosclerosis and rheumatoid arthritis (14). Another study by Cui D et al has shown reduced VCAM1 expression and macrophage/monocyte infiltration in the vascular wall of mice treated with NSPT (15). Both studies were consistent with our study that GCF NT-proBNP levels decreased 45 days after receiving SRP.

Deng et al however reported NSPT had no significant effect on CRP, total cholesterol, low-density lipoprotein cholesterol, and triglycerides (16). Also, Zeng et al concluded NSPT was associated with carotid atherosclerosis but statistical heterogeneity was substantial, hence the results were obsolete and trajected toward showing NSPT having no effects on CVD biomarkers (17). These studies showed contradictory results when compared to our study. Our study showed substantial homogeneity in results where NSPT has an effect on the NT-proBNP levels in GCF and serum in patients with periodontitis.

Gupta et al (2015) correlated the levels of sCD40 L and MCP-1 in serum and GCF of patients with chronic periodontitis before and after SRP. sCD40 L and MCP-1 are the acute precipitators of CVD in subjects with periodontitis, and Gupta et al concluded that a positive correlation observed between sCD40 L and MCP-1 levels and detected reduced levels of GCF and serum after SRP, which suggests this phenomenon as one of the pathways that may lead to the propagation of cardiovascular events in patients with periodontal disease (18). This is in accordance with our study as NT-proBNP levels are reduced post-SRP, which shows a positive correlation between CVD and periodontitis and may prevent the risk of CVD.

For this study, SRP was found to significantly reduce NT-proBNP levels in GCF in patients with chronic periodontitis compared to baseline values. This decrease in NT-proBNP levels at the end of the study can be explained by the effect of SRP on local factor removal. Therefore, it can reduce the inflammatory response and, as a result, the mediators that stimulate the production in the acute phase protein.

We were unable to compare the results of the present study on the effect of SRP on serum or GCF levels of NT-proBNP in patients with chronic periodontitis with other studies because to our knowledge this is the first study to evaluate NT-proBNP levels in GCF and serum in patients with periodontitis before and after SRP.

The significant increase in the concentration levels of NT-proBNP in serum may perhaps be due to the following reasons:

1. Time Factor: NT-proBNP is a cardiac biomarker that is detected in patients with periodontitis. The reduction of the levels in serum requires supplemental time in the blood stream to get stabilized. Also, evidences regarding CVD biomarkers suggest the recall period as 3-6 months for reevaluation.
2. Periodontal Invention: Evidence by Alka S. Waghmare et al concluded that bacteremia frequently occurs immediately after SRP (19). Similarly, in our study SRP may have led to bacteremia and therefore had aggravated the levels of serum NT-proBNP for a brief time.

This study had a number of shortcomings. The study recruited a small sample size. Further investigations with larger numbers of subjects and of a longer duration are needed to better understand the role of periodontal therapy on the improvement of the cardiac status. Blinding was done only at the statistician level. Thus, multilevel blinding can be incorporated in future studies.

Conclusion

Till date and to the best of our knowledge this is the first study that aims to compare the levels of NT-proBNP in serum and GCF in patients with chronic generalized periodontitis before and after SRP. Even with the limitations of this study, we can conclude that NSPT has a reducing effect on the serum and GCF NT-proBNP levels in chronic periodontitis patients. In addition, serum and GCF BNP levels represent a potential biomarker of chronic periodontitis and may indicate NSPT may avoid the risk of CVD events by reducing systemic inflammation caused by local factors. Hence, it can be concluded that NSPT reduces NT-proBNP concentrations in patients with chronic periodontitis and may evade the future risk of CVD.

Compliance with ethics guidelines

The study protocol is approved by the University Ethics Committee for Human Trials of M. S. Ramaiah University of Applied Sciences (Ref no. EC-2020/PG/13). Written informed consent has been obtained from the participants.

Availability of data and materials: All data generated or analyzed during this study are included in this published article (and its supplementary information files).

Authors' contribution

IF: Clinical investigator; funding; data collection; manuscript preparation

BS: Designing of the study; clinical investigator; data analysis

UY: Literature search; manuscript review

SFK: Study concept; manuscript preparation, editing and review

MN: Manuscript preparation and review

Disclosures

Conflict of interest: The authors declare no conflict of interest.

Financial support: This research received no specific grant from any funding agency in the public, commercial, or not-for-profit sectors.

References

- Leira Y, Blanco J. Brain natriuretic peptide serum levels in periodontitis. *J Periodontol Res*. 2018;53(4):575-581. [CrossRef PubMed](#)
- Jensen J, Ma LP, Fu MLX, Svaninger D, Lundberg PA, Hammarsten O. Inflammation increases NT-proBNP and the NT-proBNP/BNP ratio. *Clin Res Cardiol*. 2010;99(7):445-452. [CrossRef PubMed](#)
- Dale JC, Steindel SJ, Walsh M. Early morning blood collections: a College of American Pathologists Q-Probes study of 657 institutions. *Arch Pathol Lab Med*. 1998;122(10):865-870. [PubMed](#)
- Sorita A, Patterson A, Landazuri P, et al. The feasibility and impact of midnight routine blood draws on laboratory orders and processing time. *Am J Clin Pathol*. 2014;141(6):805-810. [CrossRef PubMed](#)
- Eke PI, Dye BA, Wei L, et al. Update on prevalence of periodontitis in adults in the United States: NHANES 2009 to 2012. *J Periodontol*. 2015;86(5):611-622. [CrossRef PubMed](#)
- Dikbas I, Tanalp J, Tomruk CO, Koksak T. Evaluation of reasons for extraction of crowned teeth: a prospective study at a university clinic. *Acta Odontol Scand*. 2013;71(3-4):848-856. [CrossRef PubMed](#)
- Bullon P, Newman HN, Battino M. Obesity, diabetes mellitus, atherosclerosis and chronic periodontitis: a shared pathology via oxidative stress and mitochondrial dysfunction? *Periodontol 2000*. 2014;64(1):139-153. [CrossRef PubMed](#)
- Iacopino AM, Cutler CW. Pathophysiological relationships between periodontitis and systemic disease: recent concepts involving serum lipids. *J Periodontol*. 2000;71(8):1375-1384. [CrossRef PubMed](#)
- Sophia K II, Suresh S, Sudhakar U Sr, et al. Comparative evaluation of serum and gingival crevicular fluid periostin levels in periodontal health and disease: a biochemical study. *Cureus*. 2020;12(3):e7218. [CrossRef PubMed](#)
- Khlgatian M, Nassar H, Chou HH, Gibson FC III, Genco CA. Fimbria-dependent activation of cell adhesion molecule expression in *Porphyromonas gingivalis*-infected endothelial cells. *Infect Immun*. 2002;70(1):257-267. [CrossRef PubMed](#)
- Dhadse P, Gattani D, Mishra R. The link between periodontal disease and cardiovascular disease: how far we have come in last two decades? *J Indian Soc Periodontol*. 2010;14(3):148-154. [CrossRef PubMed](#)
- Mohan M, Jhingran R, Bains VK, et al. Impact of scaling and root planing on C-reactive protein levels in gingival crevicular fluid and serum in chronic periodontitis patients with or without diabetes mellitus. *J Periodontal Implant Sci*. 2014;44(4):158-168. [CrossRef PubMed](#)
- Goutoudi P, Diza E, Arvanitidou M. Effect of periodontal therapy on crevicular fluid interleukin-6 and interleukin-8 levels in chronic periodontitis. *Int J Dent*. 2012;2012:362905. [CrossRef PubMed](#)
- Elmeadawy SH, El-Sharkawy HM, Elbayomy A. Effect of nonsurgical periodontal therapy on systemic pro-inflammatory and vascular endothelial biomarkers and serum lipid profile in chronic periodontitis patients. *Egyptian Dent J*. 2017;63(3):2421-2433. [CrossRef](#)
- Cui D, Li H, Lei L, Chen C, Yan F. Nonsurgical periodontal treatment reduced aortic inflammation in ApoE(-/-) mice with periodontitis. *Springerplus*. 2016;5(1):940. [CrossRef PubMed](#)
- Linkai D, Chunjie L, Qian L, Yukui Z, Hongwei Z. Periodontal treatment for cardiovascular risk factors: a systematic review. *West China J Stomatol*. 31(5):463-467. [PubMed](#)
- Zeng XT, Leng WD, Lam YY, et al. Periodontal disease and carotid atherosclerosis: a meta-analysis of 17,330 participants. *Int J Cardiol*. 2016;203:1044-1051. [CrossRef PubMed](#)
- Gupta M, Chaturvedi R, Jain A. Role of cardiovascular disease markers in periodontal infection: understanding the risk. *Indian J Dent Res*. 2015;26(3):231-236. [CrossRef PubMed](#)
- Waghmare AS, Vhanmane PB, Savitha B, Chawla RL, Bagde HS. Bacteremia following scaling and root planing: a clinico-microbiological study. *J Indian Soc Periodontol*. 2013;17(6):725-730. [CrossRef PubMed](#)



Diagnostic impact of CEA and CA 15-3 on chemotherapy monitoring of breast cancer patients

Diya Hasan

Department of Allied Medical Sciences, Zarqa College, Al-Balqa Applied University, Zarqa - Jordan

ABSTRACT

Introduction: Serum tumor markers have emerged as an effective tool to determine prognosis and treatment efficiency in different cancer types. This study aimed to explore the chemotherapy monitoring efficiency and prognostic sensitivity of tumor-associated cancer antigen 15-3 (CA 15-3) and carcinoembryonic antigen (CEA) in early (II) and late (IV) clinical stage breast cancer.

Methods: CA 15-3 and CEA serum levels were assessed in 56 breast cancer patients at early (n = 26) and late (n = 30) clinical stages with these primary inclusion criteria: those who received adjuvant chemotherapy AC (adriamycin and cyclophosphamide) or AC-T (adriamycin and cyclophosphamide followed by taxane) regimens and possessed tumors negative for human epidermal growth factor receptor 2 (HER2) based on a particle-enhanced turbidimetric assay.

Results: CA 15-3 had a higher elevation than CEA in the pretreatment group of breast cancer patients when compared to healthy controls. Late-stage patients showed higher positive serum levels than early-stage patients for both markers, with a preference for CA 15-3 over CEA. AC-T chemotherapy regimen treatment in both clinical stages revealed a significantly higher level of both markers as compared to the AC regime, with a preference for CA 15-3 over CEA in late stage. Both markers were significantly higher in the late-stage group as compared to early-stage groups for both chemotherapy regimens.

Conclusions: CA 15-3 is more efficient as a prognostic monitoring marker than CEA and reveals a positive connection between chemotherapy regimen system and staging, with increased observability in late-stage patients.

Keywords: Breast cancer, CA 15-3, CEA, Chemotherapy, Prognosis

Introduction

Breast cancer is the most common cancer among Jordanian females, accounting for 22.4% of cancer cases (1). After being diagnosed with breast cancer, the patient treatment plan includes a combination of surgery, radiation, hormone therapy, and chemotherapy. Disease progress is evaluated according to consistent measures (2) based on alterations in the size of the quantifiable lesions.

During chemotherapy treatment, metastatic breast cancer is generally examined using imaging techniques such as positron emission tomography (PET), computed tomography (CT),

and magnetic resonance imaging (MRI). These techniques are costly, and their efficiency and accuracy in treatment evaluation may strongly affect patient outcomes (3).

Measuring differences in serum tumor markers has been established as a tool for evaluation of therapy effectiveness of different cancers (4,5). Cancer antigen 15-3 (CA 15-3) and carcinoembryonic antigen (CEA) are the most frequent serum tumor markers used for breast cancer, even though their functionality remains controversial (4,6). Breast cancer markers are applied for therapy response speculations, after initial therapy observation, and as prognostic indicators.

CEA is expressed in the majority of human lung, pancreatic, and gastric cancers, in addition to breast carcinoma (7). Measurements of CEA in breast cancer are suggestive of lymph node involvement and tumor size. Consequently, CEA concentrations above 7.5 µg/L are linked to a higher possibility of subclinical metastases (8). The normal range of CEA levels was connected to a significantly better prognosis of patients at the time of diagnosis compared to those with elevated levels (9). Studies propose CEA as a useful marker for monitoring treatment response including chemotherapeutic ones (10-12).

Received: June 29, 2022

Accepted: October 3, 2022

Published online: November 7, 2022

Corresponding author:

Dr. Diya Hasan
Amman, Gardenz street
0795071521 Amman - Jordan
diyahasan@bau.edu.jo



CA 15-3 (MUC1) is a cell surface glycoprotein derived from the *MUC1* gene. It's expressed on the surface of various epithelial cell types and overexpressed in 90% of breast cancer cases (13). The elevated level of CA 15-3 is used to determine the relapse potential of breast cancer patients, and as a tool for therapeutic response evaluation at late stages (14). CA 15-3 preoperative concentrations of early breast cancer patients have a notable relation to predict their outcomes (15).

Using serum tumor markers (CA 15-3 and CEA) permits the early identification of up to 60-80% of breast cancer patient metastasis (16). The serum levels of CA 15-3 and CEA were shown to be beneficial in the management of breast cancer patients and could aid as prognostic indicators and for observing disease development (17).

This study investigated the clinical importance of serum tumor markers CA 15-3 and CEA for monitoring Jordanian breast cancer patient responses to different chemotherapy regimens and their correlation with different clinical stages in addition to their prognostic value sensitivity.

Materials and methods

Patient cohort

Fifty-six female breast cancer patients were involved in this study using these main inclusion criteria: (1) human epidermal growth factor receptor 2 (HER2)-negative and (2) received adjuvant chemotherapy regimen AC (adriamycin and cyclophosphamide) or AC-T (adriamycin, cyclophosphamide, taxane). Table I shows the patient characteristics. Patients were categorized as follows: 26 patients (46.4%) were graded as stage II and 30 patients (53.5%) were graded as stage IV, patients who did not meet the criteria in Table 1 were excluded. Stage II or less was considered as early stage and stage II and above was considered as late stage as stated by the American Joint Committee on Cancer (AJCC) staging system (18). The median age between the two groups did not show any significant difference ($p = 0.232$).

Table I - Patient features and treatment method

Patient parameter	n (%)
Age (years)	Median 49 Range 43-55
Gender	Female
Clinical stage	
Stage II	26 (46.4%)
Stage IV	30 (53.5%)
Chemotherapy regime	
AC × 4	29 (51.7%)
AC × 4 followed by T × 4	27 (48.2%)
Histological type	IDC
HER2 receptor	Negative

A = adriamycin; C = cyclophosphamide; HER = human epidermal growth factor receptor; T = taxane; IDC = Invasive ductal carcinoma.

Primary chemotherapy

The first group of AC regimen consisting of 14 stage II and 15 stage IV patients was treated with 4 cycles of adriamycin 50 mg/m² and cyclophosphamide 1000 mg/m² on day 1, which was repeated every 21 days. The second group of AC-T regimen consisting of 12 stage II and 15 stage IV patients received the previous chemotherapy regimen AC, followed by 4 cycles of taxane 80 mg/m² every 21 days. The flowchart of patients is presented in Figure 1.

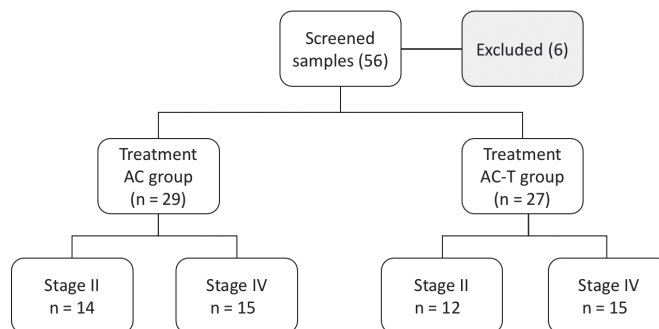


Fig. 1 - Flowchart of patients' selection. AC (Adriamycin & Cyclophosphamide) or AC-T (Adriamycin & Cyclophosphamide followed by Taxane) regimes treatments. (Based on the oncology decision according to treatment guidelines).

Sample collection

Ethical approval for this study was acquired from Al Bashir Hospital, Amman, Jordan (#3345), and written informed consent was collected from all patients. CEA and CA 15-3 blood samples were gathered from patients for diagnosis after the third month of treatment protocol (fourth cycle).

CEA and CA 15-3 measurements

The serum was isolated by centrifugation (2,500 rpm for 10 minutes) of patients' blood samples. Serum CEA and CA 15-3 levels were determined using an electrochemiluminescence immunoassay system (MODULAR ANALYTICS E170, Cobas e601; Roche, Germany): a particle-enhanced turbidimetric assay for CEA and immunoturbidimetric assay for CA 15-3. Marker assays were done using the commercial kits for CEA (Elecsys CEA, Cobas, Roche, Germany) and CA 15-3 (Elecsys CA 15-3, Cobas, Roche, Germany). A cut-off point of <5.0 µg/L (CEA) and <25.0 U/mL (CA 15-3) was used as indicated by the Roche Diagnostic Kit brochure. The CEA and CA 15-3 readings of 20 healthy females (con -) with inclusion criteria—does not have any type of cancer or chronic diseases, age ≥18 years, not on any type of medication, and 16 pre-chemotherapy breast cancer female patients (con +)—were obtained from Bio-lab laboratories.

Statistical analysis

Statistical analysis was performed using SPSS software. A t-test and Fishers test were performed to find out possible

marker-level variations between target groups. To see if the differences in proportions were statistically significant, the chi-square test was utilized. When possible, the odds ratio was utilized to assess the relationship.

Results

This study was planned to determine the correlation between CEA and CA 15-3 levels' elevation significance on monitoring response to Jordanian breast cancer female patients' treatment with different chemotherapy regimens at early and late clinical stages.

CEA and CA 15-3 levels in breast cancer

The CEA and CA 15-3 serum levels were measured in all samples using ELISA. The serum levels of CEA (1.7 µg/L) and CA 15-3 (18.7 U/mL) were significantly increased (Fig. 2; $p = 0.0005$ and $p = 0.0001$), respectively, in the pre-chemotherapy group (con +) compared to the healthy group (con -): CEA (1.09 µg/L) and CA 15-3 (8.7 U/mL). The presented data revealed differentiation between CEA and CA 15-3 serum-level elevation of studied groups (Fig. 2), as we observed a stronger increase of CA 15-3 level (Fig. 2B) compared to CEA level (Fig. 2A). These results imply that CEA and

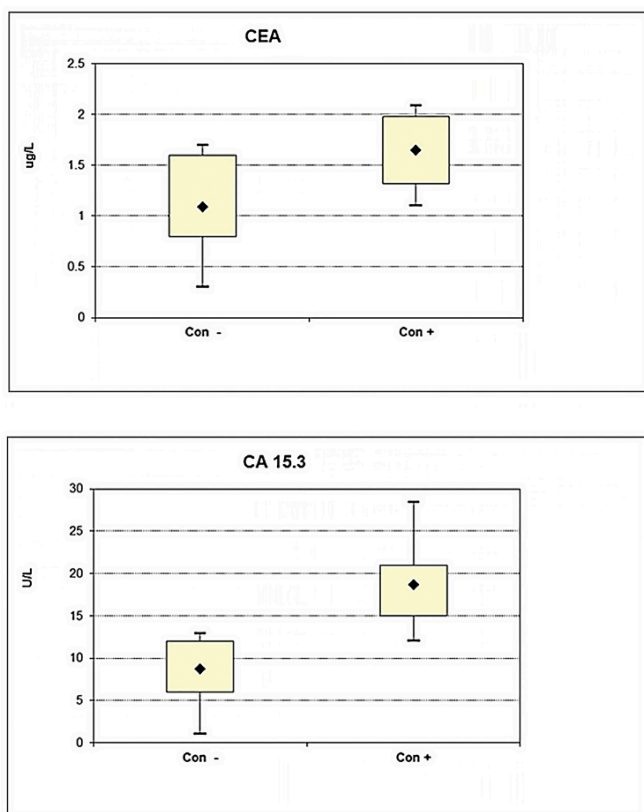


Fig. 2 - Difference in serum level between healthy non-cancer group (control -) and breast cancer patients groups before chemotherapy (control +) of (A) CEA (B) CA 15-3 markers. (*Significant increase differences for the serum levels of CEA and CA 15-3 (**** $P = 0.0005$ and **** $P = 0.0001$) respectively in pre-chemotherapy group (con +) compared to healthy ones (con -)).

CA 15-3 levels can be used efficiently to anticipate breast cancer tendency and provide a convenient detection method for breast cancer with a preference for CA 15-3 over CEA in sensitivity.

Positive serum levels of CEA and CA 15-3

In all-inclusive patient samples, elevated positive serum levels found in early and late stages were identified as follows: for CEA (II AC 4/14 [29%]), (II AC-T 4/11 [36%]), (IV AC 7/14 [50%]), and (IV AC-T 9/14 [64%]) of the breast cancer cases used the cut-off point <5.0 µg/L. As for CA 15-3 (II AC 5/14 [35.7%]), (II AC-T 7/11 [63.6%]), (IV AC 10/14 [71%]), and (IV AC-T 9/14 [64%]) of the breast cancer cases used the cut-off point <25 U/mL (Fig. 3). In total 8/25 (32%) of stage II and 16/28 (57%) of stage IV patients had higher levels of CEA than the cut-off point, while for CA 15-3 12/25 (48%) of stage II and 19/28 (68%) of stage IV patients had higher levels of CA 15-3 than the cut-off point (Fig. 3). In our study, a combined chemotherapy regimen demonstrated higher positive serum-level percentages for both markers as compared to a single chemotherapy regimen in the early-stage patient group; this elevation was notably stronger for CA 15-3 in comparison to CEA. The same result was obtained for CEA in the late-stage patient group; however, CA 15-3 behaved differently as positive serum levels were higher in a single chemotherapy regimen compared to a combined regimen. Overall, the late-stage patient group showed higher positive serum-level percentages compared to the early-stage group for both markers with a preference for CA 15-3 over CEA. These findings suggest that the serum levels of CA 15-3 might be more beneficial for observing chemotherapy response in advanced tumors than early diagnosis as compared with CEA.

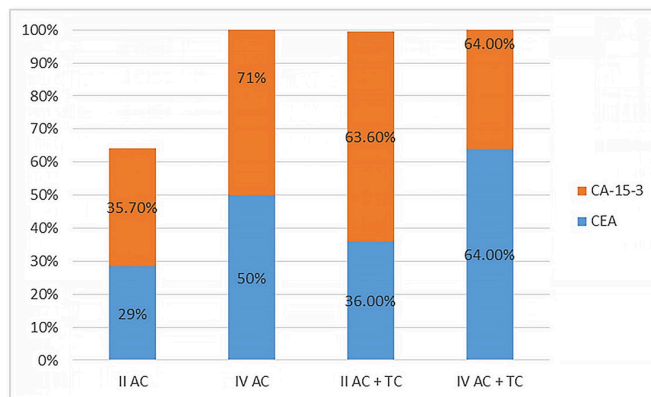


Fig. 3 - Positive serum levels of carcinoembryonic antigen (CEA) and cancer antigen (CA) 15-3 markers for both chemotherapy regimens (AC and AC-T) in early (II) and late (IV) clinical stages. AC = adriamycin and cyclophosphamide; AC-T = adriamycin and cyclophosphamide followed by taxane.

CEA and CA 15-3 levels based on chemotherapy type

Furthermore, the marker serum-level response and its association with the type of chemotherapeutic treatments in both early and late stages were investigated. Comparing the



CEA levels between both treatment regimens AC (mean rank: 2.41) and AC-T (mean rank: 2.65) in early stage, the AC (mean rank: 8.16) and AC-T (mean rank: 17.45) in late stage showed no significant changes ($p = 0.71$ and $p = 0.41$), respectively (Fig. 4A). Conversely, the CA 15-3 levels behaved differently where it had shown a significant change ($p = 0.056$) comparing the AC-T (mean rank: 144.39) to AC (mean rank: 25.55) at late stage but not at early stage ($p = 0.089$) AC (mean rank: 25.00) and AC-T (mean rank: 43.27) (Fig. 4B). This elevation in response to a combined chemotherapy regimen was observed to be stronger in the case of CA 15-3 in comparison to CEA and more specifically in the late-stage patient group.

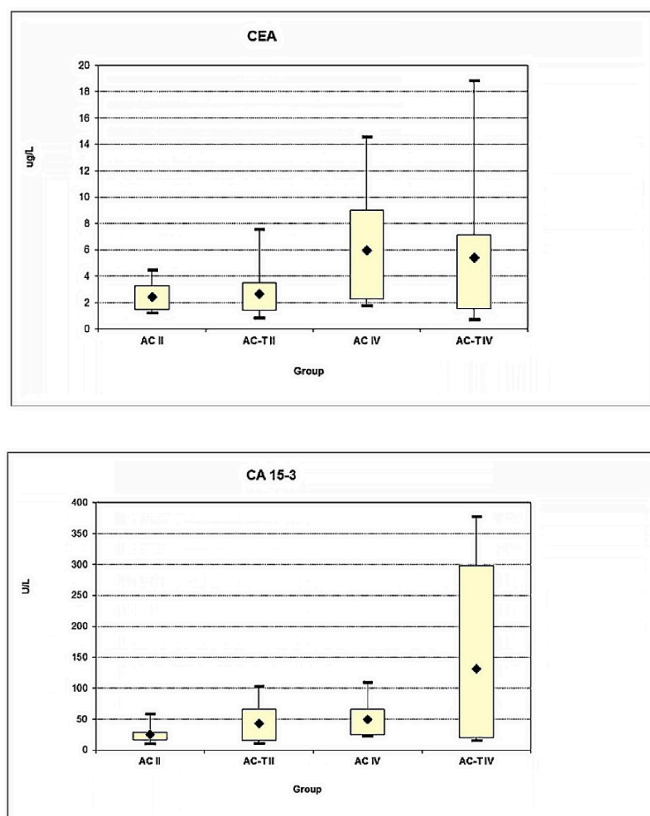


Fig. 4 - Effect of chemotherapy regime type AC or AC-T in both early (II) and late (IV) clinical stages on serum level response of (A) CEA and (B) CA 15-3 markers. (*Significant increase for the CA 15-3 serum level (* $P = 0.05$) comparing the AC-T to AC at late-stage IV).

CEA and CA 15-3 levels based on clinical stage

Analysis was performed to check if the CEA and CA 15-3 elevation response was associated with breast cancer progression in terms of different clinical stages (early and late) in each of the studied chemotherapeutic regimens. Comparing CEA levels between II (mean rank: 2.41) and IV (mean rank: 5.26) stages of AC treatment, II (mean rank: 2.65) and IV (mean rank: 5.83) stages of AC-T treatment, there was a

significant change ($p = 0.022$) in stage IV AC but not in stage IV AC-T ($p = 0.081$) (Fig. 5A). The CA 15-3 level comparison ([II (mean rank: 25.00) and IV (mean rank: 49.35) stages of AC treatment], [II (mean rank: 34.27) and IV (mean rank: 130.96) stages of AC-T treatment]) showed a significant change in stage IV compared to stage II in both AC and AC-T treatments ($p = 0.005$ and $p = 0.044$), respectively (Fig. 5B).

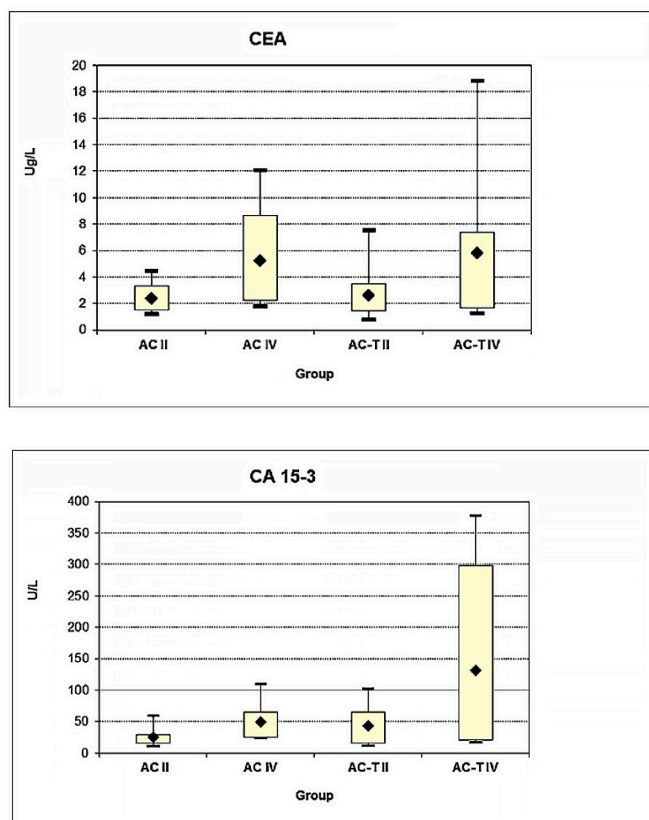


Fig. 5 - Effect of both clinical stages early (II) and late (IV) in association with chemotherapy regime type AC or AC-T on serum level response of (A) CEA and (B) CA 15-3 markers. (*Significant increase for the CEA serum level (* $P = 0.02$) for AC treatment at late-stage IV), (*Significant increase for the CA 15-3 serum level in late stage IV in both AC and AC-T treatments (* $P = 0.005$ and * $P = 0.044$) respectively).

The results revealed a significant connection between a change in marker level and clinical staging, as both CEA and CA 15-3 were significantly elevated in the late-stage patient group; more so than in the early-stage group in both chemotherapeutic regimens (Fig. 5). Collectively, these data suggest that CEA and CA 15-3 are predictive of chemotherapy response among different regimens throughout treatment and show differences between both early and late stages.

Discussion

Breast cancer is the most frequent cancer among Jordanian women. This study evaluated the significance of

using CA 15-3 and CEA for monitoring different chemotherapy regimens since assessing prognosis using diagnostic markers is believed to help in patients' therapeutic response anticipation, which is vital for evaluating the course of therapy and to avoid the side effects of worthless and inefficient treatments.

In the present study, CA 15-3 had shown a higher elevation as compared to CEA as both markers were significantly elevated in breast cancer patients at the time of diagnosis in comparison to healthy controls. These results imply that both CA 15-3 and CEA markers can efficiently predict breast cancer susceptibility and deliver benefit for breast cancer prognosis detection. The combination of both tumor markers (CA 15-3 and CEA) is important in breast cancer (19). CA 15-3 has better prognostic significance in relation to CEA (20). However, some studies have indicated that the prognostic value of CA 15-3 is lower than that of CEA (21), which demonstrates marker contradictory association in breast carcinogenesis (22).

Some studies have described the changes of CA-15-3 and CEA levels to be independent regardless of the breast cancer stage (23); however, our results showed that elevated serum levels of CEA and CA 15-3 above the cut-off point were identified in 8 (32%) and 12 (48%) of early-stage patients, and 16 (57%) and 19 (68%) of late-stage patients. More notable serum levels were elevated in the late stage than in the early stage with a preference for CA 15-3 over CEA. CA 15-3 and CEA elevation levels have been described as connected with clinic pathological parameters including advanced tumor, node, metastasis (TNM) stage (24).

The author analyzed the clinical impact of CA 15-3 and CEA to breast cancer patients with different chemotherapy regimens and in terms of different tumor clinical stages. This study found that CA 15-3 and CEA levels were shown to be higher in late stage and combined regimen as compared to early stage and single regimen, mainly with a preference for CA 15-3 at late stage over CEA. These results suggest that CA 15-3 and CEA serum levels can be an indicator for stage and chemotherapy regimen systems. Additionally, they suggest the clinical importance of CA 15-3 for follow-up as a prognostic variable during chemotherapy treatment of breast cancer patients.

CA 15-3 serum levels showed variations among breast cancer stages (9). CA 15-3 levels increase in all types of tumors; however, in breast cancer, it continues to increase as the tumor develops (25). Studies have reported that alterations of tumor marker levels are associated with a patient's therapeutic response, in addition to imaging method evaluation (26). CA 15-3 flaring (125% over the baseline) has been noticed in breast cancer patients after chemotherapy and has been linked with higher chances of disease development (27). Increased CA 15-3 levels were found for locally progressed breast cancer patients who received primary chemotherapy (AC or AC-T regimen), which is an indicator of a poor response to treatment (28). The analysis of CA 15-3 levels upregulating during the first 4-6 weeks of a new therapy should be considered because false initial rises can happen (29-33). The chemotherapy influence on the temporary elevation of CA 15-3 followed by its decline could be a consequence of unsuitable early cancelation or change of chemotherapy regimen (30,34,35).

Previous studies indicated no connection between a breast cancer patient's prior treatment and CEA levels (36). Based on our data, the CEA levels changed during the course of treatment and stages. CEA elevation for colorectal cancer patients has been noticed in the first 4-6 weeks after beginning chemotherapy (37,38). In addition, a chemotherapy regimen based on both irinotecan and oxaliplatin was found to induce a CEA flare and was correlated with good prognosis for colorectal cancer patients (39). The mechanisms by which chemotherapy induces CEA during cancer treatment remain to be elucidated. Several factors were described to have an influence and connection including hypothyroidism and inflammatory diseases (40,41). In some protocols CEA combined with CA 15-3 is used to observe the chemotherapy response for breast cancer patients, as it flares in the first 4-8 weeks of therapy as previously noted (42).

The current study promotes the option of monitoring CA 15-3 and CEA during adjuvant chemotherapy for breast cancer patients in Jordan as its results could contribute to treatment evaluation and be beneficial for customizing chemotherapeutic regimens in the future.

Conclusions

In conclusion, monitoring serum CA 15-3 and CEA levels for Jordanian breast cancer patients undergoing chemotherapy treatment provides prognostic indication and clinical information for evaluating tumor response as both markers had elevated levels with a preference for CA 15-3 over CEA in sensitivity.

Acknowledgments

The author acknowledges the biomedical scientists at Biolab Diagnostic Laboratories, represented by Dr. Amid Abdelnour, for their support of this work.

Disclosures

Conflict of interest: The authors declare that they have no conflict of interest.

Financial support: The author acknowledges the financial support from the deanship of scientific research at Al-Balqa Applied University Salt, Jordan (grant 118001).

Ethical approval: Ethical approval for this study was obtained from the ethical approval committee of Al Bashir Hospital Amman, Jordan (#3345).

References

1. Abdel-Razeq H, Mansour A, Jaddan D. Breast cancer care in Jordan. *JCO Glob Oncol*. 2020;6(6):260-268. [CrossRef PubMed](#)
2. Therasse P, Arbuuck SG, Eisenhauer EA, et al. New guidelines to evaluate the response to treatment in solid tumors. European Organization for Research and Treatment of Cancer, National Cancer Institute of the United States, National Cancer Institute of Canada. *J Natl Cancer Inst*. 2000;92(3):205-216. [CrossRef PubMed](#)
3. Alunni-Fabbroni M, Müller V, Fehm T, Janni W, Rack B. Monitoring in metastatic breast cancer: is imaging outdated

- in the era of circulating tumor cells? *Breast Care (Basel)*. 2014;9(1):16-21. [CrossRef PubMed](#)
4. Bidard FC, Hajage D, Bachelot T, et al. Assessment of circulating tumor cells and serum markers for progression-free survival prediction in metastatic breast cancer: a prospective observational study. *Breast Cancer Res*. 2012;14(1):R29. [CrossRef PubMed](#)
 5. Liu L, Xu HX, Wang WQ, et al. Serum CA125 is a novel predictive marker for pancreatic cancer metastasis and correlates with the metastasis-associated burden. *Oncotarget*. 2016;7(5):5943-5956. [CrossRef PubMed](#)
 6. Falzarano R, Viggiani V, Michienzi S, et al. Evaluation of a CLEIA automated assay system for the detection of a panel of tumor markers. *Tumour Biol*. 2013;34(5):3093-3100. [CrossRef PubMed](#)
 7. Thompson JA, Grunert F, Zimmermann W. Carcinoembryonic antigen gene family: molecular biology and clinical perspectives. *J Clin Lab Anal*. 1991;5(5):344-366. [CrossRef PubMed](#)
 8. Molina R, Auge JM, Farrus B, et al. Prospective evaluation of carcinoembryonic antigen (CEA) and carbohydrate antigen 15.3 (CA 15.3) in patients with primary locoregional breast cancer. *Clin Chem*. 2010;56(7):1148-1157. [CrossRef PubMed](#)
 9. Uehara M, Kinoshita T, Hojo T, Akashi-Tanaka S, Iwamoto E, Fukutomi T. Long-term prognostic study of carcinoembryonic antigen (CEA) and carbohydrate antigen 15-3 (CA 15-3) in breast cancer. *Int J Clin Oncol*. 2008;13(5):447-451. [CrossRef PubMed](#)
 10. Dnistrian AM, Schwartz MK, Greenberg EJ, Smith CA, Schwartz DC. CA 15-3 and carcinoembryonic antigen in the clinical evaluation of breast cancer. *Clin Chim Acta*. 1991;200(2-3):81-93. [CrossRef PubMed](#)
 11. Jezersek B, Cervek J, Rudolf Z, Novaković S. Clinical evaluation of potential usefulness of CEA, CA 15-3, and MCA in follow-up of breast cancer patients. *Cancer Lett*. 1996;110(1-2):137-144. [CrossRef PubMed](#)
 12. Robertson JF, Jaeger W, Syzendera JJ, et al; European Group for Serum Tumour Markers in Breast Cancer. The objective measurement of remission and progression in metastatic breast cancer by use of serum tumour markers. *Eur J Cancer*. 1999;35(1):47-53. [CrossRef PubMed](#)
 13. Duffy MJ, Shering S, Sherry F, McDermott E, O'Higgins N. CA 15-3: a prognostic marker in breast cancer. *Int J Biol Markers*. 2000;15(4):330-333. [CrossRef PubMed](#)
 14. Kurebayashi J. [Biomarkers in breast cancer]. *Gan To Kagaku Ryoho*. 2004;31(7):1021-1026. [PubMed](#)
 15. Shering SG, Sherry F, McDermott EW, O'Higgins NJ, Duffy MJ. Preoperative CA 15-3 concentrations predict outcome of patients with breast carcinoma. *Cancer*. 1998;83(12):2521-2527. [CrossRef PubMed](#)
 16. Jäger W, Eibner K, Löffler B, Gleixner S, Krämer S. Serial CEA and CA 15-3 measurements during follow-up of breast cancer patients. *Anticancer Res*. 2000;20(6D):5179-5182. [PubMed](#)
 17. Zhao S, Mei Y, Wang J, Zhang K, Ma R. Different levels of CEA, CA153 and CA125 in milk and benign and malignant nipple discharge. *PLoS One*. 2016;11(6):e0157639. [CrossRef PubMed](#)
 18. Edge SB, Compton CC. The American Joint Committee on Cancer: the 7th edition of the AJCC cancer staging manual and the future of TNM. *Ann Surg Oncol*. 2010;17(6):1471-4. [CrossRef PubMed](#)
 19. Vizcarra E, Lluch A, Cibrián R, et al. Value of CA 15.3 in breast cancer and comparison with CEA and TPA: a study of specificity in disease-free follow-up patients and sensitivity in patients at diagnosis of the first metastasis. *Breast Cancer Res Treat*. 1996;37(3):209-216. [CrossRef PubMed](#)
 20. Geraghty JG, Coveney EC, Sherry F, O'Higgins NJ, Duffy MJ. CA 15-3 in patients with locoregional and metastatic breast carcinoma. *Cancer*. 1992;70(12):2831-2834. [CrossRef PubMed](#)
 21. Ebeling FG, Stieber P, Untch M, et al. Serum CEA and CA 15-3 as prognostic factors in primary breast cancer. *Br J Cancer*. 2002;86(8):1217-1222. [CrossRef PubMed](#)
 22. Banin Hirata BK, Oda JM, Losi Guembarovski R, Ariza CB, de Oliveira CE, Watanabe MA. Molecular markers for breast cancer: prediction on tumor behavior. *Dis Markers*. 2014;2014:513158. [CrossRef PubMed](#)
 23. Moazzezy N, Farahany TZ, Oloomi M, Bouzari S. Relationship between preoperative serum CA 15-3 and CEA levels and clinicopathological parameters in breast cancer. *Asian Pac J Cancer Prev*. 2014;15(4):1685-1688. [CrossRef PubMed](#)
 24. Agrawal AK, Jelen M, Rudnicki J, et al. The importance of preoperative elevated serum levels of CEA and CA15-3 in patients with breast cancer in predicting its histological type. *Folia Histochem Cytobiol*. 2010;48(1):26-29. [CrossRef PubMed](#)
 25. Fu Y, Li H. Assessing clinical significance of serum CA15-3 and carcinoembryonic antigen (CEA) Levels in breast cancer patients: a meta-analysis. *Med Sci Monit*. 2016;22:3154-3162. [CrossRef PubMed](#)
 26. Yang Y, Zhang H, Zhang M, Meng Q, Cai L, Zhang Q. Elevation of serum CEA and CA15-3 levels during antitumor therapy predicts poor therapeutic response in advanced breast cancer patients. *Oncol Lett*. 2017;14(6):7549-7556. [CrossRef PubMed](#)
 27. Duffy MJ. Serum tumor markers in breast cancer: are they of clinical value? *Clin Chem*. 2006;52(3):345-351. [CrossRef PubMed](#)
 28. Al-azawi D, Kelly G, Myers E, et al. CA 15-3 is predictive of response and disease recurrence following treatment in locally advanced breast cancer. *BMC Cancer*. 2006;6(1):220. [CrossRef PubMed](#)
 29. Nisman B, Maimon O, Allweis T, et al. The prognostic significance of LIAISON(R) CA15-3 assay in primary breast cancer. *Anticancer Res*. 2013;33(1):293-299. [PubMed](#)
 30. Kim HS, Park YH, Park MJ, et al. Clinical significance of a serum CA15-3 surge and the usefulness of CA15-3 kinetics in monitoring chemotherapy response in patients with metastatic breast cancer. *Breast Cancer Res Treat*. 2009;118(1):89-97. [CrossRef PubMed](#)
 31. Agha-Hosseini F, Mirzaii-Dizgah I, Rahimi A. Correlation of serum and salivary CA15-3 levels in patients with breast cancer. *Med Oral Patol Oral Cir Bucal*. 2009;14(10):e521-e524. [CrossRef PubMed](#)
 32. Ali HQ, Mahdi NK, Al-Jowher MH. The value of CA15-3 in diagnosis, prognosis and treatment response in women with breast cancer. *J Pak Med Assoc*. 2013;63(9):1138-1141. [PubMed](#)
 33. Kobayashi S, Iwase H, Karamatsu S, Matsuo K, Masaoka A, Miyagawa T. The clinical value of serum CA15-3 assay postoperatively in breast cancer patients. *Jpn J Surg*. 1989;19(3):278-282. [CrossRef PubMed](#)
 34. Di Gioia D, Heinemann V, Nagel D, et al. Kinetics of CEA and CA15-3 correlate with treatment response in patients undergoing chemotherapy for metastatic breast cancer (MBC). *Tumour Biol*. 2011;32(4):777-785. [CrossRef PubMed](#)
 35. Devine PL, Duroux MA, Quin RJ, et al. CA15-3, CASA, MSA, and TPS as diagnostic serum markers in breast cancer. *Breast Cancer Res Treat*. 1995;34(3):245-251. [CrossRef PubMed](#)
 36. Thriveni K, Krishnamoorthy L, Ramaswamy G. Correlation study of carcino embryonic antigen & cancer antigen 15.3 in pre-treated female breast cancer patients. *Indian J Clin Biochem*. 2007;22(1):57-60. [CrossRef PubMed](#)



37. Sørbye H, Dahl O. Transient CEA increase at start of oxaliplatin combination therapy for metastatic colorectal cancer. *Acta Oncol.* 2004;43(5):495-498. [CrossRef PubMed](#)
38. Ailawadhi S, Sunga A, Rajput A, Yang GY, Smith J, Fakih M. Chemotherapy-induced carcinoembryonic antigen surge in patients with metastatic colorectal cancer. *Oncology.* 2006;70(1):49-53. [CrossRef PubMed](#)
39. Strimpakos AS, Cunningham D, Mikropoulos C, Petkar I, Barbachano Y, Chau I. The impact of carcinoembryonic antigen flare in patients with advanced colorectal cancer receiving first-line chemotherapy. *Ann Oncol.* 2010;21(5):1013-1019. [CrossRef PubMed](#)
40. Takahashi N, Shimada T, Ishibashi Y, Oyake N, Murakami Y. Transient elevation of serum tumor markers in a patient with hypothyroidism. *Am J Med Sci.* 2007;333(6):387-389. [CrossRef PubMed](#)
41. Klapdor R, Bahlo M, Babinski A. Atypical courses of serum tumor markers—4 case reports. *Anticancer Res.* 2003;23(2A):845-850. [PubMed](#)
42. Harris L, Fritsche H, Mennel R, et al; American Society of Clinical Oncology. American Society of Clinical Oncology 2007 update of recommendations for the use of tumor markers in breast cancer. *J Clin Oncol.* 2007;25(33):5287-5312. [CrossRef PubMed](#)



Journal of Circulating Biomarkers

www.aboutscience.eu

ISSN 1849-4544



ABOUTSCIENCE